Åbo Akademi University

**Terhi Maula**

# MEMBRANE PROPERTIES OF STRUCTURALLY MODIFIED CERAMIDES

## Effects on Lipid Lateral Distribution and Sphingomyelin-Interactions in Artificial Bilayer Membranes

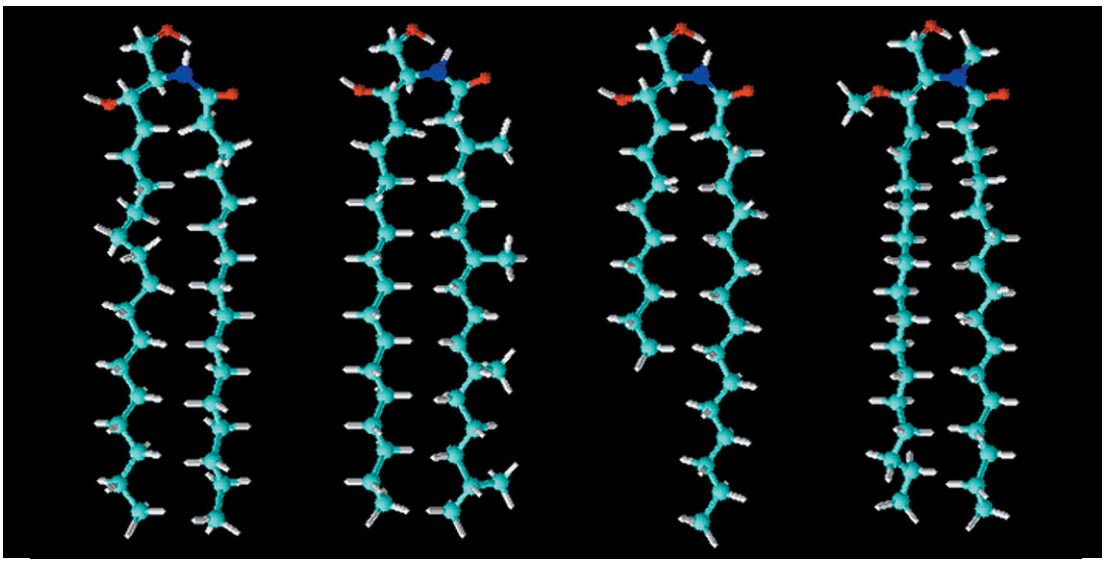

BIOCHEMISTRY
DEPARTMENT OF BIOSCIENCES
ÅBO AKADEMI UNIVERSITY
TURKU, FINLAND

2014

# MEMBRANE PROPERTIES OF STRUCTURALLY MODIFIED CERAMIDES

## effects on lipid lateral distribution and sphingomyelin-interactions in artificial bilayer membranes

**Terhi Maula**


**Biochemistry, Department of Biosciences**
**Åbo Akademi University**
**Turku, Finland**

**2014**

*Supervised by*

Professor J. Peter Slotte

Biochemistry, Department of Biosciences
Åbo Akademi University
Turku, Finland

*Reviewed by*

Docent Katariina Öörni

Wihuri Research Institute
Helsinki, Finland

MD, Docent Juha Holopainen

Department of Ophthalmology
University of Helsinki
Helsinki, Finland

*Opponent*

Professor Félix Goñi

Unidad de Biofísica & Departamento de Bioquímica
Universidad del País Vasco
Bilbao, Spain

Cover: 3D-optimized structures (drawn in ChemSketch) of (from left to right): palmitoylceramide, and the structurally modified phytanoylceramide, dodecasphing-4-enine based ceramide, and 2N(methyl)-3O(methyl)-palmitoylceramide. Carbon atoms are shown in cyan, nitrogens in blue, oxygens in red and hydrogens in white.

ISBN 978-952-12-3021-9
Painosalama Oy – Turku, Finland 2014

*To my family*

## TABLE OF CONTENTS

## LIST OF ORIGINAL PUBLICATIONS

This thesis is based on the following original publications referred to by the Roman numerals I-V throughout the thesis. The original publications have been reprinted with the permission of the copyright holders.

**I Differential ability of cholesterol-enriched and gel phase domains to resist benzyl alcohol-induced fluidization in multilamellar lipid vesicles.**
Maula T., Westerlund B., Slotte JP.
*Biochimica et Biophysica Acta 1788:2454-2461, 2009.*

**II The effects of *N*-acyl chain methylations on ceramide molecular properties in bilayer membranes.**
Maula T., Urzelai B., Slotte JP.
*European Biophysics Journal 40:857-863, 2011.*

**III Importance of the sphingoid base length for the membrane properties of ceramides.**
Maula T., Artetxe I., Grandell P-M., Slotte JP.
*Biophysical Journal 103:1870-1879, 2012.*

**IV Effects of sphingosine 2*N*- and 3*O*-methylation on palmitoyl ceramide properties in bilayer membranes.**
Maula T., Kurita M., Yamaguchi S., Yamamoto T., Katsumura S., Slotte JP.
*Biophysical Journal 101:2948-2956, 2011.*

**V Effects of sphingomyelin headgroup size on interactions with ceramide.**
Artetxe I., Sergelius C., Kurita M., Yamaguchi S., Katsumura S., Slotte JP., Maula T.
*Biophysical Journal 104:604-612, 2013.*

## CONTRIBUTION OF THE AUTHOR

The work in all of the original publications was designed by the author together with professor Slotte. In publication V, Ibai Artetxe participated in the design of the experiments.

The experimental work was performed by the author with the following exceptions: In paper II, Bakarne Urzelai performed a majority of the fluorescence quenching measurements under supervision of the author. In paper III, the work was performed by Ibai Artetxe and Pia-Maria Grandell under supervision by the author. In paper IV, one of the three ceramide analogs used in the study was synthezised by the group of professor Katsumura. In paper V, the sphingomyelin analogs were synthezised by the group of professor Katsumura, and a majority of the work was performed by Ibai Artetxe under supervision by the author, with assistance from Christian Sergelius with some of the fluorescence quenching experiments.

The author of this thesis was the principal author of papers I-IV under supervision by professor Slotte. Principal author of paper V was Ibai Artetxe under co-supervision by professor Slotte and the author of this thesis.

**Additional publications not included in the thesis:**

**Structure-activity relationship of sphingomyelin analogs with sphingomyelinase from Bacillus cereus.**
Sergelius C., Niinivehmas S., Maula T., Kurita M., Yamaguchi S., Yamamoto T., Katsumura S., Pentikäinen OT., Slotte JP.
*Biochimica et Biophysica Acta 1818:474-480, 2012.*

**2NH and 3OH are crucial structural requirements in sphingomyelin for sticholysin II binding and pore formation in bilayer membranes.**
Maula T., Isaksson YJE., García-Linares S., Niinivehmas S., Pentikäinen OT., Kurita M., Yamaguchi S., Yamamoto T., Katsumura S., Gavilanes JG., Martínez-del-Pozo Á., Slotte JP.
*Biochimica et Biophysica Acta 1828:1390-1395, 2013.*

## ACKNOWLEDGEMENTS

The work for this thesis was performed during 2008-2014 at the Department of Biosciences at Åbo Akademy University in Turku. During this period I got to know many great scientists, skilful colleagues and students, and some wonderful persons. Now, I would like to take the chance to thank the people who have had major roles in my life during the time spent producing this thesis.

First, I would like to sincerely thank my supervisor *Peter Slotte*. They say that the journey of becoming a PhD and composing a doctoral thesis requires hard work, great devotion, and lots of effort, and that it may not always be the most easiest path. In keeping with this, thank you for all the advice and guidance, and for providing excellent resources that enabled my thesis work. Thank you for the encouragement, for teaching me confidence, and for enabling this interesting journey and life-enriching experience.

I also wish to warmly thank all the past and present members of the lipid group for the wonderful working environment. A special thanks to *Bodil Westerlund*, *Thomas Nyholm*, *Katrin Halling*, *Anders Björkbom*, *Shishir Jaikishan*, *Jenny Isaksson*, *Max Lönnfors*, *Oskar Engberg*, *Helen Cooper* and *Md. Abdullah Al Sazzad*. Thank you Bodil for guiding me through the very first steps of starting a PhD and writing a manuscript. Thank you Thomas for all the guidance and practical help, for travel-company and for always being available for discussion. Shishir, my ultimate travel-companion and dear colleague: by coming from such a different cultural background, with such a great personality, you have many times made me see the world in a different (better!) way, such as when reading maps upside down in Bilbao. Thank you for so carefully carrying my luggage on conference trips, and for all the looong quiet hours spent on flights when you were asleep. Thank you Anders for sharing your excellent sense of humor, your never-ending enthusiasm for science, and for all the practical help in the lab. A special thanks to Jenny for the peer support in the exciting times of expecting. Thank you Max for taking good care of the coffee machine, and together with Helen, Oskar and Sazzad for the great company. A warm thank-you also to the many summer and gradu-students in our lab, especially *Anders Kullberg, Sofie Kvarnström, Oscar Ekholm, Daniel Lindroos, Nora Sairio, Kristian Ijäs* and *Joel Nyström*. Thank you also *Alexandra Elsing, Eva Bligt-Lindén* and *Matts Nylund* for great company over the years!

I would also like to thank all my coauthors, especially the two outstanding exchange students from Bilbao, *Bakarne Urzelai* and *Ibai Artetxe*. A special thanks goes to my coauthors from Japan, to *professor Shigeo Katsumura* and his

laboratory. Thank you also *Pia-Maria Grandell* and *Christian Sergelius* for your hard work and valuable help.

A big thanks belongs to the key staff at our department: *Elsmarie Nyman*, *Pirkko Luoma*, *Jussi Meriluoto* and *Juha-Pekka Sunila*. I would also like to express my deep gratitude to *Mark Johnson* and *Fredrik Karlsson*, the heart and soul of ISB, the graduate school that organized great scientific meetings and social activities, and offered a framework for the fluent progress of my thesis work. I would also like to warmly thank *Pia Roos-Mattjus* and *Reijo Käkelä* for serving as my thesis supervisory committee members and for showing interest towards my work. I would like to express my deepest gratitude to *Katariina Öörni* and *Juha Holopainen* for taking the time to review my thesis and for giving constructive criticism and valuable suggestions to improve its contents.

To my dear friends outside the lab I owe a huge thank-you, especially *Pauliina*, *Katja*, *Johanna*, *Mona*, and *Krista*. Thank you for everything that has had absolutely nothing to do with science! The support I have received from you in the form of true friendship has been invaluable. Thank you *Sari* and *Ansku* for all the moments shared with Hella, and a special thank-you to Ansku for all the (priceless!) help. I would also like to thank the members of *Mammaryhmä*, our little group of "fresh" mothers and their babies, for great company and for representing the core of the absolutely best thing in the world –being a mom.

I also wish to thank the most important people around me, my family. Thank you *Marja* and *Jouko,* my parents, and *Jarmo* and *Joonas,* my brothers, for all your support and interest towards my work. By your example, I have grown to experience that home is the best and safest place in the world, and what really counts in life is family, which we should never take for granted. Thank you also *Katriina* and *Pertti*, I could not wish for more pleasant, more helpful, and more sincere parents-in-law. To my guys, my dear husband *Marko* and our lovely, and very lively, son *Matias*, I only need to say one thing: you are my home.

I am deeply grateful for the generous financial support that I received over the years from Åbo Akademi University, Svenska Kulturfonden, Medicinska Understödsföreningen Liv och Hälsa r.f., the Oskar Öflund foundation, the National Doctoral Programme in Informational and Structural Biology, the Magnus Ehrnrooth foundation, and also the funding from the Sigrid Juselius foundation and Academy of Finland for professor Slotte.

*Terhi Maula*

Lokalahti, Friday, January 31, 2014

## ABSTRACT

Ceramides comprise a class of sphingolipids that exist only in small amounts in cellular membranes, but which have been associated with important roles in cellular signaling processes. The influences that ceramides have on the physical properties of bilayer membranes reach from altered thermodynamical behavior to significant impacts on the molecular order and lateral distribution of membrane lipids. Along with the idea that the membrane physical state could influence the physiological state of a cell, the membrane properties of ceramides have gained increasing interest. Therefore, membrane phenomena related to ceramides have become a subject of intense study both in cellular as well as in artificial membranes. Artificial bilayers, the so called model membranes, are substantially simpler in terms of contents and spatio-temporal variation than actual cellular membranes, and can be used to give detailed information about the properties of individual lipid species in different environments.

This thesis focuses on investigating how the different parts of the ceramide molecule, i.e., the *N*-linked acyl chain, the long-chain sphingoid base and the membrane-water interface region, govern the interactions and lateral distribution of these lipids in bilayer membranes. With the emphasis on ceramide/sphingomyelin(SM)-interactions, the relevance of the size of the SM-head group for the interaction was also studied. Ceramides with methyl-branched *N*-linked acyl chains, varying length sphingoid bases, or methylated 2*N* (amide-nitrogen) and 3*O* ($C_3$-hydroxyl) at the interface region, as well as SMs with decreased head group size, were synthesized and their bilayer properties studied by calorimetric and fluorescence spectroscopic techniques. In brief, the results showed that the packing of the ceramide acyl chains was more sensitive to methyl-branching in the mid part than in the distal end of the *N*-linked chain, and that disrupting the interfacial structure at the amide-nitrogen, as opposed to the $C_3$-hydroxyl, had greater effect on the interlipid interactions of ceramides. Interestingly, it appeared that the bilayer properties of ceramides could be more sensitive to small alterations in the length of the long-chain base than what was previously reported for the *N*-linked acyl chain. Furthermore, the data indicated that the SM-head group does not strongly influence the interactions between SMs and ceramides.

The results in this thesis illustrate the pivotal role of some essential parts of the ceramide molecules in determining their bilayer properties. The thesis provides increased understanding of the molecular aspects of ceramides that possibly affect their functions in biological membranes, and could relate to distinct effects on cell physiology.

## ABBREVIATIONS

| | |
|---|---|
| 10MeCer | N-10-methyl-hexadecanoyl-ceramide |
| 15MeCer | N-15-methyl-heptadecanoyl-ceramide |
| 16MeCer | N-16-methyl-heptadecanoyl-ceramide |
| 12:1-PCer | (hexadecanoyl)-dodecasphing-4-enine |
| 14:1-PCer | (hexadecanoyl)-tetradecasphing-4-enine |
| 16:1-PCer | (hexadecanoyl)-hexadecasphing-4-enine |
| 20:1-PCer | (hexadecanoyl)-icosasphing-4-enine |
| 7SLPC | 1-palmitoyl-2-(7-doxyl)stearoyl-*sn*-glycero-3-phosphocholine |
| BA | benzyl alcohol |
| Cer-1-P | ceramide-1-phosphate |
| CPE | N-palmitoyl-ceramide-phosphoethanolamine |
| CPEMe | N-palmitoyl-ceramide-phosphoethanolamine-N-methyl |
| $CPEMe_2$ | N-palmitoyl-ceramide-phosphoethanolamine-N,N-dimethyl |
| CTL | cholesta-5,7,9(11)-trien-3-β-ol, cholestatrienol |
| DOPC | 1,2-dioleoyl-*sn*-glycero-3-phosphocholine |
| DPG | dipalmitoylglycerol |
| DPH | 1,6-diphenyl-1,3,5-hexatriene |
| DPPC | 1,2-dipalmitoyl-*sn*-glycero-3-phosphocholine |
| DPPE | 1,2-dipalmitoyl-*sn*-glycero-3-phosphoethanolamine |
| DPPEMe | 1,2-dipalmitoyl-phosphoethanolamine-methyl |
| $DPPEMe_2$ | 1,2-dipalmitoyl-phosphoethanolamine-dimethyl |
| DSC | differential scanning calorimetry |
| $K_x$ | molar fraction partition coefficient |
| mβCD | methyl-β-cyclodextrin |
| NMeCer | 2N(methyl)-palmitoyl-D-*erythro*-ceramide |
| NMeOMeCer | 2N(methyl)-3O(methyl)-palmitoyl-D-*erythro*-ceramide |
| OMeCer | 3O(methyl)-N-palmitoyl-ceramide |
| PC | phosphatidylcholine |
| PCer (18:1-PCer) | D-*erythro*-N-palmitoyl-ceramide |
| PGalCer | D-*erythro*-N-palmitoyl-galactosylceramide |
| PhytCer | N-3,7,11,15-methyl-hexadecanoyl-ceramide |
| POPC | 1-palmitoyl-2-oleoyl-*sn*-glycero-3-phosphocholine |
| PSM | D-*erythro*-N-palmitoyl-sphingomyelin |
| SM | sphingomyelin |
| $T_m$ | gel-to-liquid crystalline phase transition temperature |
| tPA | *trans*-parinaric acid |
| tPA-Cer | N-*trans*-parinaroyl-D-erythro-sphingosine |

# 1. INTRODUCTION

Lipid bilayer membranes evolved with the need of an insulator structure that enabled concentrating the molecules of life so as to form cells, the basic building blocks of all organisms. Along with evolution, the cellular plasma membranes developed into macromolecular structures that comprise the lipid bilayer, the membrane proteins embedded within or attached to the bilayer, the cytoskeleton that connects the bilayer to the interior structures of the cell, and the glycocalyx at the external side of the bilayer serving as a site for cell-cell recognition and interactions (1).

The lipid bilayer part of the cell membrane was originally considered as a rather static structure that supported the more dynamic and functional components of the membrane: the peripheral and integral membrane proteins, which serve as activators of cellular signaling cascades and as sites for the release of second messengers into such cascades. Today, cellular membranes are acknowledged as organized assemblies of the different membrane components, with a considerable degree of dynamic heterogeneity both in time and space.

Membrane lipids are known to have direct functional roles in cellular activities as they can serve as "lipid second messengers", or as sources for the release of such signaling molecules (2, 3). Furthermore, membrane biophysical properties can influence the state and function of membrane proteins. The same applies also inversely, in that the properties of membrane proteins can influence the conformation of membrane lipids and the ordering of the lipid bilayer. Thus, the physical state of the lipid bilayer is proposed to participate in determination of the cell's physiological state (4-6).

Ceramides, the simplest of all two-chained sphingolipids, have been found to fulfill the requirements for classification as lipid second messengers (7). Their concentration rises as a result of certain extracellular ligands binding to cell membrane receptors, and the enzymes that are involved in the regulation of ceramide levels have been identified along with the specific targets for the up-regulated ceramides. Furthermore, the cellular events that are influenced by the generation of ceramides have been specified, with the induction of the same events by exogenous administration of the lipid or its analog (7).

In addition to directly influencing the proteins and enzymes of transmembrane signaling pathways, another way of participating in cellular regulation proposed for ceramides are ceramide-enriched microdomains that

influence the biophysical properties of the cell membrane. As will become evident at a later stage in this thesis, ceramides are able to influence the biophysical properties of membranes even at rather low concentrations. Such effects originate from the inherent propensity of ceramides to segregate into ceramide-rich, higly ordered domains, as well as from their influence on the lateral distribution and order of other membrane lipids.

Ceramide-rich domains have been suggested to take part in cellular signal transmission by serving a biophysical mechanism of function in signaling processes (8, 9). The ceramide-rich domains are proposed to organize and facilitate signaling processes by amplifying receptor- and stress-mediated signaling events, a process in which the coalescence of ceramide microdomains into larger ceramide-platforms is thought to play an important role (10-12). Although ceramide-mediated receptor clustering has been observed in the plasma membranes of cells (13-15) it is not yet completely understood how these signaling platforms transfer specific signaling information. The roles of ceramides in these processes seem to be multiple, but a universal role of the ceramide-rich platforms in organizing the cellular signalosome allows them to have diverse functions in distinct receptor systems, revealing a multitude of putative biomedical targets.

Understanding how the molecular properties of ceramides relate to the properties of ceramide-rich domains, and their formation, could aid in understanding the functional implications of such domains in biological membranes. The work in this thesis was performed in order to understand, in a qualitative manner, how the molecular structural details determine the interactions and lateral distribution of ceramides in bilayer membranes, including the formation of ceramide-rich domains.

In the following chapters, the reader is introduced to the main structural lipid classes with the emphasis on SMs and ceramides, and the role of ceramides as bioactive lipids. The general concept of formation of lipid bilayers is overviewed, followed by a brief review on the lamellar bilayer phases, phase transitions and lipid-lipid interactions in membranes. The use of model membranes as experimental tools is outlined, as well as the use of fluorescent probes in the study of bilayer membranes. Membrane properties of SMs and ceramides are outlined with particular attention paid on the major effects of ceramides on bilayer membranes. The review of the literature is followed by formulation of the main aims of the thesis, and a short

introduction to the methodology that was applied. The main results are outlined, followed by a discussion about their implications relative to other reported studies. Also the biological significance of the results is discussed, and finally, the thesis is closed by a concise summary of the most important findings.

# 2. REVIEW OF THE LITERATURE

## 2.1. Overview of membrane lipids

The amphiphilic nature of membrane lipids is manifested by their hydrophilic, water-soluble head groups, which are linked to the hydrophobic fatty acyl chains. Membrane lipids are conveniently divided into three main groups according to their structure: the glycerophospholipids, the sphingolipids, and the sterols. Fatty acids that consist of a polar carboxylic acid coupled to a long, aliphatic hydrocarbon chain, constitute the acyl chain moieties of more complex lipids. In such lipids, two acyl chains become linked to a glycerol moiety, or a single chain to a sphingoid base, giving rise to glycerophospholipids and sphingolipids, respectively.

### 2.1.1. The main structural lipid classes

Glycerophospholipids comprise two acyl chains ester-linked to the *sn*-1 and *sn*-2 positions, and a head group linked to the *sn*-3 position of glycerol, according to the conventional stereochemical numbering of the glycerol carbons. Also common in natural membranes are phospholipids which contain ether-linked long-chain alkyl moieties, usually at the *sn*-1 position. The major classes of glycerophospholipids in biological membranes cover the phosphatidylcholines (PCs) and phosphatidylethanolamines (PEs, both having zwitterionic head groups), the phosphatidylinositols, phosphatidylglycerols and phosphatidylserines, and the cardiolipins with a negatively charged head group.

The most abundant class of glycerophospholipids are the PCs, which account for more than 50 % of the phospholipids in eukaryotic membranes (16). The acyl chains of natural PCs are often nearly equal in length, varying mainly between 16-20 carbon atoms, with the *sn*-1 chain usually being saturated while the *sn*-2 chain is mono- or polyunsaturated with 1-6 *cis*-double bonds (17, 18). Palmitoyl-oleoyl-PC (POPC, 16:0-18:1$^{\Delta 9c}$) is one of the major components in natural membranes, and was used as the bulk lipid in most of the multicomponent bilayers that were studied in this thesis.

In sphingolipids a fatty acyl chain is amide(*N*)-linked to an aliphatic amino alcohol, the sphingoid base, which is either sphinganine or one of its derivatives (19). The sphingolipids are further structurally classified based on their head group. Ceramides are the simplest two-chained sphingolipids with no additional head group attached to the proximal hydroxyl group of the sphingoid base. The 16:0-fatty acyl species based on the sphingosine (18:1$^{\Delta 4t}$) structure, i.e., palmitoylceramide (PCer, Fig. 1A), was used as the parent ceramide in the

studies described in this thesis. Phosphosphingolipids have a phosphate-containing head group such as phosphocholine (Fig. 1B) or phosphoethanolamine attached to the proximal carbon of the sphingoid base, while glycosphingolipids contain one or several carbohydrate moieties glycosidically linked to the ceramide molecule. The most abundant phosphosphingolipids are the SMs with a phosphocholine-head.

The fatty acyl chains of natural SMs are typically longer and more saturated than the acyl chains in PCs (17, 18, 20). The 16:0-fatty acyl species based on the sphingosine structure, i.e., palmitoylsphingomyelin (PSM, Fig. 1B), was the parent SM used in this thesis. Being the most relevant lipids in this thesis, ceramides and SMs are introduced in greater detail with respect to their biosynthesis and structure in the following section, as well as with respect to their membrane properties in later sections (*sections 2.6. and 2.7.*). The simplest glycosphingolipids are the monoglycosylated glucosylceramides and galactosylceramides (GalCer), of which the former often serves as a precursor for more complex oligoglycosylated sphingolipids that may have more than 20 sugar residues in their head groups (21). Some glycosphingolipids are hydroxylated at the $C_2$ of the fatty acyl chain (22).

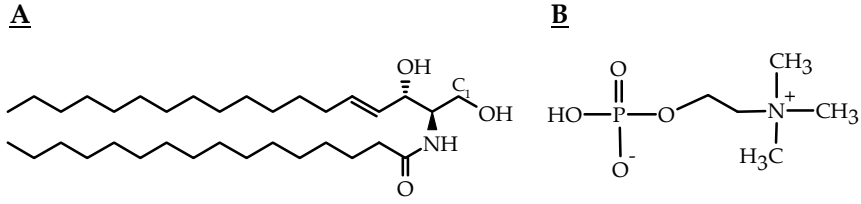


***Figure 1.*** *Molecular structures of A) PCer (also often referred to as C16-cer), and B) the phosphocholine head group of SMs. In PSM (also known as C16-SM) the head group is linked via its hydroxyl group to the $C_1$ of the sphingosine long-chain base.*

The sterols are based on the steroid backbone (23), a fused 4-ring structure, to which are attached a hydroxyl group (at $C_3$) and an aliphatic chain (at $C_{17}$, for the sterol structure see figure 6). Compared to the other main lipid classes, the sterols are more limited in structural variation. The most abundant sterol in mammalian membranes is cholesterol, which was the sterol used in the studies of this thesis. Cholesterol consists of an iso-octyl chain attached to the rigid ring structure which is in an all-*trans* configuration making the molecule flat (1). The iso-octyl chain, as well as the hydroxyl group and the methyl groups attached to

the steroid body are all β-oriented. This stereochemistry results in sidedness, making the β side of cholesterol more bulky than the smoother α side (24).

## 2.2. Ceramides and sphingomyelins

Sphingolipids are found in all eukaryotic cells with thousands of different species identified today. The abundance of sphingolipids varies between distinct cellular compartments, the SMs in the plasma membrane being most abundant and making up for some 20 to 25 % of the mammalian phospholipids (16). Ceramides, again, have an important role in formation of the permability barrier in mammalian skin tissue (25, 26), but exist at significantly lower amounts in the cellular membranes. After their synthesis, ceramides become rapidly converted into higher sphingolipids in a synthetic route described in the following section.

### 2.2.1. Generation and turnover of ceramides and SMs

The cellular *de novo*-biosynthesis of sphingolipids (reviewed in (27, 28)) is initiated in the cytosolic leaflet of the endoplasmic reticulum (ER), where palmitoyl-CoA condenses with L-serine to form 3-ketosphinganine in a reaction catalyzed by serine palmitoyltransferase ((29), Fig. 2). The 3-ketosphinganine is then reduced to sphinganine by 3-ketodihydrosphingosine reductase (30), and further *N*-acylated by a family of ceramide synthases to yield dihydroceramide (31). Ceramides with a sphingosine long-chain base are formed when the sphinganine long-chain base in dihydroceramides becomes desaturated by dihydroceramide Δ4-desaturase to yield the $C_{4\text{-}5}$ *trans*-double bond of sphingosine (32). Phytoceramides, again, are generated when the long-chain base in dihydroceramides becomes 4-hydroxylated by dihydroceramide C4-hydroxylase to yield an additional hydroxyl group at the $C_4$ (33). All natural sphingoid bases adopt the D-erythro conformation at their chiral carbons $C_2$ and $C_3$.

Ceramides are very hydrophobic in nature, having very low solubility in aqueous environments. Therefore, ceramides need to be transported from the membranes of the ER to the Golgi, the site where they become converted to higher sphingolipids. To mobilize ceramides from the ER cells use two mechanisms, vesicular transport (34) and the ceramide transfer protein CERT (35). CERT mainly transports sphingosine-based ceramides with *N*-acyl chains less than 22 carbons, but is also able to recognize and transport both dihydro- and phytoceramides (36), as well as other than C22-chain length species (36, 37), though less effectively. In the Golgi, SMs are formed from ceramides primarily transported by CERT (38).

SM-synthesis is catalyzed by SM synthases 1 and 2 which transfer phosphocholine groups from PCs to ceramides (Fig. 2). After their synthesis, SMs become sorted together with other lipids and proteins into vesicles which are transported to the plasma membrane where they fuse and release their content (39). Since SMs are transported in the inner leaflet of the vesicles, they will become constituents of the exoplasmic leaflet of the plasma membrane after vesicle fusion. A gradient in the SM content has been observed, with its abundance increasing along the secretory pathway from Golgi to the plasma membrane (40-43). SM synthase 2 is also localized at the plasma membrane where it participates in maintaining the plasma membrane SM levels (44).

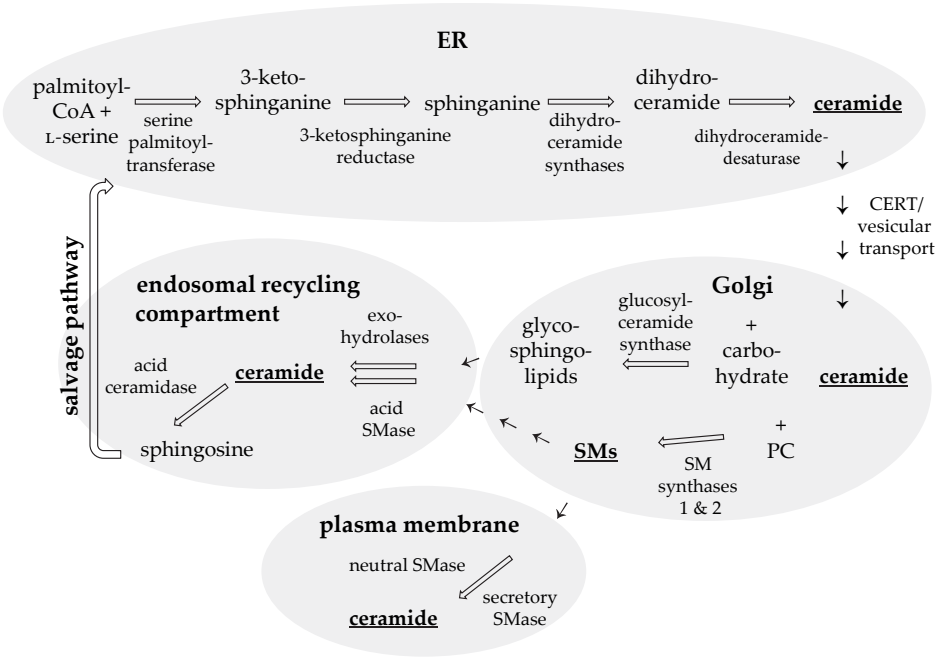


***Figure 2.*** *A simplified presentation of the generation and turnover of ceramides and SMs within distinct cellular locations. ER, endoplasmic reticulum; CERT, ceramide transfer protein; PC, phosphatidylcholine.*

The non-lysosomal turnover of SMs in the plasma membrane occurs by the actions of neutral SMase (45) and secretory (secreted acid) SMase (44) which produce locally elevated levels of ceramides. These ceramides are degraded by neutral ceramidase (46), which together with SM synthase 2 is an important regulator of ceramide metabolism in the plasma membrane. In the lysosomal

turnover of sphingolipids ceramides are regenerated from the brekdown of complex sphingolipids in the endosomal recycling compartment ((28, 47), Fig. 2). This so called "salvage pathway" is estimated to contribute from 50-90 % of the biosynthesis of sphingolipids (48, 49). The salvage pathway generates ceramides as a result of stepwise release of monosaccharide units from glycosphingolipids by exohydrolases, and by the action of acid SMase. The ceramides are further hydrolyzed by acid ceramidase to free fatty acid and sphingosine, which are released from the lysosome and either reutilized in the ER or phosphorylated to sphingosine-1-phosphate. The sphingosine-1-phosphates are further degraded by lyase activity.

The generation of ceramides by the action of SMases occurs within minutes, while the biosynthetic route generates ceramides within hours. Genetic disorders that cause dysfunctions in the fine balance between sphingolipid synthesis and degradation, with resultant accumulation of certain sphingolipid species, are related to specific medical conditions such as sphingolipidoses (50) and neuropathies (51), reflecting the importance of proper regulation of sphingolipid levels in cells.

### 2.2.2. Structural variation within ceramides and SMs

The terms "ceramides" and "SMs" virtually encounter a chemically heterogeneous group comprised of a large number of structurally closely related molecules with different tissue expression profiles and, perhaps, distinct biological functions that relate to differences in their acyl chain compositions. The sphingolipid acyl chains show variation in length and degree of unsaturation, as well as in the hydroxylation and methylation status of the chains. Some of the common structural variations observed in natural ceramides and SMs are listed below.

#### *2.2.2.1. The N-acyl chain*

In mammals, six distinct ceramide synthases (CerS1-6) with overlapping acyl-CoA preferences produce ceramides with varying *N*-acyl chain lengths (52). CerS1 mainly produces C18-ceramides (53), CerS2 produces very long-chain ceramides (C20-26) (54), and CerS5 and CerS6 predominantly produce C16-ceramides (55, 56). CerS3 prefers both middle and long-chain acyl-CoA:s (57, 58). The existence of six different CerS:s could relate to their distinct tissue expression, which was shown to correlate with the acyl chain composition of the sphingolipids in the specific tissues (54). The *N*-acyl chains of ceramides are generally saturated and may vary in length between 14 to 26, or even up to 36

carbon atoms as in skin ceramides (59-61). SMs typically contain C16-26 *N*-acyl chains (17, 18, 20), but in mammalian testes polyunsaturated very long-chain (C34) *N*-acyl chains have been found, some of which are 2-hydroxylated (62).

The most abundant unsaturated *N*-acyl chain species within ceramides and SMs are the C24:1 and C18:1 (59, 63-65). In addition, from 10-30 % up to more than 50 % of the *N*-acyl chains of some sphingolipids in certain tissues are either α- or ω-hydroxylated (59, 63, 64). Some natural ceramides contain relatively high amounts of methyl branches, which are generally located in the long-chain base, but also methyl-branched *N*-acyl chains have been found. Roughly one third of the ceramide aminoethylphosphonates of a sea anemone species were found to contain iso- and anteiso-methyl branches in acyl chains of varying length (66). Also other aquatic microorganisms (67) and invertebrates (68) possess ceramides with methyl-branched acyl chains, and they are even found in mammalian ceramides (64, 69-71). Characteristic for the methyl-branched ceramides is that they generally also contain additional hydroxyl groups, or exhibit polymethylation.

*2.2.2.2. The long-chain base*

The most common sphingoid base is sphingosine, except for in the human lens tissue, where sphinganine counts for more than half of the sphingoid bases (72). Ceramides with a phytosphingosine backbone are prevalent among fungi and plants, and in mammalians they are present in high abundance in the intestines, kidneys and skin (33, 73). Plant sphingoid bases can also contain two double bonds ($C_{4\text{-}5}$ and $C_{8\text{-}9}$) as well as methyl branches. Furthermore, some brain sphingolipids contain additional hydroxyl groups at $C_3$ or $C_6$.

While the *N*-acyl chain composition of ceramides is controlled by a repertoire of ceramide synthases, the length of the sphingoid bases is controlled in the initial step of the *de novo* synthetic pathway by the high selectivity of the serine palmitoyltransferases for fatty acyl-CoA:s with 16 ± 1 carbon atoms (74-77). This accounts for the prevalence of C18-sphingoid bases (16 carbons derived from the fatty acyl-CoA and two from serine). However, in some animal tissues other chain lengths for the sphingoid bases predominate. For example, in human skin ceramides the sphingoid base length can vary between 12 to 28 carbons (61, 78). Substantial amounts of C20-sphingoid bases have been found in mammalian gangliosides (79, 80), as well as in equine kidney sphingolipids (63). Relatively high amounts of shorter than C18-sphingoid bases are commonly found in bovine sphingolipids (72, 81, 82). Moreover, the primary sphingoid bases in insect sphingolipids are 14 or 16 carbon atoms long (83, 84).

The terms "ceramides" and "SMs" in general cover all the structural species, including those described and discussed above. It is important to note that in this thesis, these terms are primarily used to refer to the structural species that display a characteristic bilayer behavior of ceramides and SMs composed of a sphingosine backbone coupled to a saturated, unbranched, long *N*-acyl chain. Other than these structural species are separately defined when referred to.

### 2.2.3. Ceramide - a bioactive lipid

The cellular levels of free ceramides remain low under normal conditions, at a few per centages of the total lipid. However, different pro-apoptotic receptor molecules and stress stimuli, as well as developmental stages and viral infections induce significant increases in ceramide levels by the activation of acid SMase (reviewed in (85, 86)), and several lines of evidence now point to a role for endogenous ceramides in cellular activities and signaling cascades (reviewed in (86-89)). One of the most studied is the role of ceramides in initiation of apoptosis, as heat and radiation that induce apoptosis were found to cause increased ceramide levels in cells (88, 90). The C16-cer was identified as the probable mediator of death signals, while the levels of other species increased only slightly (91).

The target signaling proteins shown to be regulated by ceramides include protein kinase Cζ, kinase suppressor of Ras, a ceramide-activated protein phosphatase, and cathepsin D, to name a few (see (85, 92) for a review). Ceramides are also important in cancer biology, as they are able to suppress the growth and survival of lung-cancer derived cells (93) and fibrosarcoma tumor cells (94) by promoting or triggering apoptosis. Such findings, together with the observation of increased levels of ceramides in breast cancer tissue (95), rendered ceramides, and other sphingolipids, potential new targets in cancer therapy (96, 97).

In addition to ceramide *per se*, ceramide-1-phosphate (cer-1-P), sphingosine, and sphingosine-1-phosphate, which are all putative products in the turnover of sphingolipids, have important biological functions (98, 99). Some of the biological activities of ceramides are largerly dependent on the molecular species of the sphingoid backbone, reflecting the specificity of ceramide actions in cells. Large differences in the biological effects between ceramides (sphingosine-based) and dihydroceramides have been observed (100-103). As an example, while sphingosine-based ceramides induce apoptosis in cells, dihydroceramides are inactive (102).

Ceramides are very hydrophobic even compared to other membrane lipids, and thus exhibit very low solubility in aqueous media such as the cellular cytosol. Ceramides are therefore excpected to exert their effects on the level of membranes. Ceramides could either participate in signaling processes by directly binding and activating membrane associated proteins, or by inducing changes in the biophysical properties of cell membranes with concomitant reorganization of target proteins (7-9). The two ways of regulating cellular target proteins probably do not exclude one another, but act in unison depending on the specific pathway that is activated. Several examples of direct effects of ceramides on cellular signaling cascades exist (7). Some of these effects are mediated via organizational changes induced by ceramides in the cellular membranes, rather than direct binding of ceramides to target proteins, and this alternative mechanism of function is gaining increasing interest.

Different mechanisms for SMase activation and ceramide generation in the plasma membranes of cells have been proposed. Based on transmission electron microscopy data, it was proposed that upon stimulation intracellular vesicles that contain acid SMase fuse with the cellular plasma membrane and release the enzyme to the extracellular leaflet, where majority of the cellular SM is located (13). Another study proposed a mechanism for SMase-induced ceramide generation as a result of an apoptotic stimulus that induces membrane phospholipid scrambling, causing loss of asymmetry between the exoplasmic and cytoplasmic leaflets of the plasma membrane, rendering SM a target for hydrolysis by a neutral cytosolic SMase (104). The secreted form of SMase, which arises from the same gene as the lysosomal form and thus shares a common protein precursor with the acid SMase, has also been speculated a role in the hydrolysis of the cell surface pool of SMs (105). Secretory SMase is up-regulated and secreted by cells under inflammatory and infectious conditions (106-108), followed by a concomitant elevation in ceramide levels, presumably originating from SM-hydrolysis in the exoplasmic leaflet of the cellular plasma membrane (108).

Ceramide released from plasma membrane SM appears to transform small membrane domains into large platforms that cluster signaling proteins (13-15). Similar clustering of activated receptors is induced by the exposure of cells to exogenous ceramide (14). Receptor clustering is suggested to enhance the interactions of the receptors with other signaling molecules, enzymes, and ligands, as well as to separate them from inhibitory molecules (10-12, 85). As an example, Chiantia and coworkers demonstrated in a model membrane system that the GPI(glycosylphosphatidylinositol)-anchored protein placental alkaline

phosphatase becomes enriched in membrane domains formed by ceramides, in which it exhibits reduced lateral diffusion (109), a feature that could facilitate protein clustering and subsequent interactions with other signaling molecules. In addition to the plasma membrane, ceramides can also influence the topology of other cellular membranes, serving different functions in distinct locations (110). Furthermore, generation of ceramide can have different consequences depending on the cell type (8, 111).

The underlying biophysical properties of ceramides that account for the formation of ceramide-rich membrane domains, as well as the biophysical properties of such domains are discussed in a later section (*section 2.7.*). Before that, the underlying mechanism of how lipids assemble to form membranes, as well as the forces and interactions between lipid molecules in membranes are overviewed, followed by a brief description of the structure of biological membranes.

## 2.3. The hydrophobic effect and lipid phases

The hydrophobic effect is the major thermodynamic driving force that stabilizes lipid aggregates in aqueous solutions (112, 113). When lipids are dispersed in water they disrupt the pattern of the hydrogen bond network formed by water molecules. Subsequently, water molecules become immobilised around lipids, and the lipids try to organize the water molecules. Such an organizing effect leads to a decrease in the entropy of the system, resulting in entropic cost. The entropic cost is reduced, and the hydrogen bond network maintained, by water and the lipids separating into two phases, minimizing the contact between water and the non-polar parts of the lipids (112, 113).

The assembly of lipid-rich phases in lipid-water dispersions depends on the molecular structure, and thus, the geometrical shape of the specific lipid species. The main lipid assemblies recoqnized are the non-lamellar micellar, hexagonal and inverted hexagonal phases, as well as the lamellar bilayers (1) which are the most relevant both biologically and for this thesis. A simplified presentation of the geometrical shapes of lipids, and their consequences, are depicted in figure 3. Lipids that have a cylindrical shape, such as SMs and PCs, self-assemble to lamellar bilayers when dispersed in aqueous solutions (Fig. 3A).

The packing parameter (the lipid hydrophobic volume divided by the product of the cross-sectional area of the head group and the acyl chain length) is a simple geometrical parameter used to asses the self-association of lipids in water dispersions (18, 114). The packing parameter of cylindrical lipids that spontaneously form bilayers is close to one. The effective lipid molecular shape

gives some lipids an intrinsic curvature, which can serve as a quantitative measure of the tendency of such lipids to form curved (non-lamellar) structures. Cone-shaped lipids such as lysophospholipids with a single acyl chain have a large head group in relation to the hydrophobic volume. For such lipids the packing parameter is less than one, and they are thus prone to form micellar structures (115) and induce positive membrane curvature in bilayers ((116), Fig. 3B). If, again, the head group is relatively small, and the packing parameter exceeds one, hexagonal phases are formed as evidenced by ceramides (117), which together with similar lipids induce negative curvature in bilayer membranes ((116), Fig. 3C). In addition to the lamellar and non-lamellar phases discussed above, complex cubic phases can form under certain circumstances (118).

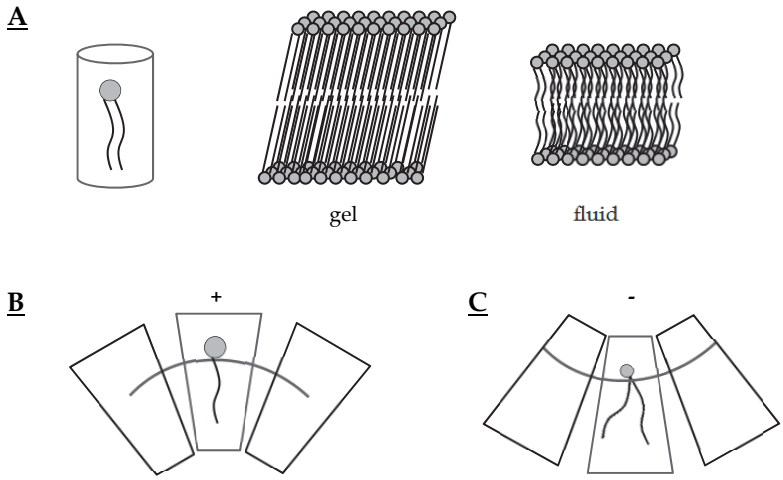


***Figure 3.*** *Simplified presentation of the geometrical shapes of membrane lipids and the gel and fluid phases of lamellar bilayers. A) Cylindrical lipids spontaneously form lamellar bilayers that display thermotropic gel-to-fluid phase transitions distinguished by in-plane structural reorganizations. B) Conical lipids induce positive membrane curvature in bilayers, while C) inverted-cone shaped lipids induce negative membrane curvature.*

The apparent polymorphism of lipids, i.e., their ability to adopt many shapes and phases, is a key feature in the shaping of biological membranes (119). As lipids assemble to higher structures such as bilayers, they will try to avoid "edges" and bend to closed structures, which causes the membrane to curve. In a biological context, locally produced curvature effects, driven by the interplay between intrinsically curved lipids and certain membrane proteins, play a major

role in enabling e.g., cellular vesicle trafficking (120). Within the lamellar bilayer phase, lipids can undergo thermotropic phase transitions with major, in-plane structural reorganizations (Fig. 3A). Such phase transitions are overviewed in the following section.

2.3.1. Lamellar bilayer phases and phase transitions

Lipid composition and structure, together with external factors that determine the physical properties of the system, influence the phase state of a lipid bilayer, and changes in the pysical properties cause transitions between the different phases. Figure 3A presents the two distinct lamellar phases that exist in bilayers below and above the main phase transition temperature ($T_m$) of a given lipid species. In general, at low temperatures the bilayer exists in a gel phase, or in a "solid-ordered" phase which is characterized by a hexagonal arrangement of the lipid head groups and extended acyl chains which adopt an all-*trans*-conformation and a tilt relative to the bilayer normal (1, 113, 121). When the temperature increases, the densely packed acyl chains become more fluid and the lipids eventually go through the gel-to-fluid (gel-to-liquid-crystalline) phase transition.

In the fluid, or "liquid-disordered" phase the lipids experience increased molecular motion and the acyl chains become untilted (1, 113, 121). The interface between the hydrophobic acyl chain region and the polar head group region becomes increasingly hydrated by the surrounding water molecules. There is also a higher incidence of *gauche* conformations in the lipid acyl chains in the fluid phase compared to the gel phase, which results in increased cross-sectional area for the individual lipid molecules. Subsequently, the bilayer expands laterally while the thickness of the bilayer decreases (1, 113).

Most of the natural unsaturated PCs display very low $T_m$:s (below 0°C (122)), while the $T_m$:s of natural SMs are considerably higher (in the range of 40-50°C) due to higher degree of saturation allowing for higher degree of interactions between the acyl chains, as well as due to the higher incidence of hydrogen bonds amongst SMs. In mixtures that contain cholesterol a "liquid-ordered" phase is further identified (123-126), with lower lateral diffusion to that observed in the fluid phase, yet significantly faster than in the gel phase (127, 128). In the liquid-ordered phase, the phospholipid acyl chain carbons that interact with cholesterol adopt an all *trans*-conformation increasing the order compared to the liquid-disordered phase.

Ceramides serve as an example of lipids for which hydration strongly influences the thermotropic properties. PCer exhibits polymorphic phase

behavior with strong hysteresis, displaying a single endothermic transition at ~95°C for the anhydrous form, while in the hydrated form it displays an exothermic transition from a metastable to a stable gel phase followed by a main endothermic transition to the melted state at 90°C (129).

In addition to the external physical factors, and the properties of the individual lipids, the phase behavior of complex lipid mixtures is determined by the interactions between the constituent lipids. The miscibility, or immiscibility, of the lipids in complex mixtures is a major determinant of the lateral organization of mixed-component bilayers, and can give rise to phase coexistence. Lipid-lipid interactions are the subject of the following section, while the lateral organization and phase coexistence in bilayer membranes are overviewed in *section 2.5.1.*.

### 2.3.2. Fundamental lipid-lipid interactions in membranes

The lipid-lipid interactions in bilayer membranes are governed by the chemical and physical properties of the individual lipid molecules (112). These interactions are non-covalent in nature, and consist of several different electrostatic interactions. These include ionic and van der Waals' interactions, as well as charge pairs and hydrogen bonds. The main interactions among lipid head groups and the membrane-water interface are charge pairs between electronegative and –positive carbons, ionic interactions manifested by charged head groups, as well as the considerably weaker hydrogen bonds which are more dependent on proper direction and distance (112).

Charge pairing has been observed between the head groups in PC-membranes (130), as well as between the methyl groups of SM and the proximal hydroxyl group of cholesterol (131). Ionic interactions can have major influence on the phase transitions of lipids, as evidenced by the significant increase in $T_m$ of negatively charged phospholipids as they bind to cations (132). Hydrogen bonds again are an important stabilizing factor for the cohesive interlipid interactions of sphingolipids, as will be discussed later. The main interactions between the aliphatic hydrocarbon chains of lipids in the membrane hydrophobic core are the attractive van der Waals' interactions, especially the London dispersion forces between two induced dipoles. These forces are a result of electron fluctuations generating temporary dipoles to minimize electron-electron repulsion between the lipid hydrocarbon chains (112).

In addition to lipid-lipid interactions, lipid-protein interactions are of great importance in biological membranes, and can have major impact on the arrangement and function of both molecules in membranes (133, 134). The

structure and properties of biological membranes, with emphasis on the development of the view on lipid lateral organization, are briefly overviewed in the following section.

## 2.4. Structure and properties of biological membranes

The bilayer structure of cell membranes was first deduced from studies performed on Langmuir monolayers. In 1925 Gortel and Grendel proposed that a bilayer is formed by two layers of amphiphilic molecules with the head groups of the molecules facing the aqueous media at both sides of the bilayer (135). Since the initial description of the bilayer structure was confirmed, it has been refined several times. Membrane proteins were first suggested to adhere to the bilayer surface at both sides, until Singer and Nicholson introduced the fluid mosaic model for membranes in 1972, including the concept of peripheral and integral membrane proteins that diffuse in the bilayer plane (136). A decade later, the fluid mosaic model was followed by the proposal of Mouritsen and Bloom for similar hydrophobic thickness of membrane lipids and proteins serving as a sorting factor that induces lateral heterogeneity in the bilayer plane (137). This idea was further developed to the membrane raft hypothesis, which suggested a dynamic clustering of sphingolipids and cholesterol into distinct lateral microdomains that float freely in the fluid bilayer, having important roles in compartmentalization of cellular processes (40-42).

Biological membranes are dynamic, spatio-temporally regulated assemblies with essential structure and functions. Cellular membranes are proposed to be highly organized platforms, with constitutive roles in regulating transmembrane trafficking and the organization of processes and reactions that are initiated or occure in the membrane. While the cellular membranes in general remain in the fluid state, domains of liquid-ordered phase, formed by cholesterol and sphingolipids, have been proposed to exist (138, 139). In such domains, the saturated acyl chains of sphingolipids would be more tightly packed than the unsaturated chains of lipids enriched outside the domains, i.e., in the non-raft membrane (Fig. 4). The increased chain packing in the rafts is thought to result in increased molecular order and an increase in the thickness of the bilayer compared to the non-raft membrane.

Explicit evidence for the equalization of SM/cholesterol-rich liquid-ordered domains with biological membrane rafts is still awaited. However, there is an intricate interplay between the metabolism and intracellular distribution of cholesterol and SMs (140), and they become co-sorted for vesicular transport from Golgi to the plasma membrane (39). Moreover, nanoscopic sphingolipid

assemblies in which the diffusion of fluorescent sphingolipid-anchors is hindered in a sterol-dependent manner have been observed in the plasma membranes of living cells (141). The observations mentioned above, together with the proposed favored interaction of cholesterol with SM relative to PC (overviewed in *section 2.6.1.*), give support for the co-localization of SM and cholesterol in lateral membrane domains with properties distinct from the "bulk" membrane.

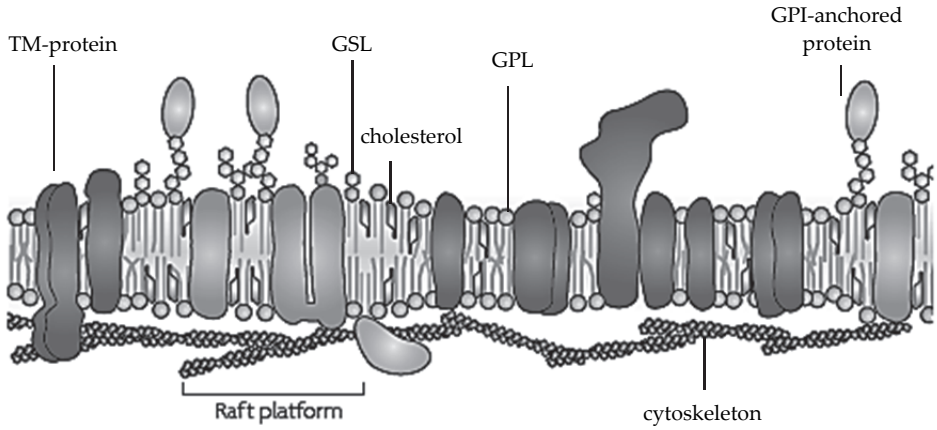


***Figure 4.*** *A schematic representation of the organization of biological membranes containing raft platforms. The raft platforms are enriched in certain trans-membrane(TM)-proteins, glycosylphosphatidylinositol(GPI)-anchored proteins, glyco-sphingolipids (GSL) and cholesterol. Glycerophospholipids (GPL) become enriched outside of the rafts together with various membrane proteins. The bilayer membrane is connected to the cytoskeleton at the cytosolic leaflet. The figure is adapted from (139) and reprinted with the permission from Nature Publishing Group.*

The raft hypothesis evoked a great deal of interest towards the lateral organization of membranes, in which lipid lateral segregation and interlipid interactions play major roles. Such properties are conveniently studied in artificial bilayer membranes (lipid vesicles) composed of natural lipids. Such membranes exhibit significantly lower level of compositional complexity compared to cell membranes. Artificial membranes and the use of fluorescent probes and fluorescently labeled lipids as tools to study lipid-lipid interactions and membrane lateral organization are overviewed in the following chapter.

## 2.5. Lipid vesicles and model membrane studies

Lipid vesicles were first described by Bangham and coworkers in early 1960's (142, 143), and they have been widely used as models for the cellular membranes

as they, by forming enclosed structures that encapsulate an aqueous solution, share fundamental similarity to the cell membrane (144, 145). Lipid vesicles can be prepared to have a distinct lateral and transbilayer structure with a dynamic nature, providing a model for the fluid bilayer component of cellular membranes. Vesicles for model membrane studies are initially prepared as large multilamellar vesicles. To reduce the size and lamellarity of these, sonication and extrusion are the most commonly used methods (146) and were also applied in the studies comprising this thesis.

The application time and intensity of the acoustic energy used to induce pressure waves that break up large vesicles in sonication prodecures influence the size of the resultant vesicles (147, 148), but in general sonication produces uni- or multilamellar vesicles with a mean diameter of 30 nm or less. In addition to the equipment energy and sonication time, also lipid composition and concentration, as well as temperature, can strongly influence the vesicle size distribution, and variation between samples produced at different times is common. A more reproducible way of regulating the size and lamellar construction of vesicles is extrusion through a defined pore size under pressure, which generates shearing forces (149, 150). Extrusion generally results into a vesicle size of up to 200 nm in diameter, with the mean size mainly influenced by lipid composition. The size, and subsequently the surface curvature of vesicles, are important matters to be considered as they can influence e.g., the rate of enzymatic reactions (151) and the lateral organization of bilayer lipids (152, 153). Further, vesicle size can influence lipid miscibility (154, 155) and the thermodynamic properties and asymmetry of membranes (156-158).

As illustrated in figure 5, which presents a molecular dynamic simulation of a dipalmitoyl-PC(DPPC)-bilayer, several regions can be distinguished in the bilayer structure of a fluid lipid (159). At the surface of the bilayer there is a region of perturbed water molecules that interact with the lipid head groups (the low head group region). Next to the surface is the interface between the hydrophilic and the hydrophobic compartments (the high head group region), followed by the region of ordered acyl chain conformations (the high tail density region). The hydrophobic core of the membrane (the low tail density region) is again more disordered with respect to the acyl chain conformations. Recently, a method for the selective labeling of the inner and outer leaflets of vesicles was developed, revealing curvature-induced differences between the packing of lipid head groups in the two leaflets (160).

It is clear that lipid-interactions in membranes are numerous and occur at different depths, gaining a further increase in complexity when bilayers are

formed by several, structurally distinct lipid species. The compositional simplicity of artificial membranes compared to biological membranes allows for more detailed and controlled studies with precisely defined mixtures of lipids, and is one of the main advantages of employing vesicles in the study of lipid-interactions and membrane lateral organization. However, the experimental use of lipid vesicles has some limitations important to keep in mind. First, it is impossible to completely control the lipid composition, both between vesicles in a given population, as well as between the two leaflets of a given bilayer, when multicomponent vesicles are generated by the conventional methods. In addition, as mentioned above, surface curvature, influenced by the vesicle size, as well as by the geometrical shape of the constituent lipids, can have major impact on the properties of the bilayers and thus, on the experimental results (151-158). To improve the resemblance between model bilayer membranes and actual cellular membranes, techniques allowing the formation of asymmetric vesicles, with distinct set of lipids in the outer and inner leaflets, respectively, have been developed (161, 162).

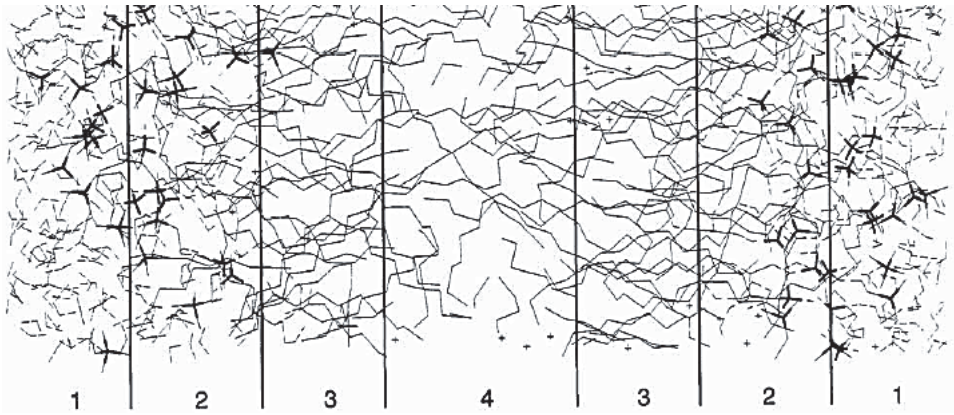


***Figure 5.*** *A snapshot of a simulated DPPC-bilayer. The dashed lines represent water molecules, the bold lines choline and phosphate groups, and the solid lines the acyl chains. The four different regions correspond to 1) low head group region, 2) high head group region, 3) high tail density region, and 4) low tail density region. The figure is adapted from (159) and reprinted with the permission from ACS Publications.*

2.5.1. Lateral organization and phase coexistence in membranes

To study the interactions and properties of lipids in membranes that mimic biological membranes, several components, usually an unsaturated

phospholipid, a saturated phospholipid and cholesterol, are mixed. In such mixtures, lipid miscibility varies depending on concentration and temperature, resulting in putative phase separation and the coexistence of fluid (liquid-disordered and liquid-ordered) and gel phases (163). The appearance of phase diagrams, and the information they contain about lipid lateral organization, vary depending on the method that is used to detect the phase separation. Several techniques, such as fluorescence spectroscopy (164, 165), fluorescence imaging (166), and nuclear magnetic resonance (NMR) (167) have been applied to compose ternary phase diagrams. Phase diagrams with ceramide as one of the components have also been established (168, 169), showing the coexistence of two distinct gel phases in a fluid membrane (169).

Three theoretical models to describe the organizing principle and phase separation in cholesterol-containing phospholipid membranes have been proposed. According to the umbrella model (170), lateral order in membranes is driven by lipid-interactions that tend to minimize the exposure of hydrophobic regions of cholesterol to water by large phospholipid head groups tilting over cholesterol. The condensed complex model, again, proposes that lateral phase separation results from temporal enrichement of reversible phospholipid-cholesterol complexes in the plane of the membrane (171). The superlattice model postulates that several locally formed regular assemblies of lipids in the plane of the membrane give rise to different phases that coexist (172).

### 2.5.2. Fluorescent probes in model membrane studies

Fluorescence spectroscopy is a widely used tool in the study of lipid-interactions and membrane lateral heterogeneity, and in general, the use of fluorescent probes or fluorescently labeled lipids relies on their preferential partitioning into either gel, ordered or fluid phases, or on the sensitivity of their spectral parameters to changes in the physical state of the surrounding micro-environment (173, 174). In addition to their lateral distribution in the plane of the membrane, the vertical location of the probes at distinct depths of a membrane allow them to report on changes occurring in the acyl chain region or in the membrane-water interface.

Two conventional membrane probes, also employed in this thesis (Fig. 6), are diphenylhexatrien (DPH) and *trans*-parinaric acid (tPA). DPH is located deep in the hydrophobic acyl chain region of bilayers, while the carboxyl group of tPA aligns between lipid head groups at the membrane interface with its tetraene chain extending between lipid acyl chains (174-176). DPH is generally considered to partition relatively equally between fluid and ordered phases (164,

177, 178) (save for the ceramide-rich gel phase (168, 179)), while tPA shows a clear preference for gel phases (168, 169, 179-181). More recently, probes in which the conjugated double bonds are an intrinsic part of a molecule that closely resembles the structure of a natural lipid have been developed and characterized. Fluorescently labeled lipid analogs relevant for this thesis are cholestatrienol (CTL), and *trans*-parinaroyl-ceramide (tPA-Cer, Fig. 6), which are used to probe the lateral membrane distribution of cholesterol (182) and long-chain, saturated ceramides, respectively (182, 183).

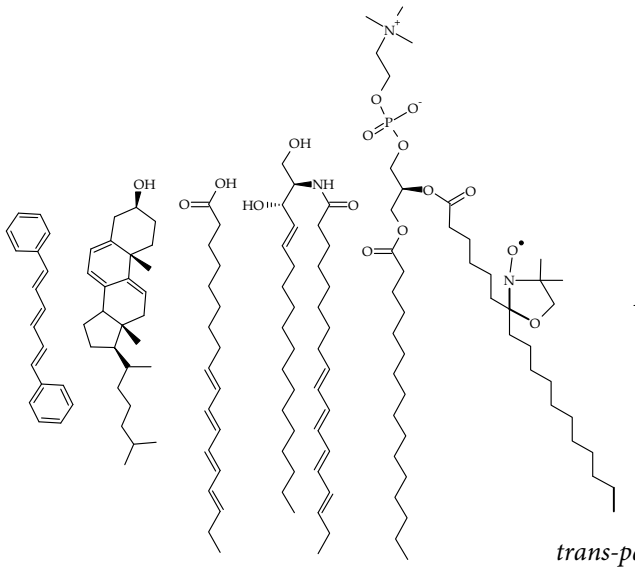

***Figure 6.*** *Molecular structures of the fluorescent probes and the quencher lipid used in this thesis (from left to right): diphenylhexatrien (DPH), cholestatrienol (CTL), trans-parinaric acid (tPA), trans-parinaroyl-ceramide (tPA-Cer), and the spin-labelled quencher lipid (7SLPC).*

Yet another lipid analog, though not fluorescent but relevant for this study, is the spin-labelled PC 7SLPC (Fig. 6). This glycerophospholipid, with a nitroxyl radical attached to $C_7$ of the *sn*-2-acyl chain, quenches fluorophores in a dynamic manner by causing a drop in their quantum yield when in close proximity to the probes (184). In bilayer membranes, the 7SLPC displays properties very similar to an unsaturated PC (184, 185). In this thesis, 7SLPC is employed to induce fluorescence quenching of CTL, tPA and tPA-Cer as a result of thermally induced melting of membrane lateral domains. Combination of fluorescent membrane probes with the state of the art techniques has been fundamental for the development of new methods to study and visualize membrane heterogeneities even in the plasma membranes of living cells (141).

## 2.6. Membrane properties of SMs

Although ceramides and SMs share the sphingoid backbone structure, their membrane properties are very different in nature, which is due to the apparent size difference between their head groups. While ceramides with their long, saturated chains and the small hydroxyl head structure are very hydrophobic and cannot form bilayers by themselves, SMs have a cylindrical molecular shape which allows them to spontaneously form bilayers in aqueous environments. Ceramides, on the other hand, tend to form hexagonal phases when present in high concentrations. Furthermore, despite of the structural similarities, ceramides and SMs interact differently with other membrane lipids such as cholesterol.

SMs and PCs share the identical phosphocholine head group (see Fig. 1B). However, there are some fundamental differences in the bilayer properties of SMs and PCs deriving from the differences in the structure of their membrane interface region, and the composition of their acyl chains. In general, the $T_m$ of SMs increases with increasing acyl chain length (186), whereas double bonds in the *N*-acyl chain lower the $T_m$ in a position-dependent manner due to reduced van der Waals' interactions (187). Likewise, methyl branches dramatically decrease the $T_m$ of SMs (188). Natural SMs often display higher $T_m$:s than natural PCs (122, 187) due to longer and more saturated acyl chains that allow for more intense van der Waals' interactions. Furthermore, possible *cis*-double bonds in the SM acyl chains are in general located further away from the interfacial region than in PCs (18). Double bonds located closer to the membrane hydrophobic core tend to disorder the acyl chain packing to a lesser degree than double bonds closer to the head group region (189).

Saturation of the *trans*-double bond in the sphingosine backbone of SMs increases the $T_m$ both for racemic (190) and enantiomerically pure species (191, 192), and induces more condensed molecular packing and acyl chain order, as well as increased bilayer order (191, 193, 194). Owing to the amide-linkage, the $C_3$-hydroxyl function, as well as the carbonyl oxygen linked to the amide, SMs can function as both hydrogen bond donors and acceptors, having more possibilities for hydrogen bond formation compared to PCs, which can only act as hydrogen bond acceptors through the oxygens in their ester-linkages (20, 195, 196). Hydrogen bonding could also contribute to the higher phase transition temperatures of natural SMs compared to natural PCs (195).

2.6.1. Phase coexistence and SM/cholesterol-interactions

When SMs are mixed with an unsaturated phospholipid they can phase separate and induce gel-fluid coexistence (164). In the presence of cholesterol the liquid-ordered phase is induced and becomes enriched in SM and cholesterol (163, 164). Numerous studies show a preferential affinity of cholesterol for SMs over other phospholipids (197-199), or indicate to a stronger interaction between SM and cholesterol relative to other phospholipids (200-205). Cholesterol has been observed to partition more favorably into bilayers that contain saturated SMs compared to bilayers that contain saturated PCs (206), and even at equal acyl chain order cholesterol shows higher affinity for SM-bilayers relative to PC-bilayers (207). However, evidence for the lack of a favored interaction between cholesterol and SM has also been presented ((208), and references therein).

Amongst other factors, the size of the SM-head group seems crucially important for SM/cholesterol-interactions in bilayers (209, 210). A systematic reduction in PSM head group size by stepwise removal of the methyl groups was shown to markedly change the molecular properties of PSM, with a noticeable decrease in the molecular area and increase in the acyl chain order, accompanied by an increase in the $T_m$. These changes, again, markedly influenced the formation of SM-sterol rich ordered domains, and decreased the overall affinity of sterol for the SM-containing bilayers (210).

## 2.7. Membrane properties of ceramides

Derived from crystal structures, infrared spectra and monolayer studies, Pascher deduced the molecular arrangement of ceramides. The rigid amide group with a planar resonance structure was found to be oriented perpendicularly towards the axes of the two hydrocarbon chains (211). Ceramides mainly interact through attractive van der Waals' forces between their extended, all-*trans* acyl chains, as well as through an extensive network of hydrogen bonds in their interfacial and head group region. Furthermore, the $C_{4\text{-}5}$ *trans*-double bond of the sphingosine base is an important structural factor that appears to promote close packing of the ceramide hydrocarbon chains (212). Saturation of this double bond (yielding dihydroceramide) was shown to induce a more expanded acyl chain conformation in monolayers (189).

The distribution of hydrogen bonds between adjacent ceramides or between ceramides and other membrane lipids is still largely unknown. However, intermolecular hydrogen bonding appears to significantly contribute to the self-condensation of natural ceramides (211). Shah and coworkers suggested, based

on differential scanning calorimetry (DSC) and X-ray diffraction data, that the sphingosine hydroxyls hydrogen bond to the amides of adjacent ceramides (129). However, a more recent molecular dynamics simulation-study suggested an interaction between the sphingosine hydroxyls and adjacent carbonyl oxygens (213). To explain the tight acyl chain packing displayed by ceramides, Li and coworkers introduced a model of an internally satisfied intramolecular hydrogen bond network that minimizes the steric repulsion between the ceramide acyl chains (214). Their model was further supported by a computational calculation of the potential and probable intra- and intermolecular hydrogen bonds formed by ceramides (215). A role for the sphingosine-double bond as a stabilizing component of the hydrogen bonds formed by ceramides has also been suggested (212, 214). Nonetheless, hydrogen bonds appear to have an important role in the interlipid interactions of ceramides.

### 2.7.1. Major effects of ceramides on membranes

Given the structure with long, conformationally ordered hydrocarbon chains and a small head structure, ceramides have a very hydrophobic nature and bind little water (216). The dense packing of ceramide acyl chains is reflected in the very high gel-to-fluid transition temperatures that pure ceramides display, with $T_m$:s of around 90°C or higher measured e.g., for C16-, C18-, and C20-cer (129, 217-219). Due to their biophysical properties, ceramides exhibit restricted miscibility with other lipids. Consequently, the influences of ceramides on membranes and membrane thermodynamics are profound, with three distinct but inter-connected effects observed, as outlined below.

#### *2.7.1.1. Ceramides increase the order of phospholipid acyl chains*

Using $^2$H-NMR spectroscopy, Huang and coworkers discovered that bovine brain ceramides enhanced the acyl chain order of saturated DPPC in the fluid state as a result of reduced *trans-gauche* isomerization of the phospholipid acyl chains (220). It was also shown that synthetic C6-, C8-, and C16-cer, but not C2-cer, were able to increase the order of DPPC acyl chains (221). Similar effects on the acyl chain order of saturated dimyristoyl-PC and DPPC bilayers by bovine brain ceramides were later observed using fluorescent probe techniques (222, 223). An enhanced acyl chain order was also shown in unsaturated POPC-bilayers as a result of incorporation of the acyl chain-defined C16-cer (224).

In accordance to the observed enhancement in phospholipid acyl chain order, an increase in the $T_m$ of dimyristoyl-PC by incorporation of C16-cer, as well as in the $T_m$ of PSM when mixed with long-chain ceramides, has been observed with

DSC (218, 225). Pinto and coworkers compared the effects of saturated versus unsaturated ceramides on POPC-bilayers, and reported that as saturated ceramides (C16, C18 and C24) increased the order of the POPC-bilayers and induced gel-fluid phase separation, the unsaturated ceramides displayed lower (C24:1) or no (C18:1) ability to induce formation of gel phases (226).

*2.7.1.2. Ceramides induce lateral microdomain formation*

Lateral segregation of ceramides into gel phase domains in a phospholipid-bilayer was first observed by Huang and coworkers who mixed DPPC with ceramides from a natural source (220). Using $^{2}$H-NMR they observed ceramide-rich microdomains in the DPPC-matrix both in gel and fluid phase membranes. The segregation of ceramides was later observed also in dimyristoyl-PC bilayers with a pyrene-labeled lipid probe, as well as with DSC (222, 227). Lateral segregation and subsequent formation of gel phase domains by ceramides was also observed in unsaturated POPC-matrix (168, 224, 228, 229). When Hsueh and coworkers studied mixtures of POPC and PCer with NMR, they observed coexistence of gel and liquid-crystalline phases over a wide range of temperatures and compositions (228). The presence of PCer was also observed to induce an ordering effect on the POPC-acyl chains, an effect also observed by Silva and coworkers (168), who reported the first complete phase diagram for the POPC/PCer-system. Characterization of the lamellar phases present in those bilayers revealed formation of ordered, rigid domains by the ceramides, with strong influence on the fluid POPC-matrix.

In addition to binary phospholipid-ceramide mixtures, the effects of ceramides have been studied in the presence of cholesterol. Ceramides were found to significantly stabilize domain formation by brain SM in the presence of cholesterol, an observation that suggested strong affinity of ceramides for sphingolipid/cholesterol-domains (230). Later, the effects of ceramides on more complex bilayers, that in general comprise of an unsaturated phospholipid, a saturated phospholipid, and in some cases cholesterol, and that exhibit fluid-fluid phase coexistence, have been studied. Incorporation of PCer into POPC/PSM-bilayers was shown to promote the formation of PSM/PCer-rich gel phase domains in the absence (169) and presence (183) of cholesterol. Similarly, formation of SM/ceramide-rich gel phase domains was observed in PC/PE/SM/cholesterol-bilayers (231). The formation of such sphingolipid-rich domains was, however, strongly dependent on the length of the ceramide *N*-acyl chain (232). Similar length-dependence was observed by Chiantia and coworkers, when they studied the effects of ceramides on liquid-ordered

domains in SM/DOPC/cholesterol-bilayers with atomic force microscopy and fluorescence correlation spectroscopy. In those mixtures, C16- and C18-Cer were found to segregate into gel phase domains that were presumed to also contain SM (233, 234), whereas ceramides with shorter *N*-acyl chains (C12, C6 or C2) did not form gel phase domains but decreased the stability and perturbed the lipid packing in the liquid-ordered domains formed by SM and cholesterol (234).

A biologically more relevant way of exploring the consequences of incorporation of ceramide into bilayers is to follow the effects of ceramide generation by the hydrolytic activity of SMase. In general, treatment of SM-containing bilayers or monolayers with SMase induces phase separation (224, 235, 236), and gives rise to transbilayer lipid redistribution (101, 237). When Holopainen and coworkers studied the effects of SMase-generated ceramide on large unilamellar vesicles composed of POPC/PSM (3/1 molar ratio), they observed rapid hydrolysis of PSM, followed by an immediate, pronounced increase in the acyl chain order, whereas the formation of ceramide-rich domains was shown to be a slower process, as reported by a pyrene-labeled lipid analog (224). However, the dynamics of domain formation by the ceramides produced as a result of SM-hydrolysis appeared to depend on the membrane curvature, as a more rapid formation of domains was observed in giant unilamellar vesicles of identical lipid composition (238).

Silva and coworkers observed that SM-hydrolysis in POPC/PSM/cholesterol-bilayers was dependent on the physical properties of the membranes, the activity being high when liquid-ordered-liquid-disordered phase separation occurred (239). They also observed that the bilayer composition, and in specific the cholesterol content, influenced the lateral segregation of the membrane lipids following ceramide generation. At the lowest cholesterol contents, ceramide/SM gel phase domains were formed, whereas at the highest cholesterol contents a SM/cholesterol ordered phase was predominating, and the ability of ceramides to form gel domains was diminished (239).

*2.7.1.3. Ceramides induce membrane structural reorganizations*

In addition to the effects of ceramides on the two-dimensional membrane structure and lipid lateral organization, curvature stress induced by ceramides can lead to alterations in the three-dimensional topology of bilayer membranes as hexagonal phases and membrane vesiculation are promoted (110). Ruiz-Argüello and coworkers were the first to demonstrate vesicle leakage and aggregation, as well as the emergence of a thermotropic lamellar-to-inverted

non-lamellar phase transition when they incorporated natural ceramides into bilayers composed of SM/PE/cholesterol or PC/PE/cholesterol (2/1/1 molar ratio) (240). Later, formation of inverted hexagonal phase by natural ceramides in dielaidoyl-PE liposomes was observed (117). The leakage of vesicle contents was also shown as a result of *in situ* ceramide generation with SMase in SM-containing mixed membranes (241, 242). The formation of non-lamellar phases by ceramides is understandable owing to its geometrical shape that intrinsically promotes negative membrane curvature.

Another major effect owing to the negative curvature induced by ceramides is membrane vesiculation, which was observed in giant unilamellar vesicles composed of POPC/PSM as they were subjected to treatment with SMase (238). In that study, treatment of the vesicles with SMase caused enrichment of the fluorescently labeled BODIPY-ceramide in domains in the outer leaflet, followed by an immediate formation of small vesicles inside the giant vesicles. In pure egg SM-vesicles, ceramide generation by SMase was shown to induce vesicle aggregation and deformations in the bilayer structure causing leakage of the aqueous content (243).

In a study of Silva and coworkers, PCer was observed to induce morphological alterations and aggregation in POPC-vesicles when its concentration increased above 10 % (168). In the same study, ceramide concentrations above 50 % and 92 % were found to give rise to cylindrical and crystalline structures, respectively. The very long-chain ceramide C24-cer has been reported to induce formation of tubular structures when mixed with POPC, likely due to its ability to form interdigitated phases in which the long acyl chains penetrate into the opposing bilayer leaflets (226, 244). In addition to inducing non-lamellar phases and membrane vesiculation, ceramides possess the unique ability to form highly structured transmembrane channels for protein diffusion in both model and natural membranes (245, 246).

### 2.7.2. Inherent affinity of ceramides for ordered phases

When Wang and Silvius performed fluorescence quenching studies with fluorescently labelled sphingolipids displaying varying head group structure, they observed a preferential partitioning of the sphingolipids into ordered domains, with modest variations in partitioning relative to the head group structure (247). In the same study, ceramide was shown to display a uniquely high affinity for ordered domains, and the authors concluded that the affinity of sphingolipids for ordered phases rests primarily in the nature of their ceramide moiety, rather than in the distinct features of the head groups (247). In other

words, ceramides are expected to interact with other saturated lipids rather than with unsaturated lipids. Busto and coworkers, again, reported a similar chain ordering effect by ceramide on PSM that was earlier discussed for PCs (*section 2.7.1.1.*), when they studied ceramide/SM-interactions in Langmuir monolayers (248). Using DSC on bilayer membranes, they also observed a ceramide-induced increase in the $T_m$ of PSM, and the coexistence of complex gel phases up to 30 mol% of ceramide, above which no PSM-rich phase was no longer seen (248).

The above mentioned studies clearly reflect an interaction between ceramides and SMs, in which the reduction of the steric repulsion between the bulky SM-head groups by ceramide (in a similar way as by cholesterol) plays an important role, maximizing the chain-chain interactions and bringing the lipids closer to each other. These interactions are further enhanced by the extensive network of hydrogen bonds formed at the membrane-water interface owing to the $C_3$-hydroxyl and $C_2$-amide functions of the sphingoid base, the $C_1$-hydroxyl function of the ceramide, and the phosphate moiety of SMs (196, 211, 249).

### 2.7.3. The bilateral effects of cholesterol and ceramide

In keeping with the proposed favorable interaction between SM and cholesterol as opposed to PC and cholesterol, and the well-documented formation of ordered phases by cholesterol together with saturated SM-species (see *section 2.6.1.*), cholesterol appears to share the volition of ceramides to interact with SM. Consequently, ceramides and cholesterol have been observed to exhibit reciprocal, concentration-dependent effects on each other's lateral distribution in membranes. In general, at high ceramide/cholesterol ratios ceramides form gel phases that also recruite SM, while at low ceramide/ cholesterol ratios ceramide-rich gel phase formation, as well as cosegregation of ceramide and SM, are abolished.

Megha and coworkers were the first to observe ceramide-induced displacement of cholesterol from ordered domains formed by a saturated PC and cholesterol (250). Shortly after, in a study of Alanko and coworkers, cholesterol was shown to be displaced from a PSM-rich ordered environment in POPC-bilayers as PCer recruited PSM to formation of a sphingolipid-rich gel phase (183). Similar displacement of cholesterol from SM-rich ordered domains, and subsequent formation of gel phase domains, was observed in giant vesicles composed of PC/PE/SM/cholesterol (231). Cholesterol-displacement, with observable consequences on its association with caveolin-1, was also observed in the cellular plasma membrane (251).

In general, short chain ceramides display lower ability to displace cholesterol than intermediate and long-chain ceramides (232, 252). Furthermore, long-chain ceramides efficiently reduce the partitioning of cholesterol into SM-containing membranes (253). Ceramides also decrease the solubility limit of cholesterol in POPC-bilayers, with eventual formation of cholesterol crystals (254). In the absence of SM, cholesterol has been shown to exhibit a destabilizing effect on ceramide-rich gel phases in PC-bilayers (255). In the absence of a fluid phospholipid, i.e., in ternary SM/ceramide/cholesterol-mixtures, cholesterol prevented the formation of a ceramide-rich gel phase, and instead a single ternary phase existed (256).

Boulgaropoulos and coworkers observed that as soon as the ceramide/SM ratio exceeded 1 in POPC/SM/ceramide/cholesterol-bilayers, the ceramides started to form crystallites (257). Ceramide crystallites were formed at significantly higher concentrations of ceramide in the absence of cholesterol, suggesting that cholesterol modulated the maximum solubility of ceramide in the bilayers (257). Even in mixed bilayers of POPC/PSM/cholesterol, high concentrations of cholesterol have been shown to solubilize ceramide-enriched domains (179, 181). More recently, it was shown that in similar mixtures, when the cholesterol content exceeds that of ceramide's the packing of the ceramide-rich gel phase is reduced (258). Apparently, even though ceramides are able to induce lateral phase separation into gel phase domains even at low concentrations, their effects on membrane organization are influenced by the membrane composition, and in particular by the concentration of cholesterol.

Taken together, the membrane behavior of ceramides is characterized by segregation into gel phase domains of high molecular order and thermal stability. This behavior originates from *i)* the need to minimize unfavorable interactions between the aqueous phase and the hydrophobic body of ceramides, *ii)* the low miscibility of ceramides in unsaturated phospholipid membranes, and *iii)* the inherent affinity of ceramides for other ordered lipids. Consequently, modifications of the structure of ceramides can be expected to affect their lateral segregation in bilayer membranes, altering their ability to form ceramide-enriched domains and to displace cholesterol from SM/cholesterol-rich domains. Interestingly, ceramides that have been chemically modified in the long-chain base near to the head group region (C1-C7) induce similar thermal stabilization of SM-rich domains, and a subsequent displacement of cholesterol, as unmodified ceramides (252). However, the length of the *N*-acyl chain remarkably affects the membrane properties of ceramides (232, 252) with effects

observed in the ability of the ceramides to form ceramide/SM-rich domains that exclude cholesterol (232, 253). In this thesis, the effects of structural alterations on ceramide bilayer properties were studied with the emphasis on *N*-acyl chain branching, the length of the sphingoid base, and the structure of the membrane-water interface. In addition, the effects of the SM-head group size, and a possible umbrella-effect, on ceramide/SM-interactions were addressed.

## 3. AIMS OF THE STUDIES

The main aims of the studies summarized in this thesis were to explore how targeted structural modifications influence the molecular properties and lipid-lipid interactions of ceramides in bilayer membranes, and to understand how the different structural aspects of ceramides affect their lateral distribution and the formation of sphingolipid-rich ordered or gel phase domains in mixed bilayers. The specific aims in each original publication are listed below.

In **paper I**, the aim was to compare the fluidizing effect of benzyl alcohol (BA) on bilayers representing liquid-disordered, cholesterol-enriched, and gel phase domains composed of different lipid species, including ceramides. This study formed the basis for the subsequent projects, in which it was studied more closely how the molecular aspects of ceramides affected their ability to form tightly packed gel phase domains of high degree of molecular order.

In **paper II,** the influence of targeted single or poly-methylation of the *N*-acyl chain on the membrane properties of ceramides was studied. The aim was to explore how the formation and thermal stability of sphingolipid-rich domains was affected by disruption of acyl chain packing at different depths along the *N*-acyl chain.

In **paper III,** the aim was to compare the membrane properties of ceramides that contained sphingoid bases of varying length. The effect of systematic reduction in sphingosine length on the interactions and lateral distribution of the ceramides was explored in order to compare the length-effects of the sphingoid base to those previously reported for ceramides containing *N*-acyl chains of different lengths.

In **paper IV,** the interface structure of ceramide was modified by introducing methyl groups to key positions. The aim was to study how disruption of interfacial properties, such as hydrogen bonding and lateral packing, affected the interlipid interactions of ceramides.

In **paper V,** the structural modifications were introduced to SM instead of ceramide. The aim was to explore how reduction in SM-head group methylation affected SM/ceramide-interactions in terms of formation and thermal stability of sphingolipid-rich domains in mixed bilayers. The study was extended to include dipalmitoylglycerol (DPG) and analogous head group analogs of PC, which allowed us to compare the role of the head group, the hydrogen bonding, and the acyl chain packing in interactions between saturated lipid species.

## 4. MATERIALS AND METHODS

The experimental approaches with the respective parameters that were examined, as well as the original publications in which the approach was applicable, are introduced in table 1. The methods and materials are described in full detail in the respective papers (I-V) while in this chapter only a brief description of the experimental procedures is given.

***TABLE 1.*** *Experimental approaches with the respective parameters examined in the original publications I-V.*

| Experimental approach | Parameter examined | Paper |
|---|---|---|
| **Fluorescence spectroscopy** | | |
| DPH-anisotropy | $T_m$, pure component | I |
| | membrane order, mixed component | I |
| tPA-anisotropy | membrane order, domain melting T | I |
| CTL-quenching | sterol-rich domain formation, sterol displacement | II-IV |
| tPA-quenching | ordered/gel domain formation, domain melting T | II-IV |
| tPA-Cer quenching | ordered/gel domain formation, domain melting T | V |
| CTL-partitioning | sterol affinity for bilayers | II-IV |
| tPA-lifetime | membrane order, domain properties, phase coexistence | III-V |
| tPA-Cer lifetime | membrane order, domain properties, phase coexistence | V |
| **Calorimetry** | | |
| DSC | lipid mixing | III-V |

### 4.1. Materials

The structural analogs of ceramide or SM were either synthesized in our laboratory (Papers II, III and IV) according to previously established protocols (259-261) or by the group of professor Shigeo Katsumura in Japan (Papers IV and V) (210, 262). The fluorescent probes CTL, tPA, tPA-Cer and the fluorescence quencher 7SLPC that was used in the quenching experiments, were synthesized in our laboratory according to (263), (259, 264, 265), (259), and (266), respectively, except for papers II and IV in which tPA was purchased from Cayman Chemical Company (Ann Arbor, MI, USA) and paper V in which 7SLPC was obtained from Avanti Polar Lipids (Alabaster, AL, USA). Lipid precursors for synthesis, as well as DPH and standard lipids were mainly obtained from Avanti Polar Lipids, Sigma-Aldrich (St. Louis, MO, USA), Larodan Fine Chemicals (Malmö, Sweden), and Molecular Probes (Leiden, the Netherlands). PSM was purified from egg yolk SM as described in Paper I. The

sources of the chemicals and the synthetic procedures are described in more detail in the original publications (I-V). The molecular structures of BA and all the sphingolipid analogs that were used in the studies prescribed in this thesis are depicted in figure 7.

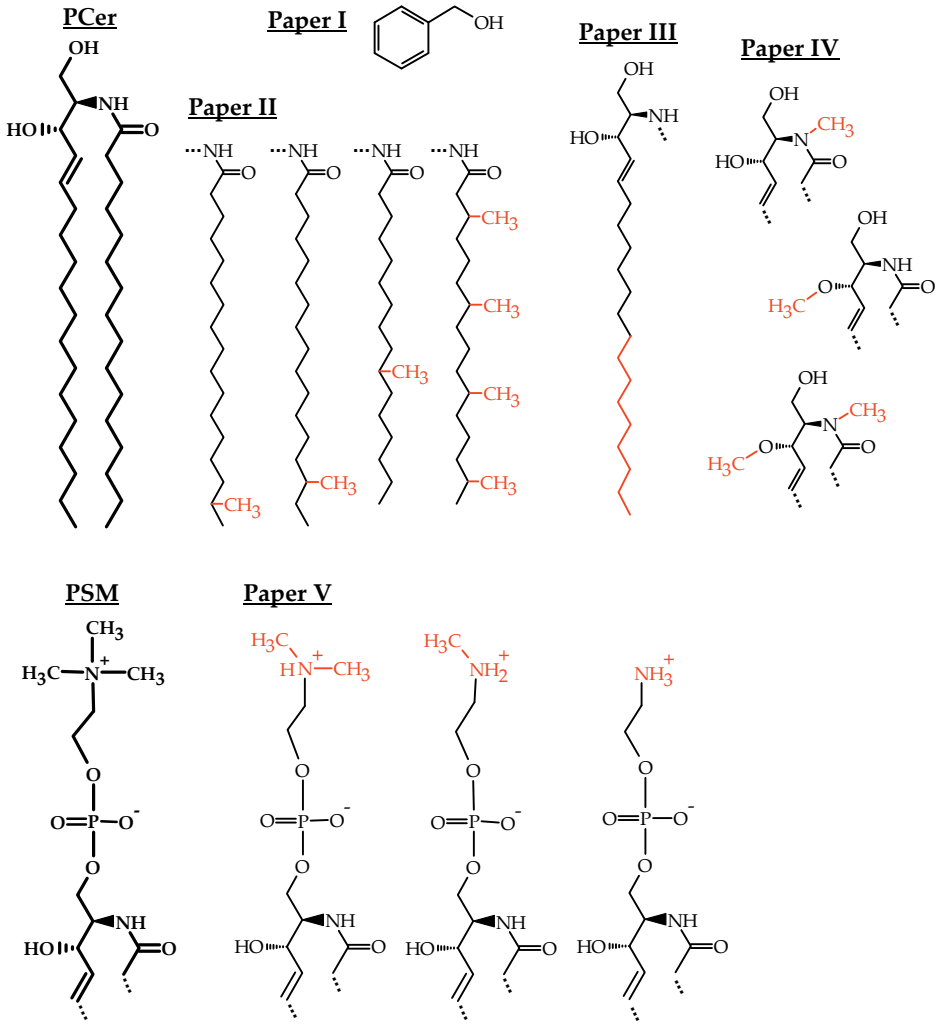


***Figure 7.*** *Molecular structures of BA (Paper I) and the sphingolipid-analogs. The parent lipid was either PCer (papers II-IV) or PSM (paper V). Paper II: the N-acyl chain was methylated at position 16, 15, or 10, or at 3, 7, 11, and 15, (16Me-, 15Me-, 10Me-, and PhytCer (phytanic), respectively). Paper III: the long-chain base length varied between 12 to 20 carbon atoms (12:1-, 14:1-, 16:1-, 18:1-, and 20:1-PCer). Paper IV: the interfacial 2N or 3O, or both, were methylated (NMe-, OMe-, and NMeOMeCer, respectively). Paper V: the PSM-head group methylation was reduced (CPEMe$_2$, CPEMe, and CPE).*

## 4.2. Preparation of lipid vesicles

All studies described in this thesis were carried out with model membrane vesicles. Except for the CTL-partitioning method that required the use of unilamellar vesicles that were prepared by extrusion (II-IV), the multilamellar vesicles used in the fluorescence measurements were prepared by sonication (I-V). For DSC, multilamellar vesicles produced by both sonication (III-V) and freeze-thaw procedures (V) were used.

The fluorescent probes and the quencher lipid were added into the membranes simultaenously with the lipids while preparing the vesicles. Sonication was in general not observed to influence the fluorescence of the probes, and it has been shown that sonication does not destroy the spin-labels on the quencher lipid (184). In general, the vesicles were prepared by hydration of dry lipid films at 65°C (for fluorescence measurements) or at a temperature above the highest gel-to-liquid phase transition temperature of the lipids represented in the sample (for DSC), followed by either sonication, extrusion or freeze-thaw.

## 4.3. Fluorescence spectroscopy

The steady-state fluorescence measurements were performed on a PTI QuantaMaster-1 spectrofluorometer (Photon Technology International, Lawrencewill, NJ, USA) operating in the T-format. The time-resolved fluorescence decays were recorded with a FluoTime 200-spectrometer with a PicoHarp 300E time-correlated single photon counting module (PicoQuant GmbH, Berlin, Germany).

### 4.3.1. Fluorescence anisotropy

The vesicles for the fluorescence anisotropy measurements were prepared at a lipid concentration of 100 μM containing either 0.25 mol% of DPH or 1 mol% of tPA. The samples were heated at a rate of 2°C/min, while the fluorescence emission intensity was continuously scanned. The excitation and emission wavelengths were 360/430 nm and 305/405 nm for DPH and tPA, respectively. The G factor was determined for each sample prior to the anisotropy measurements. The emission signal was converted to anisotropy, *r*, with the PTI FeliX32-software according to Lakowicz (267).

4.3.2. Fluorescence quenching

The fluorescence quenching was measured in samples with a lipid concentration of 50 μM. For each quenching curve, two samples were prepared. The quenched F-sample contained 1 mol% of a fluorescent probe (CTL, tPA or tPA-Cer) and 30 mol% of the quencher lipid 7SLPC. In these samples, 7SLPC replaced an equal amount of POPC that served as the bulk lipid. The unquenched $F_0$-samples contained 1 mol% of a probe, but no quencher. The excitation and emission wavelengths were 324/390 nm for CTL, and 305/405 nm for tPA and tPA-Cer. The emission data were recorded for both the F- and the $F_0$-sample as a function of temperature while the samples were heated at a rate of 5°C/min. The fluorescence quenching was reported as $F/F_0$ (calculated with the PTI FeliX32-software), which denotes the fraction of unquenched fluorescence at any given temperature (182). The method is based on collisional quenching between the fluorophores and the quencher, which display different lateral partitioning in mixed bilayers. Since the fluorophores associate with sterol-rich (CTL) or other ordered/gel phase domains (tPA and tPA-Cer), and the quencher lipid is located in the disordered bulk, this method allows the detection of lateral domains, and the respective domain melting temperatures.

4.3.3. Sterol partitioning

Sterol partitioning into mixed bilayers was determined by measuring the equilibrium partitioning of CTL (2 mol%) between large unilamellar vesicles (40 μM final lipid concentration) and methyl-β-cyclodextrin (mβCD). The molar fraction partition coefficients, $K_x$, at a given temperature were calculated from CTL-anisotropies (324/390 nm excitation and emission wavelengths), that were measured in a series of samples with equal lipid composition but increasing concentrations of mβCD (268).

4.3.4. Fluorescence lifetime

The time-resolved fluorescence decays of tPA (0.5 mol%) and tPA-Cer (1 mol%) were measured at a given temperature in samples of 100 μM lipid concentration. The fluorophores were excited by a 298 nm LED laser source and the emission data were collected at 430 nm. The data were aquired and analyzed with the FluoFit Pro-software provided by PicoQuant. The decay fits were obtained by a non-linear least squares iterative reconvolution method, based on the Marquardt-Levenberg algorithm. The justification for the number of exponentials was assessed from the reduced $\chi^2$ and a random distribution of the weighted residuals.

### 4.4. Differential scanning calorimetry

DSC was performed on samples with final lipid concentration of 1 mM for pure lipids and for binary mixtures, and 2 mM for ternary mixtures. Depending on the composition, the samples were subjected to 4-20 consecutive heating and cooling scans with a temperature gradient of 1°C/min. The data were acquired with a high-sensitivity Microcal VPDSC-instrument (Microcal, Northampton, MA, USA) and analyzed with the ORIGIN-software (Originlab, Northampton, MA, USA).

# 5. RESULTS

## 5.1. Benzyl alcohol-induced membrane fluidization

BA (also known as phenylmethanol) is a naturally occurring polar, organic compound that is used as a solvent and preservative in food and cosmetic industry, as well as in anesthethics and intravenous medications (269-271). BA is also widely used as a membrane fluidizer. It localizes in the interfacial region of bilayers with its hydroxyl group aligned with the lipid head group region, where it increases the fluidity, or decreases the molecular order, of lipid bilayers (272).

It was previously suggested that a BA-induced membrane hyperfluidization, that induced an upregulation of the cellular heat shock genes and a subsequent stress response mediated by molecular chaperones (273, 274), could relate to fluidization of SM/cholesterol-rich ordered membrane domains, which was demonstrated *in vitro* when bilayers composed of POPC/PSM/cholesterol were subjected to 40 mM BA (274). To investigate the relative effects of BA on distinct lipid phases, in paper I, we exposed bilayers that displayed gel-fluid and ordered-fluid phase separation to BA. The molecular order in the bilayers was deduced from tPA- and DPH-anisotropies measured as a function of BA-exposure.

### 5.1.1. Fluidization of gel and liquid-ordered phases by BA

Pure PSM- and DPPC-gel phases are known to exhibit a melting temperature of ~41°C (191, 275, 276). When the effects of 40 mM BA on the melting of pure PSM and DPPC gel phases was studied with DPH-anisotropy, it was found that BA decreased the $T_m$ of both saturated lipids, as well as disordered the DPPC-gel phase at temperatures below the $T_m$ (Fig. 8A). The order of the PSM gel phase was less affected before the phase transition, but the shift in $T_m$ was greater for PSM (~8°C) than for DPPC (~5°C).

The fact that BA was observed to have little influence on the order of pure gel phase lipids at low temperatures (15°C), could relate to the concentration of BA used in the study. Chen and workers reported that a much higher concentration of BA was required to disorder DPPC-vesicles below the $T_m$ than when the bilayers were in a fluid state (277). In some studies BA-concentrations below the one used in our study have been shown to reduce the $T_m$ of pure DPPC even more effectively than what was observed in our study (277-279). Factors such as the purity of the lipids could explain the observed differences. However, vesicle size or multilamellarity probably have a minor effect, since nearly identical effects of BA were observed in vesicles prepared by bath sonication, extrusion, or ethanol injection (unpublished data).

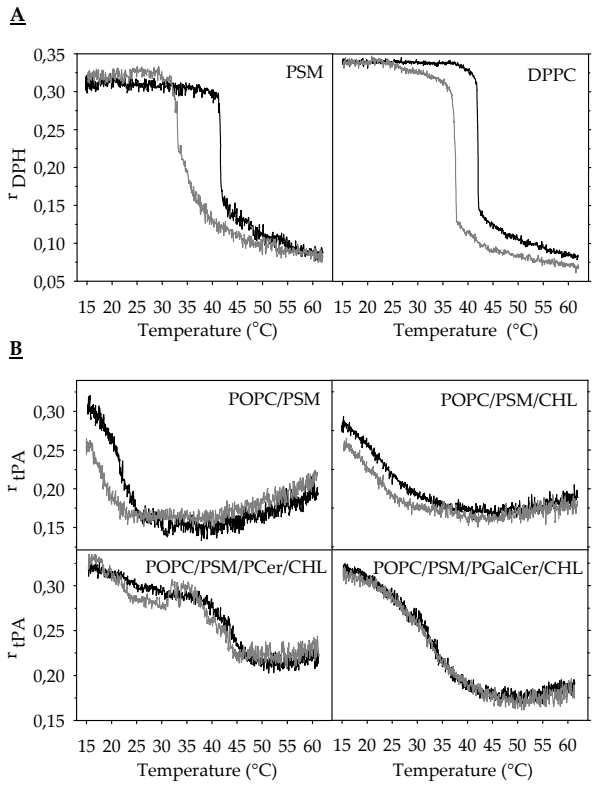


***Figure 8.*** *BA-induced fluidization of A) pure PSM- and DPPC-gel phases as detected by steady-state anisotropy of DPH (0.25 mol%), and B) ordered or gel phase domains in mixed bilayers as detected by steady state anisotropy of tPA (1 mol%). The black lines represent anisotropy from intact lipid vesicles, and the grey lines the anisotropy of an identical sample after addition of 40 mM BA. The vesicle compositions in B) were POPC/PSM, 60/30 (molar ratio); POPC/PSM/CHL, 60/30/10; POPC/PSM/PCer/CHL and POPC/PSM/PGalCer/CHL, 60/15/15/10. The figure is adapted from paper I with the permission of Elsevier.*

The mixed bilayers displaying presence of ordered or gel phase domains were studied with tPA-anisotropy (Fig. 8B). In mixed bilayers of POPC and PSM (60/30 molar ratio), where coexistence of a fluid phase and a PSM-rich gel phase is expected (164, 169, 280), BA was observed to clearly decrease the melting temperature of the PSM-gel phase. However, in bilayers of POPC/PSM/CHL (60/30/10 molar ratio), the cholesterol induced liquid-ordered domains (164) seemed slightly less sensitive to BA-induced fluidization than the PSM-gel phase domains. Thus, the presence of cholesterol, and the existence of liquid-ordered domains, appeared to increase the resistance of the bilayers against BA-induced

fluidization. This observation agrees with the earlier finding that DPPC- and egg PC-bilayers were stabilized against BA-induced effects in the presence of cholesterol (281).

5.1.2. Stabilization of the bilayers against BA by ceramides

The effects of BA on the domain melting temperature and the membrane order in bilayers containing ceramides were markedly weaker than on the other bilayers (Fig. 8B). Bilayers that were composed of POPC/PSM/PCer/CHL or POPC/PSM/PGalCer/CHL (60/15/15/10 molar ratio), displayed almost full resistance to fluidization. An interesting observation in the original paper was that although DPH-anisotropy in general reported a decrease in the molecular order for the bilayers as a result of exposure to BA, in some PCer-containing bilayers it was found to remain practically unaltered (Paper I, Fig. 4E,F). This observation, in keeping with the inability of DPH to partition into ceramide-rich phases (168, 179), suggests that PCer was able to indirectly also stabilize the fluid phase against fluidization. This conclusion would agree with the previous finding that PCer is able to enhance the acyl chain packing and molecular order of a fluid POPC (168, 228).

## 5.2. Importance of chain packing for ceramide-rich domains

In order to investigate how disruption of acyl chain packing influenced the membrane properties of ceramides, we introduced either methyl branches along the *N*-linked acyl chain, or performed a stepwise shortening of the long-chain sphingoid base, and studied the formation of ceramide-rich lateral domains and the ability of the ceramides to increase the membrane order. The methylated analogs comprised of 16MeCer and 15MeCer in which the methyl group was located near to the distal end of the acyl chain ($C_{16}$ or $C_{15}$ of an heptadecanoic acid), 10MeCer in which the methyl group located in the mid part of the (hexadecanoic) chain, and PhytCer which was polymethylated at carbons 3, 7, 11, and 15 (of a hexadecanoic acid) (Fig. 7). The sphingoid base analogs comprised of a 12, 14, 16, 18, or 20 carbons long base (containing the $C_{4\text{-}5}$ unsaturation of sphingosine) coupled to palmitic acid (Fig. 7).

5.2.1. Disruption of chain packing by methyl branches

Based on the results of Löfgren and Pascher, showing that ceramide chain packing is more sensitive to constraints in the mid part than in the distal end of the acyl chains (189), the greatest effect on formation of ceramide-rich domains was expected from the 10Me-branch and the polymethylations. The tPA-

quenching assay showed that when PCer was included to replace half of the PSM in mixed bilayers of POPC/PSM/CHL (60/30/10), the melting temperature of the ordered domains increased significantly (from ~42 to ~50°C, Fig. 9, the two lowest lines), reflecting formation of a ceramide/SM-rich phase owing to the favorable interaction between ceramides and SMs in multicomponent bilayers. Similar thermal stabilization of the ordered domains was not observed in the presence of 16MeCer and 15MeCer (with domain melting temperatures of ~42 and ~38°C, respectively).

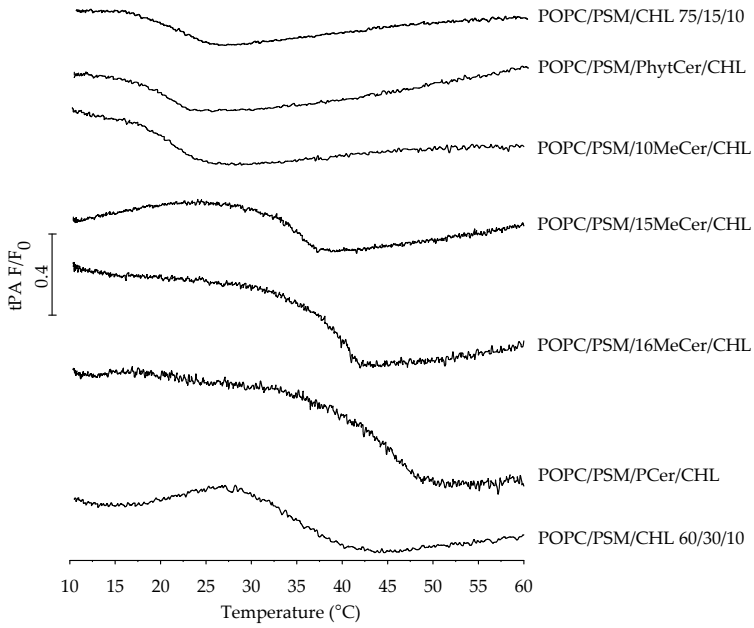


***Figure 9.*** *Formation and thermal stability of sphingolipid-rich ordered or gel phase domains in the presence of N-acyl chain methylated ceramides as reported by fluorescence quenching of tPA (1 mol%). The composition of ceramide-containing bilayers was POPC/PSM/XCer/CHL, 60/15/15/10 (molar ratio). The POPC/PSM/CHL, 75/15/10-sample is shown as a reference for bilayers with reduced amount of PSM but no ceramide. The figure is adapted from paper II with the permission of Springer.*

As expected, 10MeCer and PhytCer seemed to significantly decrease the melting temperature of the ordered domains, displaying similar thermal stability (~25 and ~23°C, respectively) as the ordered domains in bilayers that had reduced amount of PSM but no ceramide added (the POPC/PSM/CHL 75/15/10-composition). The results indicated that the methylations caused

packing constraints among the ceramide acyl chains, reducing their ability to interact with the saturated chains of PSM in the ordered domains. The magnitude of the packing constraints was highly dependent on the location of the methyl branches, but in general, the increased chain disorder caused by the methylations led to decreased thermal stability of the ordered domains.

5.2.2. Effects of chain asymmetry on chain packing

In keeping with the numerous observations that formation of ceramide-rich ordered or gel phase domains in multicomponent bilayers is highly dependent on the length of the *N*-acyl chain (232, 234, 252), modification of the sphingoid base length was expected to markedly influence the bilayer properties of ceramides. Indeed, the average fluorescence lifetimes of tPA increased with respect to the sphingoid base length of ceramide both in fluid POPC-bilayers, as well as in heterogeneous multicomponent bilayers at 23°C (Fig. 10), indicating increased molecular order with increasing sphingoid base length.

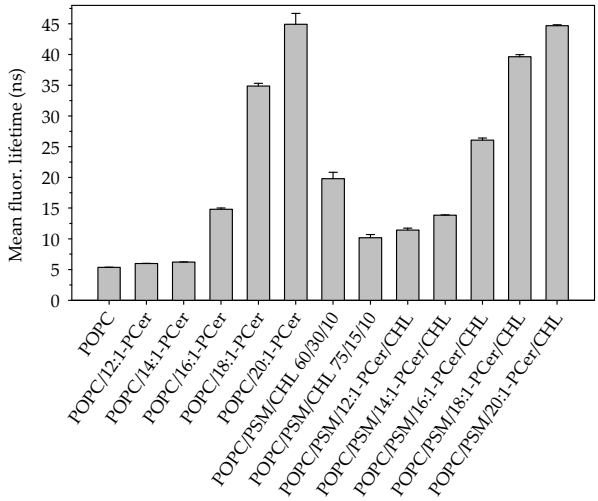


***Figure 10.*** *Effect of ceramide long-chain base length on the average order of mixed bilayers as deduced from time-resolved fluorescence decay of tPA (0.5 mol%) at 23°C. The binary bilayers were composed of POPC/X-PCer (85/15, molar ratio) and the quaternary bilayers of POPC/PSM/X-PCer/CHL, (60/15/15/10). The figure is adapted from paper III with the permission of Cell Press.*

While the average lifetime of tPA remained almost at an equal level as in pure POPC-bilayers in the presence of 12:1- and 14:1-PCer, in the presence of the ceramides with longer sphingoid bases it was significantly longer. The 16:1-, 18:1-, and 20:1-PCer were also observed to give rise to a long lifetime component that was above 30 ns, with an increasing length, intensity and amplitude with respect to the sphingoid base length (Paper III, supplementary Table 1). For 18:1-PCer this lifetime is related to the existence of a ceramide-rich gel phase (168, 169), which suggests lateral segregation of the ceramides with the C16-20 sphingoid bases from the fluid POPC.

In the multicomponent bilayers the sphingoid base analogs were observed to induce similar length-dependent increase in the average lifetime of tPA, with a marked increase in the presence of the C16-20 sphingoid base analogs. This suggested a co-segregation of the C16-20 sphingoid base analogs and PSM into sphingolipid-rich gel phase domains. This conclusion was supported by the obervation that in the presence of these ceramides, tPA reported a gel phase-implying long lifetime component above 30 ns (Paper III, supplementary Table 1), and the sphingoid base analogs were all able to mix with, and increase the main phase transition temperature of PSM in binary mixtures when studied with DSC (Paper III, Fig. 2). The increase in the melting temperature of the binary mixtures was chain-length dependent, and the low co-operativity of the DSC-melting profiles suggested presence of complex gel phases consisting of several components with presumable differences in the relative proportions of ceramide and PSM.

### 5.2.3. Branched-chain ceramides and cholesterol-rich domains

Since none of the *N*-acyl chain methylated ceramides seemed as effective in thermal stabilization of PSM-rich ordered domains as the unbranched PCer, the bilayer properties of these ceramide analogs were studied from another point of view. Ceramides have been shown to compete with cholesterol for the interactions with PSM in multicomponent bilayers with the resultant displacement of cholesterol from the SM-environment (183, 231, 250, 251). We addressed the question whether the *N*-acyl chain methylated ceramides were able to induce such cholesterol-displacement by performing CTL-quenching on POPC/PSM/CHL-bilayers in the presence of the ceramide analogs.

The results of the CTL-quenching assay are depicted in Fig 11. Since CTL is unable to partition into ceramide-rich gel phases, the absence of a detectable domain melting in the quenching assay is indicative of a ceramide-induced displacement of cholesterol from the SM-rich environment (182, 183).

Accordingly, no domains were detected by CTL in the bilayers in which PCer was present (Fig. 11). The distal monomethylations at C16 and C15 seemed to slightly weaken the ability of ceramide to displace cholesterol, as some enrichment of CTL could be observed in the presence of these ceramides relative to bilayers that contained PCer. However, even though full displacement of cholesterol was not observed in the presence of 16Me- and 15MeCer, the formation of cholesterol-rich domains was significantly interfered by these ceramides as revealed by a comparison to bilayers without any ceramide.

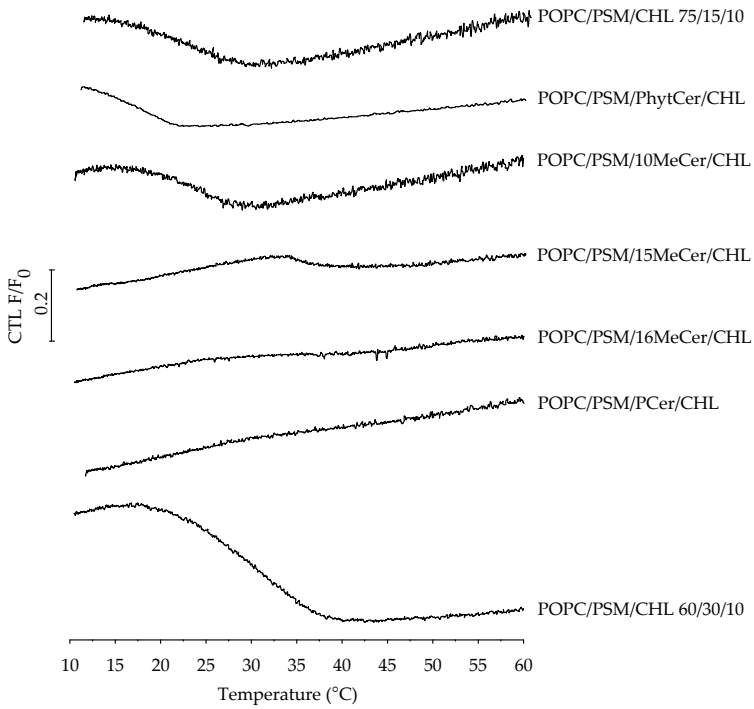


***Figure 11.*** *Effect of the N-acyl chain methylated ceramides on formation of cholesterol-rich domains in mixed bilayers as reported by fluorescence quenching of CTL (1 mol%). The composition of ceramide-containing bilayers was POPC/PSM/XCer/CHL, 60/15/15/10 (molar ratio). The POPC/PSM/CHL, 75/15/10-sample is shown as a reference for bilayers with reduced amount of PSM but no ceramide. The figure is adapted from paper II with the permission of Cell Press.*

In the original publication, 16MeCer and 15MeCer were observed to decrease the overall affinity of cholesterol for the bilayers (paper II, Fig. 3), but not as efficiently as PCer, which is consistent with the CTL-quenching data. 10MeCer and the polymethylated PhytCer were not able to displace cholesterol from the ordered domains. In fact, the thermal stability of the CTL-reported domains in the presence of these two ceramides was similar to that of the domains observed in a POPC/PSM/CHL-bilayer of 75/15/10-molar composition, that is a bilayer in which the amount of PSM was reduced but no ceramide was added. In addition, the domain melting temperatures reported by CTL were similar to those reported for these bilayers by tPA (Fig. 9). These observations suggested that 10MeCer and PhytCer either did not associate within the ordered domains or were not able to interact with PSM so as to displace cholesterol.

### 5.2.4. Chain-asymmetric ceramides and bilayer affinity of cholesterol

When the sphingoid base analogs were incorporated into POPC/PSM-bilayers, they induced a chain-length dependent thermal stabilization of the PSM-rich ordered domains, and the 16:1-, 18:1-, and 20:1-PCer proved significantly greater thermal stabilization of the PSM-rich domains than that induced by cholesterol (paper III, Fig. 3). This suggested that there could be differences between the ceramides in their ability to interact with PSM in the presence of cholesterol. In fact, only 18:1-PCer and 20:1-PCer were able to thermally stabilize the PSM-environment when cholesterol was present (paper III, supplementary Fig. 1), which was also consistent with the observation that these ceramides displaced cholesterol from the PSM-rich domains (paper III, Fig. 4).

To gain additional information about the bilayer distribution of cholesterol in the mixed bilayers, we measured the molar partition coefficient $K_x$ of CTL in equilibrium conditions in the presence of the sphingoid base analogs (Fig. 12). The partitioning assay provides information about the overall bilayer affinity of sterol, and can thus reveal ceramide-induced changes in sterol distribution independent of the lateral distribution of the ceramides. Sterol has been reported to partition more favorably into bilayers that contain PSM, or PSM and cholesterol, than into pure fluid PC-bilayers (253, 282). The assay has also been succesfully used to report on changes in sterol distribution in the presence of ceramides, PCer causing a dramatic decrease in sterol partitioning in PSM-containing bilayers (253). Indeed, a marked reduction in sterol affinity measured at 23°C was observed when half of the PSM in POPC/PSM/CHL-bilayers (60/30/10) was replaced with either 18:1-PCer or 20:1-PCer (Fig. 12).

The reduction in $K_x$ stems from the cholesterol-displacing effect of 18:1-PCer and 20:1-PCer, driving cholesterol out from the ordered PSM-environment into the more fluid POPC-phase from where it is more easily accessible to cyclodextrin. The ceramides with shorter sphingoid bases seemed to also reduce the sterol affinity, but probably for different reasons. 16:1-PCer was shown with CTL-quenching to partially displace sterol from the PSM-rich domains (paper III, Fig. 4), which explains the reduction in $K_x$. In the case of 12:1- and 14:1-PCer, the reduction in $K_x$ was probably not due to the presence of the ceramides, as much as it was a result of the reduced amount of PSM in those bilayers. Thus, in the presence of these ceramides the sterol affinity was at a similar level as for POPC/PSM/CHL-bilayers of 75/15/10-molar composition. Alternatively, the low sterol affinity in the presence of 12:1- and 14:1-PCer could relate to disordering effect of these ceramides on the PSM/cholesterol-rich phase, which has been shown for ceramides with short *N*-acyl chains (234). In general, sterol affinity was lower at 37°C than at 23°C because of the more fluid state of the bilayers at 37°C. The increasing trend in sterol affinity observed at 37°C when the sphingoid base length increased from 12 to 16 carbons could relate to a general increase in the average order of the bilayers.

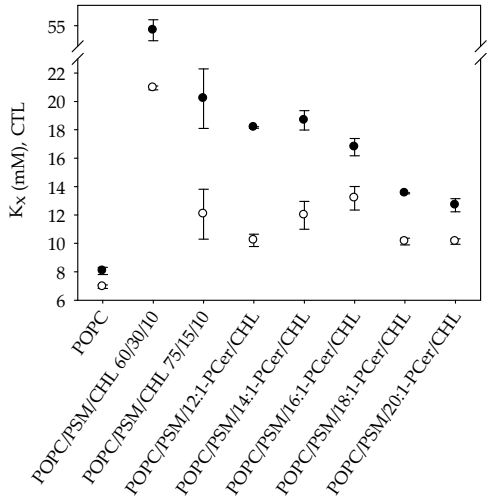


***Figure 12.*** *Sterol affinity for bilayers containing ceramides with varying length sphingoid bases as deduced from the equilibrium partitioning of CTL (2 mol%) between large unilamellar vesicles and mβCD at 23°C (black circles) and 37°C (grey circles). The affinity is expressed as the molar fraction partition coefficient $K_x$. The figure is adapted from paper III with the permission of Cell Press.*

## 5.3. Role of interfacial properties in the bilayer behavior of ceramides

To study the role of ceramides' interfacial functional groups in interlipid interactions, ceramides with methylations at 2N or 3O, or both, of the sphingoid base were synthezised, yielding NMeCer, OMeCer, and NMeOMeCer, respectively (Fig. 7). Such methylations decreased the hydrophilicity (H replaced by methyl) as well as increased the size of the interface region through the steric bulk of the methyl groups. In addition, the methyl groups attenuated hydrogen bonding. Moreover, the methyl groups could influence the properties of the $C_{4\text{-}5}$ double bond in the proximity of the $C_3$-oxygen, as well as influence the conformation of the planar amide-linkage.

### 5.3.1. Importance of the amide-group for ceramide-interactions

When studied in binary mixtures with PSM, the interface methylated ceramides were all observed to increase the $T_m$ of the PSM-gel phase (Fig. 13). However, the methylated ceramides caused a destabilization of the complex PSM/ceramide-gel phases, displaying lower $T_m$:s compared to the PSM/PCer-mixture. OMeCer proved more effective than NMeCer in thermal stabilization of PSM. The doubly methylated NMeOMeCer increased the PSM-melting temperature only by a few degrees Celsius, suggesting that the cumulative effect of the two methyl groups significantly affected the packing properties of this ceramide. Interestingly, the melting in the presence of NMeOMeCer was surprisingly cooperative compared to the other mixtures.

When the effects of the interface methylated ceramides on fluid POPC-bilayers were studied by measuring the time-resolved decays of tPA, it was observed that OMeCer increased the order of the bilayers similarly to PCer, giving rise to a long lifetime component signifying a gel phase (Table 2). However, with OMeCer the fractional intensity and fractional amplitude of this gel phase were significantly decreased compared to PCer. This is an indication of a smaller fraction of the gel phase formed by OMeCer than by PCer.

Also in the presence of NMeCer the lifetime of tPA was increased compared to the pure POPC-bilayers, but the length of the longest lifetime component was remarkably shorter in the presence of NMeCer than with OMeCer and PCer, suggesting that the molecular order in the ordered or gel phase domains formed by this ceramide was significantly decreased compared to OMeCer and PCer. The longest lifetime component of tPA was only slightly affected by the presence of the doubly methylated ceramide relative to pure POPC-bilayers, which indicates a fluid state for those bilayers.

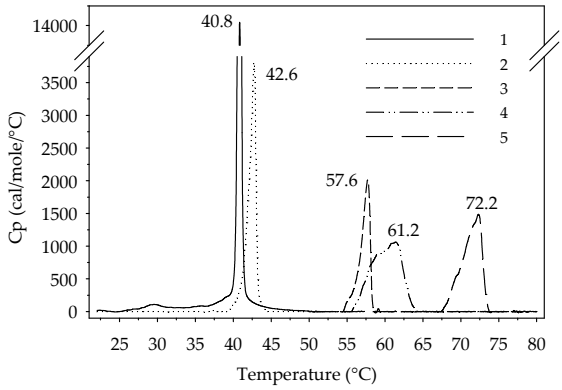


***Figure 13.*** *Mixing of the interface methylated ceramides with PSM in binary mixtures (1/1) as deduced from DSC thermograms. The specific heat capacities and the highest $T_m$ peaks of the second heating scans are shown for 1) PSM, 2) PSM/NMeOMeCer, 3) PSM/NMeCer, 4) PSM/OMeCer, and 5) PSM/PCer. The figure is adapted from paper IV with the permission of Cell Press.*

When the interface methylated ceramides were incorporated into POPC/PSM/CHL-bilayers, both NMe- and OMeCer induced a significant increase in the longest lifetime component of tPA (Table 2). However, the effect was not as strong with NMeCer as with OMeCer and PCer, indicating limitations in the structure of this ceramide, preventing as tight molecular interactions with PSM as OMeCer and PCer were able to form. This finding agreed well with the observation that PCer and OMeCer, but not NMeCer, were able to increase the thermal stability of sphingolipid-rich domains in mixed bilayers when explored by tPA-quenching (paper IV, Fig. 2).

Compared to bilayers that contained 30 mol% of PSM, the molecular order of the domains was decreased by the presence of the doubly methylated ceramide (Table 2). Together with the tPA-quenching data showing that the domain melting temperature was markedly lower in the presence of NMeOMeCer than for 30 mol% of PSM (paper IV, Fig. 2), this suggested that NMeOMeCer failed in promoting molecular order and thermal stabilization of PSM in the multicomponent bilayers. In addition, OMeCer was the only ceramide analog that was able to displace cholesterol from PSM-domains similarly to PCer, and also the most effective, after PCer, in reducing the bilayer affinity of cholesterol (paper IV, Figs. 4 and 5, respectively).

***TABLE 2.*** *Time-resolved fluorescence decays of tPA (0.5 mol%) at 23°C.*

| ***Vesicle composition*** | $\tau_1$ | $f_1$ | $\alpha_1$ | $\tau_2$ | $f_2$ | $\alpha_2$ | $\tau_3$ | $f_3$ | $\alpha_3$ |
|---|---|---|---|---|---|---|---|---|---|
| POPC | 5.8 ± 0.1 | 88.5 ± 1.8 | 66.5 ± 1.4 | 1.5 ± 0.4 | 11.5 ± 1.8 | 33.5 ± 1.4 | | | |
| POPC/PCer | 47.2 ± 1.1 | 81.4 ± 3.2 | 34.8 ± 3.8 | 5.7 ± 0.2 | 18.6 ± 3.2 | 65.2 ± 3.8 | | | |
| POPC/NMeCer | 38.6 ± 1.8 | 43.4 ± 4.9 | 11.8 ± 1.8 | 6.7 ± 0.5 | 56.6 ± 4.9 | 88.2 ± 1.8 | | | |
| POPC/OMeCer | 55.7 ± 0.8 | 50.1 ± 0.8 | 9.3 ± 0.4 | 5.7 ± 0.1 | 49.9 ± 0.8 | 90.6 ± 0.4 | | | |
| POPC/NMeOMeCer | 7.9 ± 0.3 | 90.8 ± 4.9 | 72.8 ± 4.2 | 2.1 ± 0.9 | 9.2 ± 4.9 | 27.2 ± 4.2 | | | |
| POPC/PSM/CHL 60:30:10 | 40.6 ± 0.3 | 43.7 ± 0.9 | 19.8 ± 0.3 | 18.2 ± 0.4 | 48.2 ± 0.2 | 48.7 ± 0.2 | 4.7 ± 0.4 | 8.1 ± 0.6 | 31.5 ± 0.5 |
| POPC/PSM/CHL 75:15:10 | 22.8 ± 0.5 | 36.0 ± 1.9 | 17.5 ± 1.0 | 10.8 ± 0.3 | 58.2 ± 1.3 | 59.8 ± 0.7 | 2.8 ± 0.3 | 5.7 ± 0.6 | 22.7 ± 0.3 |
| POPC/PSM/PCer/CHL | 54.8 ± 2.3 | 68.1 ± 4.4 | 34.6 ± 5.1 | 16.7 ± 2.6 | 29.1 ± 2.3 | 49.1 ± 6.6 | 4.4 ± 0.8 | 4.1 ± 1.2 | 24.5 ± 2.6 |
| POPC/PSM/NMeCer/CHL | 47.1 ± 2.3 | 56.2 ± 6.6 | 26.6 ± 3.5 | 17.7 ± 2.0 | 40.5 ± 5.2 | 50.8 ± 3.4 | 3.2 ± 1.5 | 3.3 ± 1.6 | 22.6 ± 3.1 |
| POPC/PSM/OMeCer/CHL | 52.9 ± 2.7 | 38.3 ± 3.5 | 11.0 ± 1.2 | 13.3 ± 1.6 | 56.9 ± 2.2 | 55.8 ± 1.2 | 3.1 ± 1.4 | 7.2 ± 2.6 | 34.0 ± 0.5 |
| POPC/PSM/NMeOMeCer/CHL | 35.4 ± 1.8 | 30.3 ± 6.6 | 14.2 ± 3.5 | 16.6 ± 1.2 | 63.8 ± 3.4 | 63.0 ± 1.3 | 4.1 ± 1.6 | 6.0 ± 3.2 | 22.9 ± 3.9 |

*The composition of the binary mixtures was 85/15 (molar ratio), and the ceramide-containing mixtures 60/15/15/10. τ, lifetime (ns); f, fractional intensity (%); α, fractional amplitude (%). The table is adapted from paper IV with the permission of Cell Press.*

## 5.4. Impact of the SM-head group on ceramide-interactions

To study the role of the PSM-head group in stabilization of ceramide/SM-interactions, PCer was mixed with SM-analogs in which the regular three methyl groups were reduced to two ($CPEMe_2$), one (CPEMe), or none (CPE, Fig. 7). The PCer-SM interaction seemed surprisingly stable against reduction in SM-head group methylation. Revealed by DSC, the SM-analogs were all able to form complex gel phases with PCer in binary (equimolar) mixtures (paper V, Fig. 1). The melting temperature of these gel phases increased slightly with respect to the decreasing SM-head group methylation (from 70-75°C for PCer/PSM, to 73-78°C for PCer/CPE), but the differences in the $T_m$-range of the melting of the complex gel phases were surprisingly low compared to the differences in the $T_m$ of the pure SM-analogs that were measured previously with DPH-anisotropy ((210), from 42°C for PSM to 65°C for CPE). This observation suggested that the SM-analogs interacted all very similarly with PCer, despite of the reduction in the SM-head group methylation.

To determine whether the PCer/SM-analog-interactions remained in fluid POPC-bilayers, the formation and melting of ceramide-rich domains by 7SLPC-induced quenching of tPA-Cer in mixed ternary bilayers (POPC/PCer/SM-analog, 70/15/15 molar ratio) was studied (paper V, Fig. 2). In such bilayers, coexistence of a POPC-rich fluid and PCer-rich gel phase occurs according to a previously reported ternary phase diagram for POPC/PCer/PSM mixtures (169). Formation of gel phase domains was detected by tPA-Cer in all of the mixtures, with similar domain melting temperature (~50°C) irrespective of the number of SM-head methyl groups, and of markedly higher domain melting temperature compared to bilayers that contained PCer but no SM-analog.

To confirm the above mentioned observation with a probe-free method, in order to avoid any artefact arising from differential probe partitioning between the different lipid mixtures, we studied the ternary mixtures also with DSC (Fig. 14A). Very similar melting profiles and almost identical melting temperatures for the complex gel phases present in the bilayers were observed. Furthermore, the temperature at which the bilayers had become totally fluid in the DSC scans (~48°C, Fig. 14A) agreed well with the domain melting temperature that was reported by tPA-Cer-quenching (paper V, Fig. 2). However, a detailed understanding of each of the gel phase components in the broad and complex transitions in the DSC scans is difficult, due to lack of identification of the composition of each of the components undergoing melting.

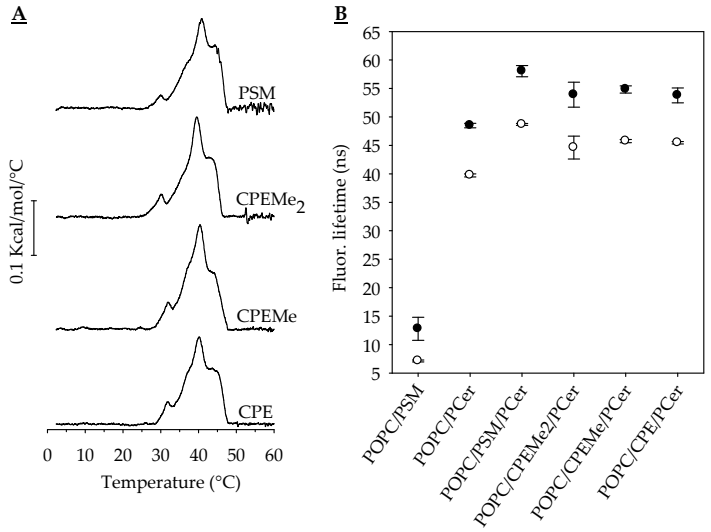


***Figure 14.*** *Thermotropic properties and order of the sphingolipid-rich domains formed by the SM-analogs and PCer in mixed bilayers as deduced from A) DSC and B) the longest lifetime component (filled circles) and the mean lifetime (open circles) of tPACer (1 mol%) at 23°C. The vesicles in A were composed of POPC/SM-analog/PCer, 70/15/15 (molar ratio). In B, the molar ratio in the binary mixtures was 85/15 and in the ternary mixtures 70/15/15. The figure is adapted from paper V with the permission of Cell Press.*

Interestingly, when not only the methyl groups, but the choline moiety altogether was removed from PSM, yielding Cer-1-P, the domain melting temperature of the PCer-co-lipid domains still remained nearly unchanged (at ~50°C, as reported by tPA-Cer-quenching, paper V, Fig. 2). This suggested that as long as the co-lipid, or SM-analog, had long and saturated acyl chains, an intact interface, and atleast the phosphate head, the lipids interacted similarly with PCer.

To gain more insight into the properties of the PCer/SM-analog gel phases that seemed very similar in terms of domain melting properties, we measured the time-resolved tPA-Cer decays in the ternary mixture bilayers at 23°C (Fig. 14B). For this purpose, we sought to first characterize the suitability of tPA-Cer for fluorescence lifetime measurements, and confirm that the linkage of tPA to a sphingosine backbone did not affect the ability of the probe to report on the properties of domains of varying degree of acyl chain order. A previous study showed that the linkage of tPA to PCs did not markedly affect the lifetime values it reported (283). When the intensity decays of tPA-Cer were compared to those of tPA in a couple of well established lipid mixtures, some small variation among

the individual lifetimes, fractional intensities and fractional amplitudes was observed, but in general, tPA-Cer was found to behave very similarly to tPA, reporting significantly longer lifetimes in ordered and gel phase domains compared to fluid bilayers (paper V, supplementary Table 1).

In agreement with previously reported phase diagrams for POPC/PSM- (164) and POPC/PCer-systems (168, 228), the tPA-Cer lifetimes indicated a fluid environment in the former and a tightly packed gel phase in the latter at 23°C in 85/15 molar ratio-mixtures (Fig. 14B). Both the longest lifetime component and the mean lifetime of tPA-Cer in the POPC/SM-mixture were significantly shorter than in the POPC/PCer-mixture. In the ternary mixture bilayers of POPC/PCer/SM-analog (70/15/15) tPA-Cer reported very long lifetimes, confirming high degree of acyl chain order and a gel-like nature for the sphingolipid-rich domains. The intensity decays clearly indicated similar molecular order and lateral acyl chain packing within the sphingolipid-rich domains irrespective of the SM-head group size.

### 5.4.1. Role of hydrogen bonding in SM/ceramide-interactions

To shed light on the possible differential roles of chain-chain interactions and hydrogen bonds in stabilization of ceramide/co-lipid-interactions we also studied mixtures of POPC, PCer and DPPC-analogs with corresponding reductions in the head group size as those in the SM-analogs. Due to inherent differences in the interface structure of PCs and SMs, the PC-analogs display reduced ability to hydrogen bonding compared to the SM-analogs. Revealed by the tPA-Cer-quenching assay, the ternary mixtures containing the PC-analogs had almost equal domain melting temperatures irrespective of the PC-analog (Fig. 15A). The domain melting temperature was, however, 4-5°C lower than that observed in the presence of the SM-analogs (paper V, Fig. 2). Clearly, the PC-analogs were able to interact with PCer very similarly despite of the differences in the PC-head group size, but the PCer/PC-analog interaction was thermally less stable than the PCer/SM-analog interaction, perhaps owing to the hydrogen bonding between the latter.

To approach this set-up from yet another point of view, we used DPG, a similar molecule to PCer, with a small hydroxyl head structure and saturated acyl chains, but reduced hydrogen bonding properties due to the glycerol interface. In ternary mixtures of POPC, DPG and SM-analogs, the melting profiles detected by tPA-Cer-quenching for laterally segregated domains formed by DPG and the analogs were very similar, with almost equal thermal stability (Fig. 15B). However, the domain melting temperatures were, again, lower than

for the PCer/SM-analog domains (paper V, Fig. 2), suggesting a possible role for hydrogen bonds in stabilization of the ceramide/SM interaction. Altogether, it seemed that any destabilizing effect owing to the reduced head group size of SM, or PC, was counterbalanced by the inherent affinity of ceramide and SM, or saturated lipid acyl chains, for each other.

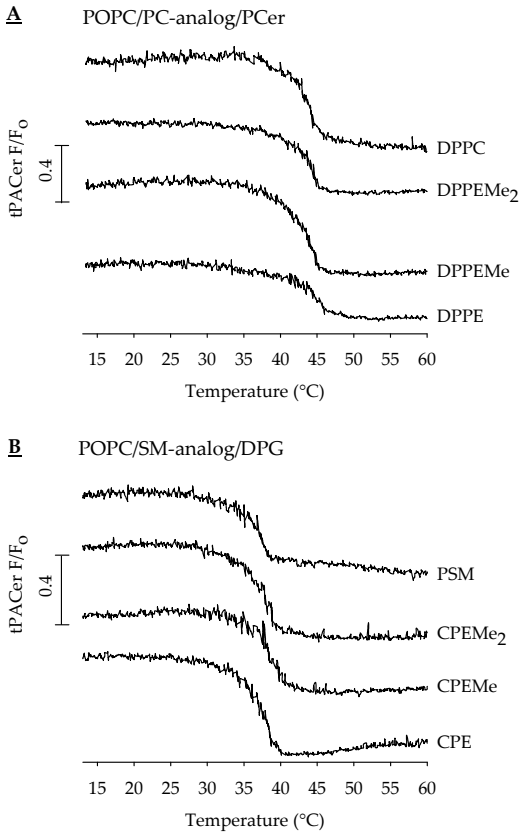


***Figure 15.*** *Formation of ordered domains by A) PC-analogs and PCer, and B) SM-analogs and DPG, as reported by fluorescence quenching of tPACer (1 mol%). Lipids in all the ternary bilayers were mixed at a molar ratio of 70/15/15. The figure is adapted from paper V with the permission of Cell Press.*

# 6. DISCUSSION

In the projects summarized in this thesis, the structural modifications that were introduced to ceramide or SM span all the topological layers of a bilayer leaflet (see Fig. 5 in *section 2.5.*). The modifications reach from the lipid head group region (paper V), through the membrane-water interface (paper IV), to the membrane hydrophobic core (papers II and III), where the region of ordered acyl chain conformations finally turns into the region of more disordered acyl chain conformations. The studies revealed that ceramides are able to form peculiarly tightly packed gel phases that, unlike gel phases formed by other lipid species included in the studies, are able to resist fluidization by BA (paper I). The formation of ceramide-rich gel phases was significantly attenuated if the lateral chain packing of ceramides was impaired in the region of ordered acyl chain conformations by introducing methyl branches to the *N*-acyl chain (paper II) or by shortening the effective length of the sphingosine long-chain base (paper III). Attenuation of hydrogen bonding and molecular packing by methylation of the amide-nitrogen markedly weakened the interlipid interactions of ceramides, suggesting an important role for the amide-nitrogen in the interfacial interactions of ceramides (paper IV). Moreover, as reducing the size of the SM-head group had practically no effect on SM/ceramide-interactions, it appeared that the interactions between SM and ceramide were governed by chain-chain interactions between their saturated chains, with some contribution from hydrogen bonding (paper V). The main results and their implications in relation to other reported studies are discussed below.

## 6.1. Membrane fluidization by benzyl alcohol

BA-induced disordering of lipid bilayers has been previously observed by several methods, including capacitance and conductance measurements (284) and studies based on electron spin resonance (285, 286), NMR (272), DSC (277), fluorescence polarization (277, 287), and X-ray diffraction (288). The results presented in this thesis give further fluorescence spectroscopy-derived proof of the membrane fluidizing effects of BA, with the added value that differences in the ability of BA to fluidize distinct lipid mixtures in which lateral phase separation occurs were observed.

In biological systems, BA has been reported to both increase and inhibit the activity of certain membrane-related enzymes (285, 289-292). The inhibition of bovine milk galactosyltransferase was dependent on the phase state of the liposomes into which the enzyme was incorporated, as inhibition was readily

observed in fluid phase membranes composed of unsaturated glycerophospholipids, whereas in gel phase bilayers formed by saturated glycerophospholipids the inhibition was attenuated (289). In our study, phase separated domains formed by PSM, DPPC, PCer and PGalCer, which are all saturated, showed variations in the ability to resist fluidization by BA, which suggests that the magnitude of the BA-effect was dependent on the thermal stability and composition of the domains, rather than on the degree of acyl chain saturation of the constituent lipids. Instead, the ability of BA to become incorporated into the laterally segregated domains was mainly affected by the degree of lateral chain packing, as well as by hydrogen bonds that stabilized the ceramide-rich domains.

It was clear from the results that also the lipid head group played an important role in the interlipid interactions within the phase separated domains, as different effects on membrane order and thermal stability were observed irrespective of the saturated lipid acyl chains. The influence of BA on the activity of certain membrane proteins could thus relate to its different effects on laterally heterogeneous membranes of varying composition, as the lateral distribution of proteins within biological membranes is assumed uneven (293, 294). Differences in the total partitioning of BA into the bilayers of varying composition could partly contribute to the observed differences between BA-effects on the different bilayers. However, such a contribution is expected minimal since BA, due to its relatively high partitioning into organic solvent *vs* water (logP ~1.10 (295)), is assumed to readily partition into membranes while exhibiting moderate solubility in water.

## 6.2. Structural modifications of ceramide

The ability of the ceramide-rich gel phase domains to resist fluidization by BA awakened our interest towards the role of the distinct parts of the ceramide molecular structure in the tight interlipid interactions occurring in such gel phases. PCer has been widely characterized in terms of its thermodynamic phase behavior and lateral distribution in multicomponent membranes. Numerous studies have shown that PCer laterally segregates from glycerophospholipids, with the resultant formation of ceramide-rich gel phase domains (168, 224, 228). Furthermore, PCer interacts with SM in more complex bilayers, recruiting SM into sphingolipid-rich gel phase domains (169, 183, 234) that displace cholesterol (183, 234).

The molecular geometry of an inverted cone, with a small polar function and conformationally ordered acyl chains allow the tight packing of PCer in

membranes. To study how disruption of acyl chain packing or the interfacial interactions affected the characteristic bilayer behavior of PCer, we introduced targeted modifications to the ceramide structure. The *N*-acyl chain was modified with methyl branches at different positions starting from the terminal end and proceeding towards the mid part of the acyl chain. The sphingosine base was modified by a stepwise shortening of its effective length, and the $C_3$-OH and the $C_2$-NH of the sphingosine base, that locate in the interfacial region, were methylated in order to prevent them from participating in the formation of hydrogen bonds.

### 6.2.1. Methyl-branching of the *N*-acyl chain

There are numerous reports about the occurrence of methyl branches in both the *N*-acyl chain and the long-chain base, including polymethylated species, of natural ceramides of varying origin (64, 66-71). In this thesis, such methylations were shown to induce structural constraints that caused less tight acyl chain packing compared to PCer. This finding is consistent with the reported effects of acyl chain methylation on the molecular space requirement and lateral head group-interactions of ceramide in monolayer studies (189). Acyl chain packing was clearly less affected by terminal methyl branches than by a methylation closer to the mid part of the *N*-acyl chain (or polymethylation), which resembles the position-dependent effects of *cis*-double bonds on the lateral interactions of ceramides (189). While *cis*-unsaturation at $C_9$ of a C18-acyl chain increased the space requirement of ceramide and promoted steric hindrance against close acyl chain packing, as well as loss of polar head group-interactions, *cis*-unsaturation of a C24-acyl chain at $C_{15}$ did not markedly affect the molecular area of the ceramide relative to the corresponding saturated acyl chain-species (189).

The effects of *N*-acyl chain methylation on membrane properties of ceramides observed in our study also agree well with a previously reported study about the membrane behavior of methylated SMs, showing that the formation of SM-rich gel phases or SM/cholesterol-rich ordered phases was less affected by terminal methylation of the SM *N*-acyl chain than by a methylation closer to the mid part of the acyl chain (188). Together with previous observations (232, 253), our results augment the important role of the *N*-acyl chain structure in the bilayer behavior of ceramides. Specific functional roles for methylated ceramides in cellular biology remain to be discovered, but based on our results, naturally occurring methyl-branched ceramides are expected to display more fluid nature relative to unbranched ceramides. Thus, methyl branches could serve similar functions as *cis*-double bonds. The fact that branched-chain ceramides are found

in marine organisms (66-68) suggests they could have importance in aqueous environments. Indeed, it was postulated that for humans, the higher water-retaining and -holding capacity of the skin surface of a newborn compared to an adult could relate to the high abundance of methyl-branched ceramides in the vernix caseosa, the waxy coating of a newborn baby (70).

6.2.2. Chain asymmetry regulated by long-chain base length

To our knowledge, there are no reports on the influence of the long-chain base length on the packing and lateral distribution of ceramides in bilayer membranes, although great variation in the length of some biological sphingoid bases has been observed (19, 27). Significantly different biophysical properties for sphingolipids containing short-chain sphingoid bases relative to long-chain sphingoid bases were suggested by Fyrst and coworkers, who characterized the long-chain bases of *Drosophila melanogaster* (84). They also suggested distinct effects of varying length sphingoid bases on membranes. In support of their hypothesis, our results showed a clear, length-dependent variation in the influences of the ceramides containing C12- to C20-sphingoid bases on the molecular order and lateral phase separation, as well as on the lateral distribution of cholesterol, in binary and more complex lipid mixtures. These findings agree in general with the effects of *N*-acyl chain length on the bilayer behavior of ceramides. Ceramides with long or intermediate long *N*-acyl chains (C10-C24) have been shown to phase separate and form high melting temperature ceramide-rich phases both in mixed SM/DOPC/cholesterol-bilayers (234) and in binary mixtures with dielaidoyl-PE (219) and dimyristoyl-PC (296).

In general, the results of all our studies performed with ceramide analogs implied that the ability of ceramides to effectively displace cholesterol from a PSM-rich environment was dependent on the ability of the ceramides to thermally stabilize the PSM-rich phase, inducing increased molecular order when half of the PSM-amount was replaced by a ceramide. Similarly, a ceramide-induced displacement of cholesterol from a SM-rich phase was proposed for ceramides with an *N*-acyl chain long enough to allow the formation of ceramide-rich gel phases that presumably also recruited SM (234).

If PCer is considered structurally symmetric in that its two acyl chains are equally long (in accordance with the calculations of Kodama and Kawasaki (297) demonstrating the symmetry of PSM), it then follows that an *N*-acyl chain *n* carbon atoms long corresponds to a $n + 2$ carbon atoms long sphingoid base. This assumption facilitates the comparison of the relative effects of varying length *N*-acyl chains to those of varying length long-chain bases. In fluid

dimyristoyl-PC monolayers, a ceramide with as short as C10 *N*-acyl chain was observed to laterally phase separate from the PC. A 10 carbons long *N*-acyl chain corresponds to a C12 long-chain base. However, in our studies, neither ceramides with C12 nor C14 long-chain bases phase-separated in fluid POPC-bilayers. Considering ceramide-induced displacement of cholesterol from a SM-rich environment, a minimum length of 8 carbons was required for the ceramide *N*-acyl chain (232), while the minimum length requirement for the long-chain base was significantly longer, 16 carbon atoms, in our study.

These observations suggest that lateral segregation of ceramides, as well as the ceramide-induced displacement of cholesterol, could be more sensitive to shortening of the long-chain base than the *N*-acyl chain. Thus, the two aliphatic chains of saturated ceramides, although being structurally identical at the membrane hydrophobic core, could display differences in their lateral packing and interlipid interactions in the core of the membrane owing to differences between the interfacial regions of the chains. As an example, shortening of the sphingosine base and the subsequent reduction in van der Waals' forces between the sphingosine and neighboring acyl chains could have induced orientational disorder about the $C_{4\text{-}5}$ *trans*-double bond which is an important factor in promoting close packing of ceramide acyl chains (189, 212), and has been suggested to play a role in stabilization of the intramolecular network of hydrogen bonds within ceramides (212, 214).

For the ceramides with short sphingoid bases the possibilities for van der Waals' interactions between the acyl chains are reduced relative to the ceramides with long sphingoid bases, which is a direct effect of the chain-mismatch. In SMs which experience chain-mismatch, rotational motions of the shorter chain have been suggested to exert disordering effects on the mismatched bonds of the longer chain that extends beyond the length of the shorter chain (297). This offered an explanation for SM-gel phases becoming destabilized when chain-mismatch occurs (298). In a similar way, the ceramides with mismatched acyl chains could have experienced perturbations in conformation, reducing their interlipid interactions. Moreover, for ceramides with mismatched chains, the terminal methyls have been suggested to occupy a larger volume relative to the terminal methyls of symmetric chains (299), reducing the degree of interlipid interactions. However, in monolayer studies ceramides with *N*-acyl chains from 10 to 16 carbons long were observed to exhibit nearly identical mean molecular areas (296), which challenges the hypothesis of a putative increase in the molecular volume of chain-mismatched sphingolipids.

Taken together, the length of the sphingoid base was shown to be a major determinant of the bilayer properties of ceramides, and in agreement with the proposal of Fyrst and coworkers (84), it could significantly influence the biophysical properties of ceramides in biological membranes. Variation in the chain-length of ceramides modulates their hydrophobicity and lateral organization in membranes, factors that could influence their translocation to distinct cellular compartments, as well as their specific functions therein. As an example, it was proposed that the increase in the abundance of C20 long-chain bases in neuronal gangliosides during aging, causing the ratio of C18 to C20 sphingoid bases to change, could induce alterations in the membrane properties of neurons, with possible implications in physiological or patholocigal processes (79).

6.2.3. 2N- and 3O-methylation of the sphingoid base

Replacing the hydrogen at 2N and 3O of the sphingoid base with a methyl group can be expected to increase the hydrophobicity and size of the interface region in PCer due to the more bulky and hydrophobic nature of a methyl group relative to a hydrogen. Furthermore, methylation of the interfacial functional groups attenuated hydrogen bonding through 2N and 3O. Our results showed that disruption of the interfacial properties of PCer at 2N and 3O differently influenced the molecular packing and the interlipid interactions of the ceramides. 2N-methylation was observed to prevent as tight intermolecular interactions that were observed for PCer and the 3O-methylated ceramide. This was manifested as a markedly reduced ability of the 2N-methylated ceramide to form highly ordered ceramide-rich phases.

Megha and coworkers conducted similar studies with ceramide analogs in which structural modifications were introduced in or near the head group region (252). In their study, a ceramide with a methyl group added to the C3 of the sphingoid base (preserving the C3-OH) was observed to form similar ordered domains as the unmodified ceramide. In the same study, the methyl group at the C3 did not appear to prevent the ceramide from displacing cholesterol from a SM-rich phase (252). These obervations agree with the largely unchanged capability of the 3O-methylated ceramide to form ceramide-rich gel phases and to displace cholesterol from a PSM-rich environment relative to PCer observed in our study. The 3O-methylation was also unlikely to disturb the local conformation around the $C_{4\text{-}5}$ double bond in the sphingoid base, which has been found to play an important role in allowing the tight acyl chain packing in sphingosine-based ceramides (189, 212).

Several models for hydrogen bonding in ceramides have been deduced based on experimental data (129, 211, 212, 214), computational theoretical calculations (215) and molecular dynamics simulations (213, 300). In light of these studies, it seems that the amide-nitrogen and the hydroxyl groups in ceramides participate in both intra- and intermolecular hydrogen bonds. However, our experiments with the 2N- and 3O-methylated ceramides indicated a more critical role for the 2NH of ceramides in their interlipid interactions. Such a conclusion agrees with the observation that in SM the NH-group is the sole hydrogen bond donor in interlipid interactions (196). Accordingly, disrupting the sole hydrogen bond-donor function in the sphingosine base (2NH) would influence the interlipid interactions to a greater degree than disrupting one of the several hydrogen bond-acceptor functions (3OH).

The 3OH in sphingosine, sticking out from the molecular structure of ceramide, is probably more flexible, and thus less sensitive to structural alterations than the 2NH, which is a part of the rigid amide link connecting the sphingosine to the *N*-acyl chain. Thus, distortion of the 2NH can be expected to influence the biophysical properties of ceramides to a greater degree than distortion of the 3OH, which was also clearly shown in our study. In addition, in a similar study about the bilayer properties of 2N- and 3O-methylated PSM-analogs, the 2N-methyl was demonstrated to be buried deeper in the bilayer than the unmodified 2NH or the 3O-methyl (301). If this were the case also for the 2N- and 3O-methylated ceramides, the 2N-methyl could have had a greater effect on the lateral packing of the ceramides, which could (at least partly) explain the observed differences between the interfacially methylated ceramides in their lateral distribution and interlipid interactions. Indeed, when Perera and coworkers used identical 2N- and 3O-methylated PCer-analogs to investigate the role of hydrogen bonding via these two functional groups in the formation of transmembrane ceramide channels, they found that the 2N-methylated ceramide displayed drastically reduced ability to pack into channels, whereas such a reduction was not observed for the 3O-methylated ceramide (302).

The results from the PSM-analog study mentioned earlier showed that the 2N-methylation had the largest effect on the thermal stability of the SM-gel phase, while the formation of SM/cholesterol-rich ordered phases was influenced to a greater extent by the 3O-methylation (301). It was also observed that the 3O-methylation markedly affected the head group dynamics of SM and increased the contact of cholesterol with water (301). In keeping with the umbrella model (170) this could have explained the observed decrease in SM/cholesterol-interactions. Interestingly, our unpublished data from

experiments that were performed in order to study how the interfacially methylated SM-analogs interacted with PCer showed that the SM/ceramide-interactions were affected more by the 2N-methylation than the 3O-methylation of SM. This, together with the results presented in this thesis, suggest that sphingolipid-sphingolipid interactions involving the amide-nitrogen are important for the cohesive properties of sphingolipids. Furthermore, the apparent differences between ceramide and cholesterol in their interactions with the interfacially methylated SMs suggested that the ceramide/SM-interactions might not be as dependent on the umbrella effect as cholesterol/SM-interactions.

### 6.3. Structural modification of the SM-head group

The importance of a phospholipid head group in shielding the hydrophobic body of other membrane lipids, with significantly smaller head groups, from unfavorable exposure to aqueous environment was initially proposed for phospholipid/cholesterol-interactions in the umbrella model (170, 303). In agreement with the proposed model, the SM-head group was found crucial for SM/cholesterol-interactions in a study that compared the interlipid interactions between cholesterol and PSM relative to SM-analogs in which the head group size was reduced by a stepwise removal of methyl groups from the phosphocholine-moiety (210). The formation of SM/cholesterol-rich ordered domains, as well as the bilayer affinity of cholesterol, were reduced in the presence of the SM-head group analogs (210).

Similarly to cholesterol, the small hydroxyl head can be expected to have limited ability to shield the hydrophobic body of ceramides from unfavorable interactions with water. However, it should be noted that although neither cholesterol nor ceramides are able to form bilayer structures alone, the lateral segregation of ceramides into ceramide-rich domains poor in glycerophospholipids in bilayers indicates that ceramides are less dependent on a possible umbrella effect. Instead, the aversion of saturated ceramides for unsaturated glycerophospholipids could be the main driving force for the lateral segregation of ceramides. Moreover, glycerophospholipids, with their lower ability to formation of hydrogen bonds relative to sphingolipids, are not able to efficiently participate in the hydrogen bond network of ceramides, which could also contribute to the lateral segregation of ceramides from glycerophospholipids.

In contrast to the aversion of unsaturated glycerophospholipids, ceramides display favorable interactions with SMs, resulting in the formation of ceramide/SM-rich ordered or gel phase domains in fluid bilayers (169, 231). Similarly to cholesterol/SM-interaction, for which the SM-head group is of

crucial importance (210), accommodation of ceramide under the phosphocholine head group of SM could partly stabilize their interactions. However, we observed no marked effects on the thermal stability or molecular order of the ceramide/SM-rich domains when the SM-head group size was reduced.

If the ceramide/SM-interaction was strongly dependent on the SM-head group size, then removal of methyl groups from the SM-phosphocholine, and the subsequent decreased ability of the SM-head group to function as an umbrella, could have been expected to reduce the interactions between PCer and the SM-analogs. In a recent molecular dynamics simulation study it was suggested that the umbrella effect becomes significant for SM/ceramide-interactions when the amount of ceramide exceeds the amount of SM in the system (249). This could explain the lack of dependence on the umbrella effect in our study, as in the mixtures that were studied the ceramide/SM molar ratio never exceeded 1. On the other hand, removing methyl groups from the PSM-head group was previously shown to decrease the molecular area and increase the acyl chain order of SM (210). Consequently, as the role of the head group as a limiting factor in lateral packing was reduced, the $T_m$ of the pure SM-analogs increased in relation to a decrease in the head group size (210). In keeping with this, the SM-analogs could have been expected to increase the thermal stability and molecular order of the ceramide-rich domains relative to PSM. However, such an effect was not observed, indicating that although a decrease in the head group size increased the SM-acyl chain order, it did not seem to promote increased lateral packing within ceramide/SM-rich domains.

In our study, small head group lipids with saturated chains (PCer and DPG) were observed to cosegregate with saturated phospholipids (SM-analogs and PC-analogs) irrespective of the size of the phospholipid head group. This suggests that the association of saturated acyl chains was entropically favored. In support of this conclusion, sphingolipids have been shown to favorably partition into ordered phases regardless of the polar head structure (247). From such an observation, it was concluded that the inherent affinity of sphingolipids for ordered phases originates primarily from the nature of their ceramide moiety, rather than from special features of their head groups. Due to differences in the interface structure of SMs and PCs, the capability of PCs to participate in interlipid hydrogen bonding is reduced relative to SMs (196). In line with this, the pure PC-analogs displayed constantly lower $T_m$:s than the SM-analogs (210). A possible role for hydrogen bonds in stabilization of the SM-ceramide interactions was indicated in our study, since replacing the SM-analogs with

analogous saturated PC-analogs caused a decrease in the thermal stability of the ceramide/co-lipid domains.

Altogether, any stabilizing effect arising from increased acyl chain packing as the SM-head group size was reduced could have been counterbalanced by a destabilizing effect arising from disturbed head group-interactions, and vice versa. Nonetheless, the SM-head group did not appear to strongly participate in the SM/ceramide-interaction. Instead, entropic contribution from the favored interaction of saturated acyl chains that interact through van der Waals' forces seemed dominant in controlling the interlipid interactions of ceramides and SMs, with some contribution from interfacial hydrogen bonding.

## 6.4. General aspects of the studies

Summarizing the results from the studies that included structurally modified ceramides (papers II-IV) reveals that in addition to PCer, the 20:1-PCer (in which the sphingoid base was 2 carbons longer relative to PCer) and OMeCer (in which the 3O of the PCer-sphingoid base was methylated) were the only ceramides that were able to thermally stabilize PSM-rich domains (when half of the PSM amount in multicomponent bilayers was replaced by one the ceramides). These ceramides were also the only ones able to effectively displace cholesterol from PSM/ceramide-rich domains, which is indicative of a dependency of the displacing-ability on the capability to thermally stabilize the PSM-rich phase. Such a thermal stabilization would be mediated by an increase in the molecular order of the domains induced by the ceramides, which was observed to occur in the presence of the above mentioned ceramides. However, even 16:1-PCer (with a 16 carbons long sphingoid base) and NMeCer (in which the 2N of the PCer-sphingoid base was methylated) were able to form gel phases in fluid POPC-bilayers, as well as to increase the order of the PSM-rich domains (when half of the PSM was replaced by these ceramides). These ceramides were, however, not able to effectively displace cholesterol from those domains, nor to thermally stabilize the PSM-rich domains. These observations suggest that although 16:1-PCer and NMeCer exhibited a relatively ordered nature, their interactions with PSM were markedly reduced, and they were not able to compete with cholesterol so as to displace it.

In the lack of thoughrough biophysical characterization of the complex mixtures containing the ceramide analogs, the complete phase behavior and the relative amounts of ordered or gel phases compared to fluid phase in the bilayers are not known. This fact in some cases complicates the interpretation of the results presented in this thesis. Especially for such analogs that displayed a more

fluid nature relative to PCer, with subsequent inability to recruit PSM to highly ordered gel phases that displace cholesterol, the lateral distribution in the complex bilayers remains unresolved. Such ceramides could either be excluded from PSM/cholesterol-rich phases, or coexist within such phases.

It should be noted that the studies presented in this thesis were conducted with a limited variety of binary and quaternary compositions. The effects of ceramides on lipid lateral distribution in membranes is highly dependent on the relative concentrations of ceramide and cholesterol. High contents of cholesterol are known to destabilize (255, 258) as well as to solubilize (179, 181) ceramide rich gel phases. However, the aim of the presented studies was to compare the bilayer behavior of the structurally modified ceramides to that of PCer, with emphasis on the formation of ceramide(/SM)-rich gel phases and the subsequent effects on the membrane lateral distribution of cholesterol. Thus, bilayer compositions in which such phenomena in principle could be observed were selected.

## 6.5. Ceramide and cholesterol, competitors or interplayers?

Ceramide-induced alterations in the membrane lateral localization of cholesterol was one of the main features of the ceramide analogs studied in this thesis. In keeping with this, the underlying molecular-level driving force for the ceramide-induced effects on cholesterol distribution deserve to be discussed. Ceramides and cholesterol have well-documented mutual effects on each other in membranes, with two main phenomena identified depending on the composition of the membranes: *i)* a ceramide-induced displacement of cholesterol from highly ordered phases, and *ii)* a cholesterol-induced destabilization and solubilization of ceramide-rich phases (see *section 2.7.3.*). In general, the former phenomenon predominates in membranes displaying low cholesterol content, whereas the latter is effective at high cholesterol content.

It has been reported, based on X-ray diffraction experiments, that as soon as the ceramide/SM ratio exceeds 1 in POPC/SM/PCer/cholesterol-bilayers ceramide starts to form membrane-insoluble crystallites (257). This was interpreted as a limited ability of the SM/ceramide-rich gel phase to recruit POPC-molecules due to their preferential interaction with cholesterol over ceramide. In that study the relative amount of POPC equaled the total amount of sphingolipid. In another study the affinity for POPC-bilayers was shown the be higher for ceramide than for cholesterol, and at the solubility limit of ceramide (67 mol%) addition of cholesterol resulted in formation of membrane insoluble cholesterol crystals (254). Formation of ceramide or cholesterol crystals, as well

as limitations in the formation of sphingolipid-rich gel phases due to POPC, are unlikely to have occurred in the quaternary mixtures examined in our studies since the ceramide/SM ratio never exceeded 1, and the relative amount of POPC was double to that of total sphingolipid and sixfold relative to cholesterol. Though, it cannot be precluded that in other membrane compositions, especially in the presence of higher amounts of cholesterol, the relative differences in bilayer behavior between the ceramide analogs and PCer could have been more pronounced. Correspondingly, at lower relative amounts of cholesterol more subtle differences might have been observed.

It was initially proposed that the driving force for the ceramide-induced displacement of cholesterol from ordered phases resides in the high degree of molecular packing in the ceramide-rich ordered phases causing cholesterol to be excluded from those, and/or in the competition between ceramide and cholesterol for an umbrella effect mediated by a phospholipid (250). In light of our studies, showing that ceramide is not similarly dependent on the SM-head group as cholesterol, and that the tight ceramide/SM-interaction is mainly mediated by their saturated acyl chains, a more prominent role for chain packing relative to competition for an umbrella seems likely.

It is clear from the literature that the influences that cholesterol and ceramide have on each other in membranes are complex and highly dependent on the membrane composition (see *section 2.7.3.*). The initial models of displacement of cholesterol by ceramide, or ceramide-gel phase solubilization by cholesterol, are starting to become challenged by a model in which, at certain conditions, ceramides and cholesterol are able to interact and colocalize in membranes. In the absence of a fluid phase, SM, cholesterol and ceramide have been reported to form a single, ternary phase, in which all the lipids coexist (256). Moreover, cholesterol has been shown to increase the miscibility of ceramide with glycerophospholipids (181, 304). Interestingly, specific antibodies raised against cholesterol/ceramide-complexes (that do not recognize these two lipids if not complexed, nor induce complex formation *per se*) have been used to detect colocalized ceramide and cholesterol in late endosomes and in Golgi membranes in cells (305-307). In line with the low levels of ceramide in plasma membranes, no antibody binding was observed at the plasma membrane (307). However, it would be interesting to see if any antibody binding to the plasma membrane is observed if ceramide generation in the plasma membrane was stimulated by SM-hydrolysis. At least in the stratum corneum of mammalian skin, which contains high levels of ceramides and cholesterol, these two lipids closely interact to contribute to the permeability barrier (25, 26).

Based on observations from model membrane studies, ceramides induce significant alterations in membrane properties already at low concentrations. Ceramides increase the molecular order of membranes and induce curvature effects with resultant alterations in membrane structure and the lateral distribution of other membrane components. The cellular plasma membrane plays pivotal roles in vesiculation processes and in cell-cell communication, and is centrally involved in cellular signal transmission and substance transport. Moreover, the plasma membrane is connected to the cellular cytoskeleton, to which many signaling proteins are intimately linked. Thus, even subtle alterations in the levels of ceramides, with resultant changes in the organization or topology of the plasma membrane, could have significant influences on cellular physiology and signaling processes.

The biological functions of ceramide-rich domains in cellular membranes could include direct trapping of certain signaling proteins within such domains, facilitating their interactions with other proteins of signaling cascades, as well as the alteration of the general biophysical properties of membranes, influencing regions in close vicinity to the highly ordered ceramide-rich domains. As an example, it has been shown that the raft-associated phosphatase GPI-PLAP and ganglioside GM1 become enriched in ceramide-rich domains in model membranes, exhibiting reduced lateral diffusion within the domains (109). Ceramides also induce alterations in the bending ridigity of fluid membranes, with putative influence on the membrane lateral pressure profile and subsequently on the activity of e.g., membrane ion channels (257, 308). This serves as an example of a ceramide-induced alteration in the general biophysical properties of a membrane, with resultant influence on the activity of non-raft proteins.

Although techniques have been developed in order to allow similar studies to be performed in cellular membranes as in model membranes, the significantly more complex and dynamic nature of cellular membranes complicates as detailed, molecular-level studies. The strong dependence of lipid (and protein) lateral distribution and intermolecular interactions on the composition of a membrane, as well as the marked effects that certain, relatively small variations in lipid structure possess on the bilayer behavior of lipids as demonstrated in this thesis, augment the complexity of intermolecular interactions in membranes. This complexity is even greater in cellular membranes, in which thousands of lipid species exist together with a variety of membrane-associated proteins and cytoskeletal components, adding to the network of intermolecular interactions.

## 7. CONCLUSIONS

The resistance of ceramide-rich gel phase domains to fluidization by benzyl alcohol observed in paper I was related to the high degree of intermolecular cohesion and lateral packing within the domains. Based on the observations in papers II-IV, these properties are strongly dependent on the molecular structure of ceramides. Structural features that contribute to the cohesive properties of ceramides in bilayer membranes are: *i)* effective lateral packing of the *N*-acyl chain, which is more sensitive to packing defects in the mid part relative to the terminal end, *ii)* matching hydrophobic length of the *N*-acyl chain and the sphingoid base, of which the latter, at certain circumstances, seems more sensitive to shortening of its effective length, and *iii)* the interlipid interactions mediated via the amide-nitrogen (Fig. 16). Therefore, natural ceramides with a sphingoid base shorter than 18 carbon atoms, or with methyl-branched acyl chains, are expected to display a markedly more fluid nature in cellular membranes compared to long-chain, unbranched ceramides.

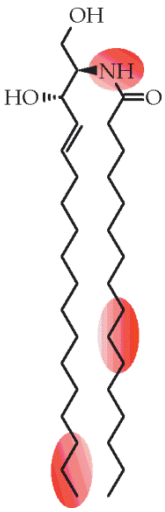


***Figure 16.*** *Regions in ceramide structure found most sensitive to structural alterations in this thesis. Methyl-branching of the N-acyl chain was studied in paper II, the length of the sphingoid base was issued in paper III, and the roles of 2NH and 3OH in the interfacial interactions were investigated in paper IV.*

Based on the results in paper V, ceramide/SM-interactions are mainly stabilized by ceramides' aversion for unsaturated lipids and the attractive van der Waals' forces between the acyl chains of the two saturated sphingolipids. Some contribution to the interactions between ceramides and SMs can be concluded to stem from hydrogen bonding, while the SM-head group does not appear to strongly participate in the interactions. In this respect, the ceramide-SM interaction differs markedly from the cholesterol-SM interaction which is

stabilized, to a significant degree, by the umbrella effect mediated by the SM-head group.

As demonstrated in this thesis, the molecular structure of ceramides determine the influences that these lipids exert on the lateral distribution of other membrane lipids and the membrane biophysical properties. In keeping with this, differences in the bilayer behavior and membrane effects of structurally distinct ceramides could relate to specific biological functions in distinct cell or tissue types.

# REFERENCES


1. Yeagle, P. L. 2005. The structure of biological membranes. CRC Press, Boca Raton, FL.

2. Spiegel, S., D. Foster, and R. Kolesnick. 1996. Signal transduction through lipid second messengers. Curr. Opin. Cell Biol. 8: 159-167.

3. Eyster, K. M. 2007. The membrane and lipids as integral participants in signal transduction: lipid signal transduction for the non-lipid biochemist. Adv. Physiol Educ. 31: 5-16.

4. Kinnunen, P. K. 1991. On the principles of functional ordering in biological membranes. Chem. Phys. Lipids 57: 375-399.

5. Kinnunen, P. K., A. Koiv, J. Y. Lehtonen, M. Rytomaa, and P. Mustonen. 1994. Lipid dynamics and peripheral interactions of proteins with membrane surfaces. Chem. Phys. Lipids 73: 181-207.

6. Holopainen, J. M. 2001. Ceramide - a messenger of cell death. A biophysical approach. Institute of biomedicine, Biomedicum Helsinki, University of Helsinki, Helsinki.

7. Futerman, A. H. 2002. Ceramide Signaling. Kluwer Academic/Plenum Publishers, New York, USA.

8. Kolesnick, R. N., F. M. Goni, and A. Alonso. 2000. Compartmentalization of ceramide signaling: physical foundations and biological effects. J. Cell Physiol 184: 285-300.

9. Cremesti, A. E., F. M. Goni, and R. Kolesnick. 2002. Role of sphingomyelinase and ceramide in modulating rafts: do biophysical properties determine biologic outcome? FEBS Lett. 531: 47-53.

10. Bollinger, C. R., V. Teichgraber, and E. Gulbins. 2005. Ceramide-enriched membrane domains. Biochim. Biophys. Acta 1746: 284-294.

11. Zhang, Y., X. Li, K. A. Becker, and E. Gulbins. 2009. Ceramide-enriched membrane domains--structure and function. Biochim. Biophys. Acta 1788: 178-183.

12. Stancevic, B., and R. Kolesnick. 2010. Ceramide-rich platforms in transmembrane signaling. FEBS Lett. 584: 1728-1740.

13. Grassme, H., A. Jekle, A. Riehle, H. Schwarz, J. Berger, K. Sandhoff, R. Kolesnick, and E. Gulbins. 2001. CD95 signaling via ceramide-rich membrane rafts. J. Biol. Chem. 276: 20589-20596.

14. Grassme, H., H. Schwarz, and E. Gulbins. 2001. Molecular mechanisms of ceramide-mediated CD95 clustering. Biochem. Biophys. Res. Commun. 284: 1016-1030.

15. Grassme, H., V. Jendrossek, J. Bock, A. Riehle, and E. Gulbins. 2002. Ceramide-rich membrane rafts mediate CD40 clustering. J. Immunol. 168: 298-307.

16. van Meer, G., D. R. Voelker, and G. W. Feigenson. 2008. Membrane lipids: where they are and how they behave. Nat. Rev. Mol. Cell Biol. 9: 112-124.

17. Dougherty, R. M., C. Galli, A. Ferro-Luzzi, and J. M. Iacono. 1987. Lipid and phospholipid fatty acid composition of plasma, red blood cells, and platelets and how they are affected by dietary lipids: a study of normal subjects from Italy, Finland, and the USA. Am. J. Clin. Nutr. 45: 443-455.

18. Barenholz, Y., and T. E. Thompson. 1999. Sphingomyelin: biophysical aspects. Chem. Phys. Lipids 102: 29-34.

19. Pruett, S. T., A. Bushnev, K. Hagedorn, M. Adiga, C. A. Haynes, M. C. Sullards, D. C. Liotta, and A. H. Merrill, Jr. 2008. Biodiversity of sphingoid bases ("sphingosines") and related amino alcohols. J. Lipid Res. 49: 1621-1639.

20. Barenholz, Y., and T. E. Thompson. 1980. Sphingomyelins in bilayers and biological membranes. Biochim. Biophys. Acta 604: 129-158.

21. Tettamanti, G. 2004. Ganglioside/glycosphingolipid turnover: new concepts. Glycoconj. J. 20: 301-317.

22. Kishimoto, Y., and N. Kawamura. 1979. Ceramide metabolism in brain. Mol. Cell Biochem. 23: 17-25.

23. Ikonen, E., and M. Jansen. 2008. Cellular sterol trafficking and metabolism: spotlight on structure. Curr. Opin. Cell Biol. 20: 371-377.

24. Rog, T., M. Pasenkiewicz-Gierula, I. Vattulainen, and M. Karttunen. 2009. Ordering effects of cholesterol and its analogues. Biochim. Biophys. Acta 1788: 97-121.

25. Norlen, L., I. Plasencia, and L. Bagatolli. 2008. Stratum corneum lipid organization as observed by atomic force, confocal and two-photon excitation fluorescence microscopy. Int. J. Cosmet. Sci. 30: 391-411.

26. van Smeden, J., M. Janssens, G. S. Gooris, and J. A. Bouwstra. 2013. The Important Role of Stratum Corneum Lipids for the Cutaneous Barrier Function. Biochim. Biophys. Acta In Press.

27. Merrill, A. H., Jr. 2002. De novo sphingolipid biosynthesis: a necessary, but dangerous, pathway. J. Biol. Chem. 277: 25843-25846.

28. Gault, C. R., L. M. Obeid, and Y. A. Hannun. 2010. An overview of sphingolipid metabolism: from synthesis to breakdown. Adv. Exp. Med. Biol. 688: 1-23.

29. Hanada, K. 2003. Serine palmitoyltransferase, a key enzyme of sphingolipid metabolism. Biochim. Biophys. Acta 1632: 16-30.

30. Kihara, A., and Y. Igarashi. 2004. FVT-1 is a mammalian 3-ketodihydrosphingosine reductase with an active site that faces the cytosolic side of the endoplasmic reticulum membrane. J. Biol. Chem. 279: 49243-49250.

31. Mullen, T. D., Y. A. Hannun, and L. M. Obeid. 2012. Ceramide synthases at the centre of sphingolipid metabolism and biology. Biochem. J. 441: 789-802.

32. Geeraert, L., G. P. Mannaerts, and P. P. Van Veldhoven. 1997. Conversion of dihydroceramide into ceramide: involvement of a desaturase. Biochem. J. 327 ( Pt 1): 125-132.

33. Mizutani, Y., A. Kihara, and Y. Igarashi. 2004. Identification of the human sphingolipid C4-hydroxylase, hDES2, and its up-regulation during keratinocyte differentiation. FEBS Lett. 563: 93-97.

34. Watson, P., and D. J. Stephens. 2005. ER-to-Golgi transport: form and formation of vesicular and tubular carriers. Biochim. Biophys. Acta 1744: 304-315.

35. Hanada, K., K. Kumagai, N. Tomishige, and M. Kawano. 2007. CERT and intracellular trafficking of ceramide. Biochim. Biophys. Acta 1771: 644-653.

36. Kumagai, K., M. Kawano, F. Shinkai-Ouchi, M. Nishijima, and K. Hanada. 2007. Interorganelle trafficking of ceramide is regulated by phosphorylation-dependent cooperativity between the PH and START domains of CERT. J. Biol. Chem. 282: 17758-17766.

37. Kudo, N., K. Kumagai, N. Tomishige, T. Yamaji, S. Wakatsuki, M. Nishijima, K. Hanada, and R. Kato. 2008. Structural basis for specific lipid recognition by CERT responsible for nonvesicular trafficking of ceramide. Proc. Natl. Acad. Sci. U. S. A 105: 488-493.

38. Hanada, K., K. Kumagai, S. Yasuda, Y. Miura, M. Kawano, M. Fukasawa, and M. Nishijima. 2003. Molecular machinery for non-vesicular trafficking of ceramide. Nature 426: 803-809.

39. Klemm, R. W., C. S. Ejsing, M. A. Surma, H. J. Kaiser, M. J. Gerl, J. L. Sampaio, R. Q. de, C. Ferguson, T. J. Proszynski, A. Shevchenko, and K. Simons. 2009. Segregation of sphingolipids and sterols during formation of secretory vesicles at the trans-Golgi network. J. Cell Biol. 185: 601-612.

40. van Meer, G., E. H. Stelzer, R. W. Wijnaendts-van-Resandt, and K. Simons. 1987. Sorting of sphingolipids in epithelial (Madin-Darby canine kidney) cells. J. Cell Biol. 105: 1623-1635.

41. Simons, K., and G. van Meer. 1988. Lipid sorting in epithelial cells. Biochemistry 27: 6197-6202.

42. van Meer, G., and K. Simons. 1988. Lipid polarity and sorting in epithelial cells. J. Cell Biochem. 36: 51-58.

43. van Meer, G., and J. C. Holthuis. 2000. Sphingolipid transport in eukaryotic cells. Biochim. Biophys. Acta 1486: 145-170.

44. Milhas, D., C. J. Clarke, and Y. A. Hannun. 2010. Sphingomyelin metabolism at the plasma membrane: implications for bioactive sphingolipids. FEBS Lett. 584: 1887-1894.

45. Marchesini, N., and Y. A. Hannun. 2004. Acid and neutral sphingomyelinases: roles and mechanisms of regulation. Biochem. Cell Biol. 82: 27-44.

46. Tani, M., Y. Igarashi, and M. Ito. 2005. Involvement of neutral ceramidase in ceramide metabolism at the plasma membrane and in extracellular milieu. J. Biol. Chem. 280: 36592-36600.

47. Kitatani, K., J. Idkowiak-Baldys, and Y. A. Hannun. 2008. The sphingolipid salvage pathway in ceramide metabolism and signaling. Cell Signal. 20: 1010-1018.

48. Gillard, B. K., R. G. Clement, and D. M. Marcus. 1998. Variations among cell lines in the synthesis of sphingolipids in de novo and recycling pathways. Glycobiology 8: 885-890.

49. Tettamanti, G., R. Bassi, P. Viani, and L. Riboni. 2003. Salvage pathways in glycosphingolipid metabolism. Biochimie 85: 423-437.

50. Sabourdy, F., B. Kedjouar, S. C. Sorli, S. Colie, D. Milhas, Y. Salma, and T. Levade. 2008. Functions of sphingolipid metabolism in mammals--lessons from genetic defects. Biochim. Biophys. Acta 1781: 145-183.

51. Dawkins, J. L., D. J. Hulme, S. B. Brahmbhatt, M. Auer-Grumbach, and G. A. Nicholson. 2001. Mutations in SPTLC1, encoding serine palmitoyltransferase, long chain base subunit-1, cause hereditary sensory neuropathy type I. Nat. Genet. 27: 309-312.

52. Levy, M., and A. H. Futerman. 2010. Mammalian ceramide synthases. IUBMB. Life 62: 347-356.

53. Venkataraman, K., C. Riebeling, J. Bodennec, H. Riezman, J. C. Allegood, M. C. Sullards, A. H. Merrill, Jr., and A. H. Futerman. 2002. Upstream of growth and differentiation factor 1 (uog1), a

mammalian homolog of the yeast longevity assurance gene 1 (LAG1), regulates N-stearoyl-sphinganine (C18-(dihydro)ceramide) synthesis in a fumonisin B1-independent manner in mammalian cells. J. Biol. Chem. 277: 35642-35649.

54. Laviad, E. L., L. Albee, I. Pankova-Kholmyansky, S. Epstein, H. Park, A. H. Merrill, Jr., and A. H. Futerman. 2008. Characterization of ceramide synthase 2: tissue distribution, substrate specificity, and inhibition by sphingosine 1-phosphate. J. Biol. Chem. 283: 5677-5684.

55. Riebeling, C., J. C. Allegood, E. Wang, A. H. Merrill, Jr., and A. H. Futerman. 2003. Two mammalian longevity assurance gene (LAG1) family members, trh1 and trh4, regulate dihydroceramide synthesis using different fatty acyl-CoA donors. J. Biol. Chem. 278: 43452-43459.

56. Mizutani, Y., A. Kihara, and Y. Igarashi. 2005. Mammalian Lass6 and its related family members regulate synthesis of specific ceramides. Biochem. J. 390: 263-271.

57. Mizutani, Y., A. Kihara, and Y. Igarashi. 2006. LASS3 (longevity assurance homologue 3) is a mainly testis-specific (dihydro)ceramide synthase with relatively broad substrate specificity. Biochem. J. 398: 531-538.

58. Mizutani, Y., A. Kihara, H. Chiba, H. Tojo, and Y. Igarashi. 2008. 2-Hydroxy-ceramide synthesis by ceramide synthase family: enzymatic basis for the preference of FA chain length. J. Lipid Res. 49: 2356-2364.

59. O'Brien, J. S., and G. Rouser. 1964. The fatty acid composition of brain sphingolipids: sphingomyelin, ceramide, cerebroside, and cerebroside sulfate. J. Lipid Res. 5: 339-342.

60. Fahy, E., S. Subramaniam, H. A. Brown, C. K. Glass, A. H. Merrill, Jr., R. C. Murphy, C. R. Raetz, D. W. Russell, Y. Seyama, W. Shaw, T. Shimizu, F. Spener, G. van Meer, M. S. VanNieuwenhze, S. H. White, J. L. Witztum, and E. A. Dennis. 2005. A comprehensive classification system for lipids. J. Lipid Res. 46: 839-861.

61. Farwanah, H., B. Pierstorff, C. E. Schmelzer, K. Raith, R. H. Neubert, T. Kolter, and K. Sandhoff. 2007. Separation and mass spectrometric characterization of covalently bound skin ceramides using LC/APCI-MS and Nano-ESI-MS/MS. J. Chromatogr. B Analyt. Technol. Biomed. Life Sci. 852: 562-570.

62. Robinson, B. S., D. W. Johnson, and A. Poulos. 1992. Novel molecular species of sphingomyelin containing 2-hydroxylated polyenoic very-long-chain fatty acids in mammalian testes and spermatozoa. J. Biol. Chem. 267: 1746-1751.

63. Hara, A., and T. Taketomi. 1975. Long chain base and fatty acid compositions of equine kidney sphingolipids. J. Biochem. 78: 527-536.

64. Yasugi, E., T. Kasama, and Y. Seyama. 1991. Composition of long chain bases in ceramide of the guinea pig Harderian gland. J. Biochem. 110: 202-206.

65. Ardail, D., I. Popa, K. Alcantara, A. Pons, J. P. Zanetta, P. Louisot, L. Thomas, and J. Portoukalian. 2001. Occurrence of ceramides and neutral glycolipids with unusual long-chain base composition in purified rat liver mitochondria. FEBS Lett. 488: 160-164.

66. Karlsson, K. A., and B. E. Samuelsson. 1974. The structure of ceramide aminoethylphosphonate from the sea anemone, Metridium senile. Biochim. Biophys. Acta 337: 204-213.

67. Tanaka, I., I, S. Matsuoka, M. Murata, and K. Tachibana. 1998. A new ceramide with a novel branched-chain fatty acid isolated from the epiphytic dinoflagellate coolia monotis. J. Nat. Prod. 61: 685-688.

68. Tian, X. R., H. F. Tang, Y. S. Li, H. W. Lin, N. Ma, W. Zhang, and M. N. Yao. 2009. Ceramides and cerebrosides from the marine bryozoan Bugula neritina inhabiting South China Sea. J. Asian Nat. Prod. Res. 11: 1005-1012.

69. Yasugi, E., T. Kasama, and Y. Seyama. 1987. Branched long chain bases in cerebrosides of the guinea pig Harderian gland. J. Biochem. 102: 1477-1482.

70. Oku, H., K. Mimura, Y. Tokitsu, K. Onaga, H. Iwasaki, and I. Chinen. 2000. Biased distribution of the branched-chain fatty acids in ceramides of vernix caseosa. Lipids 35: 373-381.

71. Yasugi, E., T. Kasama, and Y. Seyama. 1988. Identification of 10-methylsphinganine in cerebrosides of the guinea pig harderian gland. J. Biochem. 103: 889-893.

72. Byrdwell, W. C., and R. H. Perry. 2007. Liquid chromatography with dual parallel mass spectrometry and 31P nuclear magnetic resonance spectroscopy for analysis of sphingomyelin and dihydrosphingomyelin. II. Bovine milk sphingolipids. J. Chromatogr. A 1146: 164-185.

73. Omae, F., M. Miyazaki, A. Enomoto, M. Suzuki, Y. Suzuki, and A. Suzuki. 2004. DES2 protein is responsible for phytoceramide biosynthesis in the mouse small intestine. Biochem. J. 379: 687-695.

74. Williams, R. D., E. Wang, and A. H. Merrill, Jr. 1984. Enzymology of long-chain base synthesis by liver: characterization of serine palmitoyltransferase in rat liver microsomes. Arch. Biochem. Biophys. 228: 282-291.

75. Merrill, A. H., Jr., D. W. Nixon, and R. D. Williams. 1985. Activities of serine palmitoyltransferase (3-ketosphinganine synthase) in microsomes from different rat tissues. J. Lipid Res. 26: 617-622.

76. Merrill, A. H., Jr., E. Wang, and R. E. Mullins. 1988. Kinetics of long-chain (sphingoid) base biosynthesis in intact LM cells: effects of varying the extracellular concentrations of serine and fatty acid precursors of this pathway. Biochemistry 27: 340-345.

77. Merrill, A. H., Jr., and R. D. Williams. 1984. Utilization of different fatty acyl-CoA thioesters by serine palmitoyltransferase from rat brain. J. Lipid Res. 25: 185-188.

78. Pons, A., P. Timmerman, Y. Leroy, and J. P. Zanetta. 2002. Gas-chromatography/mass-spectrometry analysis of human skin constituents as heptafluorobutyrate derivatives with special reference to long-chain bases. J. Lipid Res. 43: 794-804.

79. Sonnino, S., and V. Chigorno. 2000. Ganglioside molecular species containing C18- and C20-sphingosine in mammalian nervous tissues and neuronal cell cultures. Biochim. Biophys. Acta 1469: 63-77.

80. Keranen, A. 1976. Fatty acids and long-chain bases of gangliosides of human gastrointestinal mucosa. Chem. Phys. Lipids 17: 14-21.

81. Karlsson, A. A., P. Michelsen, and G. Odham. 1998. Molecular species of sphingomyelin: determination by high-performance liquid chromatography/mass spectrometry with electrospray and high-performance liquid chromatography/tandem mass spectrometry with atmospheric pressure chemical ionization. J. Mass Spectrom. 33: 1192-1198.

82. Ramstedt, B., P. Leppimaki, M. Axberg, and J. P. Slotte. 1999. Analysis of natural and synthetic sphingomyelins using high-performance thin-layer chromatography. Eur. J. Biochem. 266: 997-1002.

83. Wiegandt, H. 1992. Insect glycolipids. Biochim. Biophys. Acta 1123: 117-126.

84. Fyrst, H., D. R. Herr, G. L. Harris, and J. D. Saba. 2004. Characterization of free endogenous C14 and C16 sphingoid bases from Drosophila melanogaster. J. Lipid Res. 45: 54-62.

85. Gulbins, E. 2003. Regulation of death receptor signaling and apoptosis by ceramide. Pharmacol. Res. 47: 393-399.

86. Mathias, S., L. A. Pena, and R. N. Kolesnick. 1998. Signal transduction of stress via ceramide. Biochem. J. 335 ( Pt 3): 465-480.

87. Pushkareva, M., L. M. Obeid, and Y. A. Hannun. 1995. Ceramide: an endogenous regulator of apoptosis and growth suppression. Immunol. Today 16: 294-297.

88. Hannun, Y. A. 1996. Functions of ceramide in coordinating cellular responses to stress. Science 274: 1855-1859.

89. Jenkins, G. M. 2003. The emerging role for sphingolipids in the eukaryotic heat shock response. Cell Mol. Life Sci. 60: 701-710.

90. Hannun, Y. A., and C. Luberto. 2000. Ceramide in the eukaryotic stress response. Trends Cell Biol. 10: 73-80.

91. Thomas, R. L., Jr., C. M. Matsko, M. T. Lotze, and A. A. Amoscato. 1999. Mass spectrometric identification of increased C16 ceramide levels during apoptosis. J. Biol. Chem. 274: 30580-30588.

92. Ruvolo, P. P. 2003. Intracellular signal transduction pathways activated by ceramide and its metabolites. Pharmacol. Res. 47: 383-392.

93. Kurinna, S. M., C. C. Tsao, A. F. Nica, T. Jiffar, and P. P. Ruvolo. 2004. Ceramide promotes apoptosis in lung cancer-derived A549 cells by a mechanism involving c-Jun NH2-terminal kinase. Cancer Res. 64: 7852-7856.

94. Pruschy, M., H. Resch, Y. Q. Shi, N. Aalame, C. Glanzmann, and S. Bodis. 1999. Ceramide triggers p53-dependent apoptosis in genetically defined fibrosarcoma tumour cells. Br. J. Cancer 80: 693-698.

95. Schiffmann, S., J. Sandner, K. Birod, I. Wobst, C. Angioni, E. Ruckhaberle, M. Kaufmann, H. Ackermann, J. Lotsch, H. Schmidt, G. Geisslinger, and S. Grosch. 2009. Ceramide synthases and ceramide levels are increased in breast cancer tissue. Carcinogenesis 30: 745-752.

96. Huang, W. C., C. L. Chen, Y. S. Lin, and C. F. Lin. 2011. Apoptotic sphingolipid ceramide in cancer therapy. J. Lipids 2011: 565316.

97. Reynolds, C. P., B. J. Maurer, and R. N. Kolesnick. 2004. Ceramide synthesis and metabolism as a target for cancer therapy. Cancer Lett. 206: 169-180.

98. Kihara, A., S. Mitsutake, Y. Mizutani, and Y. Igarashi. 2007. Metabolism and biological functions of two phosphorylated sphingolipids, sphingosine 1-phosphate and ceramide 1-phosphate. Prog. Lipid Res. 46: 126-144.

99. Hannun, Y. A., and L. M. Obeid. 2008. Principles of bioactive lipid signalling: lessons from sphingolipids. Nat. Rev. Mol. Cell Biol. 9: 139-150.

100. Kok, J. W., M. Nikolova-Karakashian, K. Klappe, C. Alexander, and A. H. Merrill, Jr. 1997. Dihydroceramide biology. Structure-specific metabolism and intracellular localization. J. Biol. Chem. 272: 21128-21136.

101. Contreras, F. X., G. Basanez, A. Alonso, A. Herrmann, and F. M. Goni. 2005. Asymmetric addition of ceramides but not dihydroceramides promotes transbilayer (flip-flop) lipid motion in membranes. Biophys. J. 88: 348-359.

102. Bielawska, A., H. M. Crane, D. Liotta, L. M. Obeid, and Y. A. Hannun. 1993. Selectivity of ceramide-mediated biology. Lack of activity of erythro-dihydroceramide. J. Biol. Chem. 268: 26226-26232.

103. Chalfant, C. E., Z. Szulc, P. Roddy, A. Bielawska, and Y. A. Hannun. 2004. The structural requirements for ceramide activation of serine-threonine protein phosphatases. J. Lipid Res. 45: 496-506.

104. Tepper, A. D., P. Ruurs, T. Wiedmer, P. J. Sims, J. Borst, and W. J. van Blitterswijk. 2000. Sphingomyelin hydrolysis to ceramide during the execution phase of apoptosis results from phospholipid scrambling and alters cell-surface morphology. J. Cell Biol. 150: 155-164.

105. Tabas, I. 1999. Secretory sphingomyelinase. Chem. Phys. Lipids 102: 123-130.

106. Marathe, S., S. L. Schissel, M. J. Yellin, N. Beatini, R. Mintzer, K. J. Williams, and I. Tabas. 1998. Human vascular endothelial cells are a rich and regulatable source of secretory sphingomyelinase. Implications for early atherogenesis and ceramide-mediated cell signaling. J. Biol. Chem. 273: 4081-4088.

107. Wong, M. L., B. Xie, N. Beatini, P. Phu, S. Marathe, A. Johns, P. W. Gold, E. Hirsch, K. J. Williams, J. Licinio, and I. Tabas. 2000. Acute systemic inflammation up-regulates secretory sphingomyelinase in vivo: a possible link between inflammatory cytokines and atherogenesis. Proc. Natl. Acad. Sci. U. S. A 97: 8681-8686.

108. Jenkins, R. W., D. Canals, J. Idkowiak-Baldys, F. Simbari, P. Roddy, D. M. Perry, K. Kitatani, C. Luberto, and Y. A. Hannun. 2010. Regulated secretion of acid sphingomyelinase: implications for selectivity of ceramide formation. J. Biol. Chem. 285: 35706-35718.

109. Chiantia, S., J. Ries, G. Chwastek, D. Carrer, Z. Li, R. Bittman, and P. Schwille. 2008. Role of ceramide in membrane protein organization investigated by combined AFM and FCS. Biochim. Biophys. Acta 1778: 1356-1364.

110. van Blitterswijk, W. J., A. H. van der Luit, R. J. Veldman, M. Verheij, and J. Borst. 2003. Ceramide: second messenger or modulator of membrane structure and dynamics? Biochem. J. 369: 199-211.

111. Kolesnick, R. N. 1991. Sphingomyelin and derivatives as cellular signals. Prog. Lipid Res. 30: 1-38.

112. van Holde, K. E., W. C. Johnson, and P. S. Ho. 1998. Principles of physical biochemistry. Prentice-Hall, Inc., New Jersey.

113. Heimburg, T. 2007. Thermal biophysics of membranes. Wiley-VCH Verlag GmbH & Co KGaA, Weinheim, Germany.

114. Israelachvili, J. 1991. Intermolecular and surface forces. Academic Press, San Diego.

115. Li, Z., E. Mintzer, and R. Bittman. 2004. The critical micelle concentrations of lysophosphatidic acid and sphingosylphosphorylcholine. Chem. Phys. Lipids 130: 197-201.

116. Kooijman, E. E., V. Chupin, N. L. Fuller, M. M. Kozlov, B. de Kruijff, K. N. Burger, and P. R. Rand. 2005. Spontaneous curvature of phosphatidic acid and lysophosphatidic acid. Biochemistry 44: 2097-2102.

117. Veiga, M. P., J. L. Arrondo, F. M. Goni, and A. Alonso. 1999. Ceramides in phospholipid membranes: effects on bilayer stability and transition to nonlamellar phases. Biophys. J. 76: 342-350.

118. Tenchov, B., and R. Koynova. 2012. Cubic phases in membrane lipids. Eur. Biophys. J. 41: 841-850.

119. Frolov, V. A., A. V. Shnyrova, and J. Zimmerberg. 2011. Lipid polymorphisms and membrane shape. Cold Spring Harb. Perspect. Biol. 3: a004747.

120. McMahon, H. T., and J. L. Gallop. 2005. Membrane curvature and mechanisms of dynamic cell membrane remodelling. Nature 438: 590-596.

121. Huang, C., and S. Li. 1999. Calorimetric and molecular mechanics studies of the thermotropic phase behavior of membrane phospholipids. Biochim. Biophys. Acta 1422: 273-307.

122. Koynova, R., and M. Caffrey. 1998. Phases and phase transitions of the phosphatidylcholines. Biochim. Biophys. Acta 1376: 91-145.

123. Ipsen, J. H., G. Karlstrom, O. G. Mouritsen, H. Wennerstrom, and M. J. Zuckermann. 1987. Phase equilibria in the phosphatidylcholine-cholesterol system. Biochim. Biophys. Acta 905: 162-172.

124. Vist, M. R., and J. H. Davis. 1990. Phase equilibria of cholesterol/dipalmitoylphosphatidylcholine mixtures: 2H nuclear magnetic resonance and differential scanning calorimetry. Biochemistry 29: 451-464.

125. Thewalt, J. L., and M. Bloom. 1992. Phosphatidylcholine: cholesterol phase diagrams. Biophys. J. 63: 1176-1181.

126. Quinn, P. J., and C. Wolf. 2009. The liquid-ordered phase in membranes. Biochim. Biophys. Acta 1788: 33-46.

127. Lindblom, G., and G. Oradd. 2009. Lipid lateral diffusion and membrane heterogeneity. Biochim. Biophys. Acta 1788: 234-244.

128. Filippov, A., G. Oradd, and G. Lindblom. 2004. Lipid lateral diffusion in ordered and disordered phases in raft mixtures. Biophys. J. 86: 891-896.

129. Shah, J., J. M. Atienza, R. I. Duclos, Jr., A. V. Rawlings, Z. Dong, and G. G. Shipley. 1995. Structural and thermotropic properties of synthetic C16:0 (palmitoyl) ceramide: effect of hydration. J. Lipid Res. 36: 1936-1944.

130. Pasenkiewicz-Gierula, M., Y. Takaoka, H. Miyagawa, K. Kitamura, and A. Kusumi. 1999. Charge pairing of headgroups in phosphatidylcholine membranes: A molecular dynamics simulation study. Biophys. J. 76: 1228-1240.

131. Aittoniemi, J., P. S. Niemela, M. T. Hyvonen, M. Karttunen, and I. Vattulainen. 2007. Insight into the putative specific interactions between cholesterol, sphingomyelin, and palmitoyl-oleoyl phosphatidylcholine. Biophys. J. 92: 1125-1137.

132. Hauser, H. 1991. Effect of inorganic cations on phase transitions. Chem. Phys. Lipids 57: 309-325.

133. Lee, A. G. 2005. How lipids and proteins interact in a membrane: a molecular approach. Mol. Biosyst. 1: 203-212.

134. Marsh, D. 2008. Protein modulation of lipids, and vice-versa, in membranes. Biochim. Biophys. Acta 1778: 1545-1575.

135. Gorter, E., and F. Grendel. 1925. On bimolecular layers of lipoids on the chromocytes of the blood. J. Exp. Med. 41: 439-443.

136. Singer, S. J., and G. L. Nicolson. 1972. The fluid mosaic model of the structure of cell membranes. Science 175: 720-731.

137. Mouritsen, O. G., and M. Bloom. 1984. Mattress model of lipid-protein interactions in membranes. Biophys. J. 46: 141-153.

138. Simons, K., and W. L. Vaz. 2004. Model systems, lipid rafts, and cell membranes. Annu. Rev. Biophys. Biomol. Struct. 33: 269-295.

139. Simons, K., and M. J. Gerl. 2010. Revitalizing membrane rafts: new tools and insights. Nat. Rev. Mol. Cell Biol. 11: 688-699.

140. Ridgway, N. D. 2000. Interactions between metabolism and intracellular distribution of cholesterol and sphingomyelin. Biochim. Biophys. Acta 1484: 129-141.

141. Eggeling, C., C. Ringemann, R. Medda, G. Schwarzmann, K. Sandhoff, S. Polyakova, V. N. Belov, B. Hein, M. C. von, A. Schonle, and S. W. Hell. 2009. Direct observation of the nanoscale dynamics of membrane lipids in a living cell. Nature 457: 1159-1162.

142. Bangham, A. D., and R. W. Horne. 1964. Negative staining of phospholipids and their structural modification by surface-active agents as observed in the electron microscope. J. Mol. Biol. 8: 660-668.

143. Bangham, A. D., M. M. Standish, and J. C. Watkins. 1965. Diffusion of univalent ions across the lamellae of swollen phospholipids. J. Mol. Biol. 13: 238-252.

144. Sessa, G., and G. Weissmann. 1968. Phospholipid spherules (liposomes) as a model for biological membranes. J. Lipid Res. 9: 310-318.

145. Chan, Y. H., and S. G. Boxer. 2007. Model membrane systems and their applications. Curr. Opin. Chem. Biol. 11: 581-587.

146. Szoka, F., Jr., and D. Papahadjopoulos. 1980. Comparative properties and methods of preparation of lipid vesicles (liposomes). Annu. Rev. Biophys. Bioeng. 9: 467-508.

147. Maulucci, G., S. M. De, G. Arcovito, F. Boffi, A. C. Castellano, and G. Briganti. 2005. Particle size distribution in DMPC vesicles solutions undergoing different sonication times. Biophys. J. 88: 3545-3550.

148. Richardson, E. S., W. G. Pitt, and D. J. Woodbury. 2007. The role of cavitation in liposome formation. Biophys. J. 93: 4100-4107.

149. Mayer, L. D., M. J. Hope, and P. R. Cullis. 1986. Vesicles of variable sizes produced by a rapid extrusion procedure. Biochim. Biophys. Acta 858: 161-168.

150. MacDonald, R. C., R. I. MacDonald, B. P. Menco, K. Takeshita, N. K. Subbarao, and L. R. Hu. 1991. Small-volume extrusion apparatus for preparation of large, unilamellar vesicles. Biochim. Biophys. Acta 1061: 297-303.

151. Ahyayauch, H., A. V. Villar, A. Alonso, and F. M. Goni. 2005. Modulation of PI-specific phospholipase C by membrane curvature and molecular order. Biochemistry 44: 11592-11600.

152. Roux, A., D. Cuvelier, P. Nassoy, J. Prost, P. Bassereau, and B. Goud. 2005. Role of curvature and phase transition in lipid sorting and fission of membrane tubules. EMBO J. 24: 1537-1545.

153. Pencer, J., A. Jackson, N. Kucerka, M. P. Nieh, and J. Katsaras. 2008. The influence of curvature on membrane domains. Eur. Biophys. J. 37: 665-671.

154. Nordlund, J. R., C. F. Schmidt, S. N. Dicken, and T. E. Thompson. 1981. Transbilayer distribution of phosphatidylethanolamine in large and small unilamellar vesicles. Biochemistry 20: 3237-3241.

155. Brumm, T., K. Jorgensen, O. G. Mouritsen, and T. M. Bayerl. 1996. The effect of increasing membrane curvature on the phase transition and mixing behavior of a dimyristoyl-sn-glycero-3-phosphatidylcholine/ distearoyl-sn-glycero-3-phosphatidylcholine lipid mixture as studied by Fourier transform infrared spectroscopy and differential scanning calorimetry. Biophys. J. 70: 1373-1379.

156. Boni, L. T., S. R. Minchey, W. R. Perkins, P. L. Ahl, J. L. Slater, M. W. Tate, S. M. Gruner, and A. S. Janoff. 1993. Curvature dependent induction of the interdigitated gel phase in DPPC vesicles. Biochim. Biophys. Acta 1146: 247-257.

157. Nagano, H., T. Nakanishi, H. Yao, and K. Ema. 1995. Effect of vesicle size on the heat capacity anomaly at the gel to liquid-crystalline phase transition in unilamellar vesicles of dimyristoylphosphatidylcholine. Phys. Rev. E. Stat. Phys. Plasmas. Fluids Relat Interdiscip. Topics. 52: 4244-4250.

158. Kucerka, N., J. Pencer, J. N. Sachs, J. F. Nagle, and J. Katsaras. 2007. Curvature effect on the structure of phospholipid bilayers. Langmuir 23: 1292-1299.

159. Marrink, S. J., and H. J. Berendsen. 1994. Simulation of water transport through a lipid membrane. J. Chem. Phys. 98: 4155-4168.

160. Chiantia, S., A. S. Klymchenko, and E. London. 2012. A novel leaflet-selective fluorescence labeling technique reveals differences between inner and outer leaflets at high bilayer curvature. Biochim. Biophys. Acta 1818: 1284-1290.

161. Cheng, H. T., Megha, and E. London. 2009. Preparation and properties of asymmetric vesicles that mimic cell membranes: effect upon lipid raft formation and transmembrane helix orientation. J. Biol. Chem. 284: 6079-6092.

162. Cheng, H. T., and E. London. 2011. Preparation and properties of asymmetric large unilamellar vesicles: interleaflet coupling in asymmetric vesicles is dependent on temperature but not curvature. Biophys. J. 100: 2671-2678.

163. Marsh, D. 2009. Cholesterol-induced fluid membrane domains: a compendium of lipid-raft ternary phase diagrams. Biochim. Biophys. Acta 1788: 2114-2123.

164. de Almeida, R. F., A. Fedorov, and M. Prieto. 2003. Sphingomyelin/phosphatidylcholine/cholesterol phase diagram: boundaries and composition of lipid rafts. Biophys. J. 85: 2406-2416.

165. Nyholm, T. K., D. Lindroos, B. Westerlund, and J. P. Slotte. 2011. Construction of a DOPC/PSM/cholesterol phase diagram based on the fluorescence properties of trans-parinaric acid. Langmuir 27: 8339-8350.

166. Veatch, S. L., and S. L. Keller. 2005. Miscibility phase diagrams of giant vesicles containing sphingomyelin. Phys. Rev. Lett. 94: 148101.

167. Bunge, A., P. Muller, M. Stockl, A. Herrmann, and D. Huster. 2008. Characterization of the ternary mixture of sphingomyelin, POPC, and cholesterol: support for an inhomogeneous lipid distribution at high temperatures. Biophys. J. 94: 2680-2690.

168. Silva, L., R. F. de Almeida, A. Fedorov, A. P. Matos, and M. Prieto. 2006. Ceramide-platform formation and -induced biophysical changes in a fluid phospholipid membrane. Mol. Membr. Biol. 23: 137-148.

169. Castro, B. M., R. F. de Almeida, L. C. Silva, A. Fedorov, and M. Prieto. 2007. Formation of ceramide/sphingomyelin gel domains in the presence of an unsaturated phospholipid: a quantitative multiprobe approach. Biophys. J. 93: 1639-1650.

170. Huang, J., and G. W. Feigenson. 1999. A microscopic interaction model of maximum solubility of cholesterol in lipid bilayers. Biophys. J. 76: 2142-2157.

171. Radhakrishnan, A., and H. M. McConnell. 1999. Condensed complexes of cholesterol and phospholipids. Biophys. J. 77: 1507-1517.

172. Somerharju, P., J. A. Virtanen, K. H. Cheng, and M. Hermansson. 2009. The superlattice model of lateral organization of membranes and its implications on membrane lipid homeostasis. Biochim. Biophys. Acta 1788: 12-23.

173. Lentz, B. R. 1993. Use of fluorescent probes to monitor molecular order and motions within liposome bilayers. Chem. Phys. Lipids 64: 99-116.

174. Borenstain, V., and Y. Barenholz. 1993. Characterization of liposomes and other lipid assemblies by multiprobe fluorescence polarization. Chem. Phys. Lipids 64: 117-127.

175. Franova, M., J. Repakova, P. Capkova, J. M. Holopainen, and I. Vattulainen. 2010. Effects of DPH on DPPC-cholesterol membranes with varying concentrations of cholesterol: from local perturbations to limitations in fluorescence anisotropy experiments. J. Phys. Chem. B 114: 2704-2711.

176. Castanho, M., M. Prieto, and A. U. Acuna. 1996. The transverse location of the fluorescent probe trans-parinaric acid in lipid bilayers. Biochim. Biophys. Acta 1279: 164-168.

177. Lentz, B. R., Y. Barenholz, and T. E. Thompson. 1976. Fluorescence depolarization studies of phase transitions and fluidity in phospholipid bilayers. 2 Two-component phosphatidylcholine liposomes. Biochemistry 15: 4529-4537.

178. Andrich, M. P., and J. M. Vanderkooi. 1976. Temperature dependence of 1,6-diphenyl-1,3,5-hexatriene fluorescence in phophoslipid artificial membranes. Biochemistry 15: 1257-1261.

179. Silva, L. C., R. F. de Almeida, B. M. Castro, A. Fedorov, and M. Prieto. 2007. Ceramide-domain formation and collapse in lipid rafts: membrane reorganization by an apoptotic lipid. Biophys. J. 92: 502-516.

180. Sklar, L. A. 1980. The partition of cis-parinaric acid and trans-parinaric acid among aqueous, fluid lipid, and solid lipid phases. Mol. Cell Biochem. 32: 169-177.

181. Castro, B. M., L. C. Silva, A. Fedorov, R. F. de Almeida, and M. Prieto. 2009. Cholesterol-rich fluid membranes solubilize ceramide domains: implications for the structure and dynamics of mammalian intracellular and plasma membranes. J. Biol. Chem. 284: 22978-22987.

182. Bjorkqvist, Y. J., T. K. Nyholm, J. P. Slotte, and B. Ramstedt. 2005. Domain formation and stability in complex lipid bilayers as reported by cholestatrienol. Biophys. J. 88: 4054-4063.

183. Alanko, S. M., K. K. Halling, S. Maunula, J. P. Slotte, and B. Ramstedt. 2005. Displacement of sterols from sterol/sphingomyelin domains in fluid bilayer membranes by competing molecules. Biochim. Biophys. Acta 1715: 111-121.

184. London, E., and G. W. Feigenson. 1981. Fluorescence quenching in model membranes. 1. Characterization of quenching caused by a spin-labeled phospholipid. Biochemistry 20: 1932-1938.

185. Ahmed, S. N., D. A. Brown, and E. London. 1997. On the origin of sphingolipid/cholesterol-rich detergent-insoluble cell membranes: physiological concentrations of cholesterol and sphingolipid induce formation of a detergent-insoluble, liquid-ordered lipid phase in model membranes. Biochemistry 36: 10944-10953.

186. Sripada, P. K., P. R. Maulik, J. A. Hamilton, and G. G. Shipley. 1987. Partial synthesis and properties of a series of N-acyl sphingomyelins. J. Lipid Res. 28: 710-718.

187. Koynova, R., and M. Caffrey. 1995. Phases and phase transitions of the sphingolipids. Biochim. Biophys. Acta 1255: 213-236.

188. Jaikishan, S., A. Bjorkbom, and J. P. Slotte. 2010. Sphingomyelin analogs with branched N-acyl chains: the position of branching dramatically affects acyl chain order and sterol interactions in bilayer membranes. Biochim. Biophys. Acta 1798: 1987-1994.

189. Lofgren, H., and I. Pascher. 1977. Molecular arrangements of sphingolipids. The monolayer behaviour of ceramides. Chem. Phys. Lipids 20: 273-284.

190. Barenholz, Y., J. Suurkuusk, D. Mountcastle, T. E. Thompson, and R. L. Biltonen. 1976. A calorimetric study of the thermotropic behavior of aqueous dispersions of natural and synthetic sphingomyelins. Biochemistry 15: 2441-2447.

191. Kuikka, M., B. Ramstedt, H. Ohvo-Rekila, J. Tuuf, and J. P. Slotte. 2001. Membrane properties of D-erythro-N-acyl sphingomyelins and their corresponding dihydro species. Biophys. J. 80: 2327-2337.

192. Nyholm, T. K., M. Nylund, and J. P. Slotte. 2003. A calorimetric study of binary mixtures of dihydrosphingomyelin and sterols, sphingomyelin, or phosphatidylcholine. Biophys. J. 84: 3138-3146.

193. Nyholm, T., M. Nylund, A. Soderholm, and J. P. Slotte. 2003. Properties of palmitoyl phosphatidylcholine, sphingomyelin, and dihydrosphingomyelin bilayer membranes as reported by different fluorescent reporter molecules. Biophys. J. 84: 987-997.

194. Ollila, F., and J. P. Slotte. 2002. Partitioning of Triton X-100, deoxycholate and C(10)EO(8) into bilayers composed of native and hydrogenated egg yolk sphingomyelin. Biochim. Biophys. Acta 1564: 281-288.

195. Ramstedt, B., and J. P. Slotte. 2002. Membrane properties of sphingomyelins. FEBS Lett. 531: 33-37.

196. Niemela, P., M. T. Hyvonen, and I. Vattulainen. 2004. Structure and dynamics of sphingomyelin bilayer: insight gained through systematic comparison to phosphatidylcholine. Biophys. J. 87: 2976-2989.

197. Demel, R. A., J. W. Jansen, P. W. van Dijck, and L. L. van Deenen. 1977. The preferential interaction of cholesterol with different classes of phospholipids. Biochim. Biophys. Acta 465: 1-10.

198. van Dijck, P. W. 1979. Negatively charged phospholipids and their position in the cholesterol affinity sequence. Biochim. Biophys. Acta 555: 89-101.

199. Niu, S. L., and B. J. Litman. 2002. Determination of membrane cholesterol partition coefficient using a lipid vesicle-cyclodextrin binary system: effect of phospholipid acyl chain unsaturation and headgroup composition. Biophys. J. 83: 3408-3415.

200. Ohvo, H., and J. P. Slotte. 1996. Cyclodextrin-mediated removal of sterols from monolayers: effects of sterol structure and phospholipids on desorption rate. Biochemistry 35: 8018-8024.

201. Mattjus, P., and J. P. Slotte. 1996. Does cholesterol discriminate between sphingomyelin and phosphatidylcholine in mixed monolayers containing both phospholipids? Chem. Phys. Lipids 81: 69-80.

202. Needham, D., and R. S. Nunn. 1990. Elastic deformation and failure of lipid bilayer membranes containing cholesterol. Biophys. J. 58: 997-1009.

203. Ramstedt, B., and J. P. Slotte. 1999. Interaction of cholesterol with sphingomyelins and acyl-chain-matched phosphatidylcholines: a comparative study of the effect of the chain length. Biophys. J. 76: 908-915.

204. Li, X. M., M. M. Momsen, J. M. Smaby, H. L. Brockman, and R. E. Brown. 2001. Cholesterol decreases the interfacial elasticity and detergent solubility of sphingomyelins. Biochemistry 40: 5954-5963.

205. Rog, T., and M. Pasenkiewicz-Gierula. 2006. Cholesterol-sphingomyelin interactions: a molecular dynamics simulation study. Biophys. J. 91: 3756-3767.

206. Leventis, R., and J. R. Silvius. 2001. Use of cyclodextrins to monitor transbilayer movement and differential lipid affinities of cholesterol. Biophys. J. 81: 2257-2267.

207. Lonnfors, M., J. P. Doux, J. A. Killian, T. K. Nyholm, and J. P. Slotte. 2011. Sterols have higher affinity for sphingomyelin than for phosphatidylcholine bilayers even at equal acyl-chain order. Biophys. J. 100: 2633-2641.

208. Holopainen, J. M., A. J. Metso, J. P. Mattila, A. Jutila, and P. K. Kinnunen. 2004. Evidence for the lack of a specific interaction between cholesterol and sphingomyelin. Biophys. J. 86: 1510-1520.

209. Terova, B., R. Heczko, and J. P. Slotte. 2005. On the importance of the phosphocholine methyl groups for sphingomyelin/cholesterol interactions in membranes: a study with ceramide phosphoethanolamine. Biophys. J. 88: 2661-2669.

210. Bjorkbom, A., T. Rog, K. Kaszuba, M. Kurita, S. Yamaguchi, M. Lonnfors, T. K. Nyholm, I. Vattulainen, S. Katsumura, and J. P. Slotte. 2010. Effect of sphingomyelin headgroup size on molecular properties and interactions with cholesterol. Biophys. J. 99: 3300-3308.

211. Pascher, I. 1976. Molecular arrangements in sphingolipids. Conformation and hydrogen bonding of ceramide and their implication on membrane stability and permeability. Biochim. Biophys. Acta 455: 433-451.

212. Brockman, H. L., M. M. Momsen, R. E. Brown, L. He, J. Chun, H. S. Byun, and R. Bittman. 2004. The 4,5-double bond of ceramide regulates its dipole potential, elastic properties, and packing behavior. Biophys. J. 87: 1722-1731.

213. Pandit, S. A., and H. L. Scott. 2006. Molecular-dynamics simulation of a ceramide bilayer. J. Chem. Phys. 124: 14708-14715.

214. Li, L., X. Tang, K. G. Taylor, D. B. DuPre, and M. C. Yappert. 2002. Conformational characterization of ceramides by nuclear magnetic resonance spectroscopy. Biophys. J. 82: 2067-2080.

215. Vorobyov, I., M. C. Yappert, and D. B. DuPré. 2002. Energetic and topological analyses of cooperative σH- and πH-bonding interactions. J. Phys. Chem. A 106: 10691-10699.

216. Jendrasiak, G. L., and R. L. Smith. 2001. The effect of the choline head group on phospholipid hydration. Chem. Phys. Lipids 113: 55-66.

217. Chen, H., R. Mendelsohn, M. E. Rerek, and D. J. Moore. 2000. Fourier transform infrared spectroscopy and differential scanning calorimetry studies of fatty acid homogeneous ceramide 2. Biochim. Biophys. Acta 1468: 293-303.

218. Westerlund, B., P. M. Grandell, Y. J. Isaksson, and J. P. Slotte. 2010. Ceramide acyl chain length markedly influences miscibility with palmitoyl sphingomyelin in bilayer membranes. Eur. Biophys. J. 39: 1117-1128.

219. Sot, J., F. J. Aranda, M. I. Collado, F. M. Goni, and A. Alonso. 2005. Different effects of long- and short-chain ceramides on the gel-fluid and lamellar-hexagonal transitions of phospholipids: a calorimetric, NMR, and x-ray diffraction study. Biophys. J. 88: 3368-3380.

220. Huang, H. W., E. M. Goldberg, and R. Zidovetzki. 1996. Ceramide induces structural defects into phosphatidylcholine bilayers and activates phospholipase A2. Biochem. Biophys. Res. Commun. 220: 834-838.

221. Huang, H. W., E. M. Goldberg, and R. Zidovetzki. 1998. Ceramides perturb the structure of phosphatidylcholine bilayers and modulate the activity of phospholipase A2. Eur. Biophys. J. 27: 361-366.

222. Holopainen, J. M., J. Y. Lehtonen, and P. K. Kinnunen. 1997. Lipid microdomains in dimyristoylphosphatidylcholine-ceramide liposomes. Chem. Phys. Lipids 88: 1-13.

223. Massey, J. B. 2001. Interaction of ceramides with phosphatidylcholine, sphingomyelin and sphingomyelin/cholesterol bilayers. Biochim. Biophys. Acta 1510: 167-184.

224. Holopainen, J. M., M. Subramanian, and P. K. Kinnunen. 1998. Sphingomyelinase induces lipid microdomain formation in a fluid phosphatidylcholine/sphingomyelin membrane. Biochemistry 37: 17562-17570.

225. Holopainen, J. M., J. Lemmich, F. Richter, O. G. Mouritsen, G. Rapp, and P. K. Kinnunen. 2000. Dimyristoylphosphatidylcholine/C16:0-ceramide binary liposomes studied by differential scanning calorimetry and wide- and small-angle x-ray scattering. Biophys. J. 78: 2459-2469.

226. Pinto, S. N., L. C. Silva, A. H. Futerman, and M. Prieto. 2011. Effect of ceramide structure on membrane biophysical properties: the role of acyl chain length and unsaturation. Biochim. Biophys. Acta 1808: 2753-2760.

227. Carrer, D. C., and B. Maggio. 1999. Phase behavior and molecular interactions in mixtures of ceramide with dipalmitoylphosphatidylcholine. J. Lipid Res. 40: 1978-1989.

228. Hsueh, Y. W., R. Giles, N. Kitson, and J. Thewalt. 2002. The effect of ceramide on phosphatidylcholine membranes: a deuterium NMR study. Biophys. J. 82: 3089-3095.

229. Fidorra, M., L. Duelund, C. Leidy, A. C. Simonsen, and L. A. Bagatolli. 2006. Absence of fluid-ordered/fluid-disordered phase coexistence in ceramide/POPC mixtures containing cholesterol. Biophys. J. 90: 4437-4451.

230. Xu, X., R. Bittman, G. Duportail, D. Heissler, C. Vilcheze, and E. London. 2001. Effect of the structure of natural sterols and sphingolipids on the formation of ordered sphingolipid/sterol

domains (rafts). Comparison of cholesterol to plant, fungal, and disease-associated sterols and comparison of sphingomyelin, cerebrosides, and ceramide. J. Biol. Chem. 276: 33540-33546.

231. Sot, J., M. Ibarguren, J. V. Busto, L. R. Montes, F. M. Goni, and A. Alonso. 2008. Cholesterol displacement by ceramide in sphingomyelin-containing liquid-ordered domains, and generation of gel regions in giant lipidic vesicles. FEBS Lett. 582: 3230-3236.

232. Nybond, S., Y. J. Bjorkqvist, B. Ramstedt, and J. P. Slotte. 2005. Acyl chain length affects ceramide action on sterol/sphingomyelin-rich domains. Biochim. Biophys. Acta 1718: 61-66.

233. Chiantia, S., N. Kahya, J. Ries, and P. Schwille. 2006. Effects of ceramide on liquid-ordered domains investigated by simultaneous AFM and FCS. Biophys. J. 90: 4500-4508.

234. Chiantia, S., N. Kahya, and P. Schwille. 2007. Raft domain reorganization driven by short- and long-chain ceramide: a combined AFM and FCS study. Langmuir 23: 7659-7665.

235. Fanani, M. L., S. Hartel, R. G. Oliveira, and B. Maggio. 2002. Bidirectional control of sphingomyelinase activity and surface topography in lipid monolayers. Biophys. J. 83: 3416-3424.

236. Hartel, S., M. L. Fanani, and B. Maggio. 2005. Shape transitions and lattice structuring of ceramide-enriched domains generated by sphingomyelinase in lipid monolayers. Biophys. J. 88: 287-304.

237. Contreras, F. X., A. V. Villar, A. Alonso, R. N. Kolesnick, and F. M. Goni. 2003. Sphingomyelinase activity causes transbilayer lipid translocation in model and cell membranes. J. Biol. Chem. 278: 37169-37174.

238. Holopainen, J. M., M. I. Angelova, and P. K. Kinnunen. 2000. Vectorial budding of vesicles by asymmetrical enzymatic formation of ceramide in giant liposomes. Biophys. J. 78: 830-838.

239. Silva, L. C., A. H. Futerman, and M. Prieto. 2009. Lipid raft composition modulates sphingomyelinase activity and ceramide-induced membrane physical alterations. Biophys. J. 96: 3210-3222.

240. Ruiz-Arguello, M. B., G. Basanez, F. M. Goni, and A. Alonso. 1996. Different effects of enzyme-generated ceramides and diacylglycerols in phospholipid membrane fusion and leakage. J. Biol. Chem. 271: 26616-26621.

241. Basanez, G., M. B. Ruiz-Arguello, A. Alonso, F. M. Goni, G. Karlsson, and K. Edwards. 1997. Morphological changes induced by phospholipase C and by sphingomyelinase on large unilamellar vesicles: a cryo-transmission electron microscopy study of liposome fusion. Biophys. J. 72: 2630-2637.

242. Montes, L. R., M. B. Ruiz-Arguello, F. M. Goni, and A. Alonso. 2002. Membrane restructuring via ceramide results in enhanced solute efflux. J. Biol. Chem. 277: 11788-11794.

243. Ruiz-Arguello, M. B., M. P. Veiga, J. L. Arrondo, F. M. Goni, and A. Alonso. 2002. Sphingomyelinase cleavage of sphingomyelin in pure and mixed lipid membranes. Influence of the physical state of the sphingolipid. Chem. Phys. Lipids 114: 11-20.

244. Pinto, S. N., L. C. Silva, R. F. de Almeida, and M. Prieto. 2008. Membrane domain formation, interdigitation, and morphological alterations induced by the very long chain asymmetric C24:1 ceramide. Biophys. J. 95: 2867-2879.

245. Siskind, L. J., and M. Colombini. 2000. The lipids C2- and C16-ceramide form large stable channels. Implications for apoptosis. J. Biol. Chem. 275: 38640-38644.

246. Siskind, L. J., R. N. Kolesnick, and M. Colombini. 2002. Ceramide channels increase the permeability of the mitochondrial outer membrane to small proteins. J. Biol. Chem. 277: 26796-26803.

247. Wang, T. Y., and J. R. Silvius. 2003. Sphingolipid partitioning into ordered domains in cholesterol-free and cholesterol-containing lipid bilayers. Biophys. J. 84: 367-378.

248. Busto, J. V., M. L. Fanani, L. De Tullio, J. Sot, B. Maggio, F. M. Goni, and A. Alonso. 2009. Coexistence of immiscible mixtures of palmitoylsphingomyelin and palmitoylceramide in monolayers and bilayers. Biophys. J. 97: 2717-2726.

249. Metcalf, R., and S. A. Pandit. 2012. Mixing properties of sphingomyelin ceramide bilayers: a simulation study. J. Phys. Chem. B 116: 4500-4509.

250. Megha, and E. London. 2004. Ceramide selectively displaces cholesterol from ordered lipid domains (rafts): implications for lipid raft structure and function. J. Biol. Chem. 279: 9997-10004.

251. Yu, C., M. Alterman, and R. T. Dobrowsky. 2005. Ceramide displaces cholesterol from lipid rafts and decreases the association of the cholesterol binding protein caveolin-1. J. Lipid Res. 46: 1678-1691.

252. Megha, P. Sawatzki, T. Kolter, R. Bittman, and E. London. 2007. Effect of ceramide N-acyl chain and polar headgroup structure on the properties of ordered lipid domains (lipid rafts). Biochim. Biophys. Acta 1768: 2205-2212.

253. Nyholm, T. K., P. M. Grandell, B. Westerlund, and J. P. Slotte. 2010. Sterol affinity for bilayer membranes is affected by their ceramide content and the ceramide chain length. Biochim. Biophys. Acta 1798: 1008-1013.

254. Ali, M. R., K. H. Cheng, and J. Huang. 2006. Ceramide drives cholesterol out of the ordered lipid bilayer phase into the crystal phase in 1-palmitoyl-2-oleoyl-sn-glycero-3-phosphocholine/cholesterol/ceramide ternary mixtures. Biochemistry 45: 12629-12638.

255. Staneva, G., C. Chachaty, C. Wolf, K. Koumanov, and P. J. Quinn. 2008. The role of sphingomyelin in regulating phase coexistence in complex lipid model membranes: competition between ceramide and cholesterol. Biochim. Biophys. Acta 1778: 2727-2739.

256. Busto, J. V., J. Sot, J. Requejo-Isidro, F. M. Goni, and A. Alonso. 2010. Cholesterol displaces palmitoylceramide from its tight packing with palmitoylsphingomyelin in the absence of a liquid-disordered phase. Biophys. J. 99: 1119-1128.

257. Boulgaropoulos, B., M. Rappolt, B. Sartori, H. Amenitsch, and G. Pabst. 2012. Lipid sorting by ceramide and the consequences for membrane proteins. Biophys. J. 102: 2031-2038.

258. Pinto, S. N., F. Fernandes, A. Fedorov, A. H. Futerman, L. C. Silva, and M. Prieto. 2013. A combined fluorescence spectroscopy, confocal and 2-photon microscopy approach to re-evaluate the properties of sphingolipid domains. Biochim. Biophys. Acta 1828: 2099-2110.

259. Cohen, R., Y. Barenholz, S. Gatt, and A. Dagan. 1984. Preparation and characterization of well defined D-erythro sphingomyelins. Chem. Phys. Lipids 35: 371-384.

260. Zhang, L., L. I. Hellgren, and X. Xu. 2006. Enzymatic production of ceramide from sphingomyelin. J. Biotechnol. 123: 93-105.

261. Bittman, R., and C. A. Verbicky. 2000. Methanolysis of sphingomyelin. Toward an epimerization-free methodology for the preparation of D-erythro-sphingosylphosphocholine. J. Lipid Res. 41: 2089-2093.

262. Yamamoto, T., H. Hasegawa, T. Hakogi, and S. Katsumura. 2006. Versatile synthetic method for sphingolipids and functionalized sphingosine derivatives via olefin cross metathesis. Org. Lett. 8: 5569-5572.

263. Fischer, R. T., F. A. Stephenson, A. Shafiee, and F. Schroeder. 1984. delta 5,7,9(11)-Cholestatrien-3 beta-ol: a fluorescent cholesterol analogue. Chem. Phys. Lipids 36: 1-14.

264. Kuklev, D. V., and W. L. Smith. 2004. Synthesis of four isomers of parinaric acid. Chem. Phys. Lipids 131: 215-222.

265. Sklar, L. A., B. S. Hudson, and R. D. Simoni. 1977. Conjugated polyene fatty acids as fluorescent probes: synthetic phospholipid membrane studies. Biochemistry 16: 819-828.

266. Bittman, R. 1993. Chemical preparation of glycerolipids: a review of recent syntheses in Phospholipids Handbook. G. Cevec, editor. Marcel Dekker, Inc., 154-155.

267. Lakowicz, J. R. 1999. Principles of fluorescence spectroscopy. Kluvert Academic/Plenum Publishers, New York.

268. Nystrom, J. H., M. Lonnfors, and T. K. Nyholm. 2010. Transmembrane peptides influence the affinity of sterols for phospholipid bilayers. Biophys. J. 99: 526-533.

269. Wilson, L., and S. Martin. 1999. Benzyl alcohol as an alternative local anesthetic. Ann. Emerg. Med. 33: 495-499.

270. Bartfield, J. M., H. E. May-Wheeling, N. Raccio-Robak, and S. Y. Lai. 2001. Benzyl alcohol with epinephrine as an alternative to lidocaine with epinephrine. J. Emerg. Med. 21: 375-379.

271. Kazemifard, A. G., D. E. Moore, A. Mohammadi, and A. Kebriyaeezadeh. 2003. Capillary gas chromatography determination of benzaldehyde arising from benzyl alcohol used as preservative in injectable formulations. J. Pharm. Biomed. Anal. 31: 685-691.

272. Pope, J. M., D. Dubro, J. W. Done, and P. W. Westerman. 1986. The ordering of benzyl alcohol and its influence on phospholipid order in bilayer membranes. J. Am. Chem. Soc. 108: 5426-5433.

273. Balogh, G., I. Horvath, E. Nagy, Z. Hoyk, S. Benko, O. Bensaude, and L. Vigh. 2005. The hyperfluidization of mammalian cell membranes acts as a signal to initiate the heat shock protein response. FEBS J. 272: 6077-6086.

274. Nagy, E., Z. Balogi, I. Gombos, M. Akerfelt, A. Bjorkbom, G. Balogh, Z. Torok, A. Maslyanko, A. Fiszer-Kierzkowska, K. Lisowska, P. J. Slotte, L. Sistonen, I. Horvath, and L. Vigh. 2007. Hyperfluidization-coupled membrane microdomain reorganization is linked to activation of the heat shock response in a murine melanoma cell line. Proc. Natl. Acad. Sci. U. S. A 104: 7945-7950.

275. Xu, H., and C. H. Huang. 1987. Scanning calorimetric study of fully hydrated asymmetric phosphatidylcholines with one acyl chain twice as long as the other. Biochemistry 26: 1036-1043.

276. Ramstedt, B., and J. P. Slotte. 1999. Comparison of the biophysical properties of racemic and d-erythro-N-acyl sphingomyelins. Biophys. J. 77: 1498-1506.

277. Chen, C. H., K. Hoye, and L. G. Roth. 1996. Thermodynamic and fluorescence studies of the underlying factors in benzyl alcohol-induced lipid interdigitated phase. Arch. Biochem. Biophys. 333: 401-406.

278. Ebihara, L., J. E. Hall, R. C. MacDonald, T. J. McIntosh, and S. A. Simon. 1979. Effect of benzyl alcohol on lipid bilayers. A comparisons of bilayer systems. Biophys. J. 28: 185-196.

279. Konopasek, I., J. Vecer, K. Strzalka, and E. Amler. 2004. Short-lived fluorescence component of DPH reports on lipid--water interface of biological membranes. Chem. Phys. Lipids 130: 135-144.

280. Halling, K. K., B. Ramstedt, J. H. Nystrom, J. P. Slotte, and T. K. Nyholm. 2008. Cholesterol interactions with fluid-phase phospholipids: effect on the lateral organization of the bilayer. Biophys. J. 95: 3861-3871.

281. Colley, C. M., and J. C. Metcalfe. 1972. The localisation of small molecules in lipid bilayers. FEBS Lett. 24: 241-246.

282. Tsamaloukas, A., H. Szadkowska, and H. Heerklotz. 2006. Thermodynamic comparison of the interactions of cholesterol with unsaturated phospholipid and sphingomyelins. Biophys. J. 90: 4479-4487.

283. Wolber, P. K., and B. S. Hudson. 1981. Fluorescence lifetime and time-resolved polarization anisotropy studies of acyl chain order and dynamics in lipid bilayers. Biochemistry 20: 2800-2810.

284. Reyes, J., and R. Latorre. 1979. Effect of the anesthetics benzyl alcohol and chloroform on bilayers made from monolayers. Biophys. J. 28: 259-279.

285. Gordon, L. M., R. D. Sauerheber, J. A. Esgate, I. Dipple, R. J. Marchmont, and M. D. Houslay. 1980. The increase in bilayer fluidity of rat liver plasma membranes achieved by the local anesthetic benzyl alcohol affects the activity of intrinsic membrane enzymes. J. Biol. Chem. 255: 4519-4527.

286. Sauerheber, R. D., J. A. Esgate, and C. E. Kuhn. 1982. Alcohols inhibit adipocyte basal and insulin-stimulated glucose uptake and increase the membrane lipid fluidity. Biochim. Biophys. Acta 691: 115-124.

287. Balasubramanian, S. V., R. M. Straubinger, and M. E. Morris. 1997. Salicylic acid induces changes in the physical properties of model and native kidney membranes. J. Pharm. Sci. 86: 199-204.

288. McIntosh, T. J., R. V. McDaniel, and S. A. Simon. 1983. Induction of an interdigitated gel phase in fully hydrated phosphatidylcholine bilayers. Biochim. Biophys. Acta 731: 109-114.

289. Mitranic, M. M., J. M. Boggs, and M. A. Moscarello. 1982. The effect of linoleic acid and benzyl alcohol on the activity of glycosyltransferases of rat liver Golgi membranes and some soluble glycosyltransferases. Biochim. Biophys. Acta 693: 75-84.

290. Voorheis, H. P., and B. R. Martin. 1982. Local anaesthetics including benzyl alcohol activate the adenylate cyclase in Trypanosoma brucei by a calcium-dependent mechanism. Eur. J. Biochem. 123: 371-376.

291. de Foresta, B., M. Rogard, M. M. le, and J. Gallay. 1987. Effects of temperature and benzyl alcohol on the structure and adenylate cyclase activity of plasma membranes from bovine adrenal cortex. Biochim. Biophys. Acta 905: 240-256.

292. Needham, L., and M. D. Houslay. 1988. Tosyl-lysyl chloromethylketone detects conformational changes in the catalytic unit of adenylate cyclase induced by receptor and G-protein stimulation. Biochem. Biophys. Res. Commun. 156: 855-859.

293. Lingwood, D., H. J. Kaiser, I. Levental, and K. Simons. 2009. Lipid rafts as functional heterogeneity in cell membranes. Biochem. Soc. Trans. 37: 955-960.

294. Lingwood, D., and K. Simons. 2010. Lipid rafts as a membrane-organizing principle. Science 327: 46-50.

295. Sangster, J. 1989. Octanol-water partition coefficients of simple organic compounds. J. Phys. Chem. Ref. Data 18: 1111-1227.

296. Karttunen, M., M. P. Haataja, M. Saily, I. Vattulainen, and J. M. Holopainen. 2009. Lipid domain morphologies in phosphatidylcholine-ceramide monolayers. Langmuir 25: 4595-4600.

297. Kodama, M., and Y. Kawasaki. 2010. Structural role of mismatched C-C bonds in a series of d-erythro-sphingomyelins as studied by DSC and electron microscopy. Chem. Phys. Lipids 163: 514-523.

298. Jaikishan, S., and J. P. Slotte. 2011. Effect of hydrophobic mismatch and interdigitation on sterol/sphingomyelin interaction in ternary bilayer membranes. Biochim. Biophys. Acta 1808: 1940-1945.

299. Carrer, D. C., S. Schreier, M. Patrito, and B. Maggio. 2006. Effects of a short-chain ceramide on bilayer domain formation, thickness, and chain mobililty: DMPC and asymmetric ceramide mixtures. Biophys. J. 90: 2394-2403.

300. Guo, S., T. C. Moore, C. R. Iacovella, L. A. Strickland, and C. McCabe. 2013. Simulation study of the structure and phase behavior of ceramide bilayers and the role of lipid headgroup chemistry. J. Chem. Theory. Comput. 9: 5116-5126.

301. Bjorkbom, A., T. Rog, P. Kankaanpaa, D. Lindroos, K. Kaszuba, M. Kurita, S. Yamaguchi, T. Yamamoto, S. Jaikishan, L. Paavolainen, J. Paivarinne, T. K. Nyholm, S. Katsumura, I. Vattulainen, and J. P. Slotte. 2011. N- and O-methylation of sphingomyelin markedly affects its membrane properties and interactions with cholesterol. Biochim. Biophys. Acta 1808: 1179-1186.

302. Perera, M. N., V. Ganesan, L. J. Siskind, Z. M. Szulc, J. Bielawski, A. Bielawska, R. Bittman, and M. Colombini. 2012. Ceramide channels: influence of molecular structure on channel formation in membranes. Biochim. Biophys. Acta 1818: 1291-1301.

303. Huang, J., J. T. Buboltz, and G. W. Feigenson. 1999. Maximum solubility of cholesterol in phosphatidylcholine and phosphatidylethanolamine bilayers. Biochim. Biophys. Acta 1417: 89-100.

304. Staneva, G., A. Momchilova, C. Wolf, P. J. Quinn, and K. Koumanov. 2009. Membrane microdomains: role of ceramides in the maintenance of their structure and functions. Biochim. Biophys. Acta 1788: 666-675.

305. Scheffer, L., I. Fargion, and L. Addadi. 2006. Structural recognition of cholesterol-ceramide monolayers by a specific monoclonal antibody. Chembiochem. 7: 1680-1682.

306. Scheffer, L., A. H. Futerman, and L. Addadi. 2007. Antibody labeling of cholesterol/ceramide ordered domains in cell membranes. Chembiochem. 8: 2286-2294.

307. Goldschmidt-Arzi, M., E. Shimoni, H. Sabanay, A. H. Futerman, and L. Addadi. 2011. Intracellular localization of organized lipid domains of C16-ceramide/cholesterol. J. Struct. Biol. 175: 21-30.

308. Pabst, G., B. Boulgaropoulos, E. Gander, B. R. Sarangi, H. Amenitsch, V. A. Raghunathan, and P. Laggner. 2009. Effect of ceramide on nonraft proteins. J. Membr. Biol. 231: 125-132.

TERHI MAULA (née Kuru) was born on February 25, 1984 in Kolari, Finland. She graduated from Åbo Akademi University in 2008 with a Master of Science in Biochemistry. This PhD thesis project in Biochemistry has taken place during 2008-2014 under the supervision of Professor Peter Slotte at the Department of Biosciences.

ISBN 978-952-12-3021-9